AD-A034 504 M AND S COMPUTING INC HUNTSVILLE ALA F/G 17/9
PAR AURORAL STUDY. VOLUME IV. IONOSPHERIC SCINTILLATION OF SATE--ETC(U)
SEP 76 M J MITCHELL, J L BROWN DASG60-74-C-0026
UNCLASSIFIED 76-0042 NL

1 OF 1
AD-A
034 504

END
DATE
3-11-77
NTIS

PAR AURORAL STUDY

VOLUME IV. IONOSPHERIC SCINTILLATION OF SATELLITE TRACKS DURING AURORA

M AND S COMPUTING, INCORPORATED
HUNTSVILLE, ALABAMA

1 SEPTEMBER 1976

UNCLASSIFIED
SECURITY CLASSIFICATION OF THIS PAGE (When Data Entered)

REPORT DOCUMENTATION PAGE		READ INSTRUCTIONS BEFORE COMPLETING FORM
1. REPORT NUMBER Volume IV	2. GOVT ACCESSION NO.	3. RECIPIENT'S CATALOG NUMBER
4. TITLE (and Subtitle) PAR Auroral Study		5. TYPE OF REPORT & PERIOD COVERED Interim-One of six volumes
		6. PERFORMING ORG. REPORT NUMBER 76-0042
7. AUTHOR(s) M. J. Mitchell et al		8. CONTRACT OR GRANT NUMBER(s) Army DASG60-74-C-0026
9. PERFORMING ORGANIZATION NAME AND ADDRESS M&S Computing Inc. P. O. Box 5183 Huntsville, Alabama 35805		10. PROGRAM ELEMENT, PROJECT, TASK AREA & WORK UNIT NUMBERS Not Applicable
11. CONTROLLING OFFICE NAME AND ADDRESS U. S. Army Ballistic Missile Def Sys Cmd BMDSC-WE, P. O. Box 1500 Huntsville, Ala. 35807		12. REPORT DATE 1 Sep 76 13. NUMBER OF PAGES 82
14. MONITORING AGENCY NAME & ADDRESS(if different from Controlling Office) U. S. Army Ballistic Missile Def Sys Cmd BMDSC-WE, P. O. Box 1500 Huntsville, Ala. 35807		15. SECURITY CLASS. (of this report) UNCLASSIFIED 15a. DECLASSIFICATION/DOWNGRADING SCHEDULE Not Applicable

16. DISTRIBUTION STATEMENT (of this Report)

Unlimited Distribution

17. DISTRIBUTION STATEMENT (of the abstract entered in Block 20, if different from Report)

Unlimited Distribution

18. SUPPLEMENTARY NOTES This is one of six volumes of reports that present the aurora borealis data collected by a multi-megawatt phased array radar. The radar has excellent sensitivity and range resolution affording very precise aurora detail.

19. KEY WORDS (Continue on reverse side if necessary and identify by block number)

Aurora Borcalis, phased array radar, radar/aurora efforts, back scattering characteristics, radar reflectivity, geomagnetic field effects, ionospheric scintillation.

20. ABSTRACT (Continue on reverse side if necessary and identify by block number)

This report describes data collected in connection with research of aurora borealis effects on the performance of phased array radar. In particular, the effects and deviations of ionospheric scintillations are discussed.

PREFACE

This report describes the track portion of the aurora borealis research effort being performed by M&S Computing, Inc., for the Army Ballistic Missile Defense Systems Command in Huntsville, Alabama. The primary objective of the study is to advance the understanding of the auroral phenomenon, especially of its interactions with radar. The primary data gathering instrument is the Safeguard Perimeter Acquisition Radar in North Dakota. This radar has been used to collect large quantities of high resolution auroral backscatter data with the simultaneous tracking of a number of selected satellites.

The data presented here results from an analysis of ionospheric scintillation effects on satellites tracked during periods of intense auroral activity. This study was performed by M&S Computing, Inc., under Contract No. DASG60-74-C-0026 for the Army Ballistic Missile Defense Systems Command in Huntsville, Alabama. PAR Auroral Study, Volume IV, dated September 1, 1976, constitutes M&S Computing's Report No. 76-0042.

Prepared by:

J. L. Brown

Approved by:

W. E. Salter

W. E. Salter

TABLE OF CONTENTS

LIST OF FIGURES

LIST OF TABLES

1. INTRODUCTION

As a part of the Safeguard Perimeter Acquisition Radar (PAR) Auroral Experiment, a number of satellites were tracked concurrently with the collection of auroral backscatter data. This data was taken because previous work had indicated the possibility of significant scintillation effects at the PAR frequency during periods of auroral activity. These effects appear as rapid fluctuations in signal power and apparent target position and are thought to be caused by irregularities in the ionospheric F region. Certain of these characteristics are known to be related to the magnetic disturbances associated with auroral activity. Scintillation is of great concern in radar systems because it alters the statistical properties of the target. These alterations take the form of changes in the mean and standard deviation of the target's instantaneous Radar Cross Section (RCS) and of uncertainties about the angular position of the target. The perturbations to the RCS cause inaccurate estimates of the target's optical size and shape. This can increase the difficulty of target discrimination to the point of impossibility. Angular scintillations can reduce the resolution between close objects since there can be overlap in the apparent locations of the two objects. Furthermore it can perturb the track prediction algorithms and reduce the mean amplitude of the return by increasing the chances of a detection at a low gain point of the beam. In extreme cases this may even result in a Signal to Noise Ratio (SNR) below the system threshold or a total miss, either of which would be treated as a missed pulse and result in degradation of system performance. The effects of ionospheric scintillation are most significant to radars such as the PAR which must perform critical target discriminating functions.

This report is Volume IV of the PAR Auroral Study. Volumes I, II, and III are concerned primarily with the analysis of auroral backscatter. Volume V will contain studies of related subjects and phenomena.

This volume is presented in six sections. Section 1 provides an overview and a brief summary of the morphology of ionospheric scintillation. It also will provide an introduction to related literature. Section 2 describes the experiment and the techniques used in the analysis. Section 3 presents the results of that analysis, and Section 4 contains a discussion of the data of Section 3. Section 5 contains the concluding remarks, and Section 6 lists the references utilized in this study. In addition to these five sections, an appendix is included which contains composite plots of azimuth, elevation, range, and amplitude versus elapsed time in track for those tracks not discussed elsewhere in the report.

1.1 General Background

Scintillation is the term used to describe rapid random changes in measured target signal power and angular position. It also refers in some instances to slower fading effects. For the purposes of this report, the terms amplitude scintillation, angle scintillation, and fading will be used to refer to rapid fluctuations in signal strength, rapid fluctuations in apparent angular position, and slow variations in signal strength, respectively.

Detailed surveys of ionospheric scintillation effects are available in the literature (References 2, 13, 16, and 18), and for those desiring further information Jones' Index (Reference 15) should prove useful. Here we shall present only a brief overview of the general morphology and some details of the UHF Scintillation effects.

Scintillation is caused by irregularities in the ionospheric electron density. These irregularities usually range in height from 200 to 600 km and occur predominantly in the ionospheric F-layer at heights from 225 to 400 km (see References 4 and 5). Irregularities due to sporadic E and small Travelling Ionospheric Disturbances (TID's) in the F-layer (References 9 and 10) also produce scintillations but are usually less frequent and not very severe. During scintillation, signal power may be enhanced by 6 to 8 dB and decreased to the noise level during the course of the track.

The degree of amplitude scintillation also has a frequency dependence (Reference 12). At lower frequencies amplitude scintillation decreases as a function of λ but at higher frequencies occurs more as a function of λ^2. For some special geometries, however, the scintillations may increase as λ decreases (Reference 25). This is referred to as "inversion."

The scale size of the irregularities is dependent on frequency but is generally on the order of 1 kilometer in the smallest (transverse) dimension (References 7 and 14). They are generally grouped in a large-scale, field-aligned structure and demonstrate an aspect sensitivity similar to that of radar aurora (References 11 and 21).

The geographic morphology of ionospheric scintillations limits them to three regions, an equatorial region and two polar regions. Scintillation in the equatorial region extends from -15° to $+15^{\circ}$ latitude and scintillation occurs mainly at night between 2100 and 2400 hours local time. The fading rate for equatorial scintillations is generally two to ten times slower than that in the polar regions. Equatorial scintillation also exhibits a strong seasonal dependence with maxima at the equinoxes and minima at the solstices. The two polar regions, arctic and antarctic, each form a band structure with a high and low latitude boundary. Scintillations above the high latitude boundary in the polar cap region are generally characterized by sudden and short-lived periods of high scintillation. Within the boundaries, in the irregularity region, the scintillations are usually less severe but of longer duration and uniformity. The lower scintillation boundary is defined as the latitude at which the mean scintillation index at 40 MHz is 50%. It is not always a sharp boundary.

Although the irregularity region has a field-aligned structure and moves toward the equator during periods of high magnetic activity (Reference 2), in a fashion similar to the auroral oval, it is considerably offset from the auroral oval. At night the Auroral oval generally lies in the region from 63° invariant

latitude to 71° invariant latitude. This puts it entirely within the irregularity region which, at midnight, usually extends from 57° to 77° (References 6, 9, 22, 23, 24, and 25).

1.2 Related Literature

Several studies have been conducted in the UHF band: Evans (Reference 8); Little, Reid, Stiltner, and Merritt (Reference 17); Millman and Anderson (Reference 19); Millman and Moceyunas (Reference 20); Porcello and Hughes (Reference 22); and Unger, Hardin, and Horan (Reference 27). Of these, the study conducted by Evans is most extensive and complete.

Evans collected data at 400 MHz from 2376 beacon satellites. His results confirm the existence of a scintillation boundary effect for 400 MHz scintillations and places this boundary near 46° geographic latitude. He also reports an increased probability of scintillation as ir ariant latitude increases and finds considerable correlation between the occurrence of auroral clutter and scintillation. Figure 1-1 depicts the distribution in invariant latitude of 3-second tracking intervals exhibiting values exceeding three levels of scintillation indexes (top) and traverse-angle scintillation (bottom). It provides a summary of the probabilities of occurrence for scintillation as observed by Evans. His index S is defined by the equation:

$$S^2 = \frac{\langle A^4 \rangle - \langle A^2 \rangle^2}{\langle A^2 \rangle^2} \quad (1)$$

This index does not translate easily into that used in this and other studies. However, values of $S < .4$ are relatively insignificant. In the above equation the symbols $\langle\ \rangle$ denote the ensemble average.

SCINTILLATION INDEX PROBABILITIES

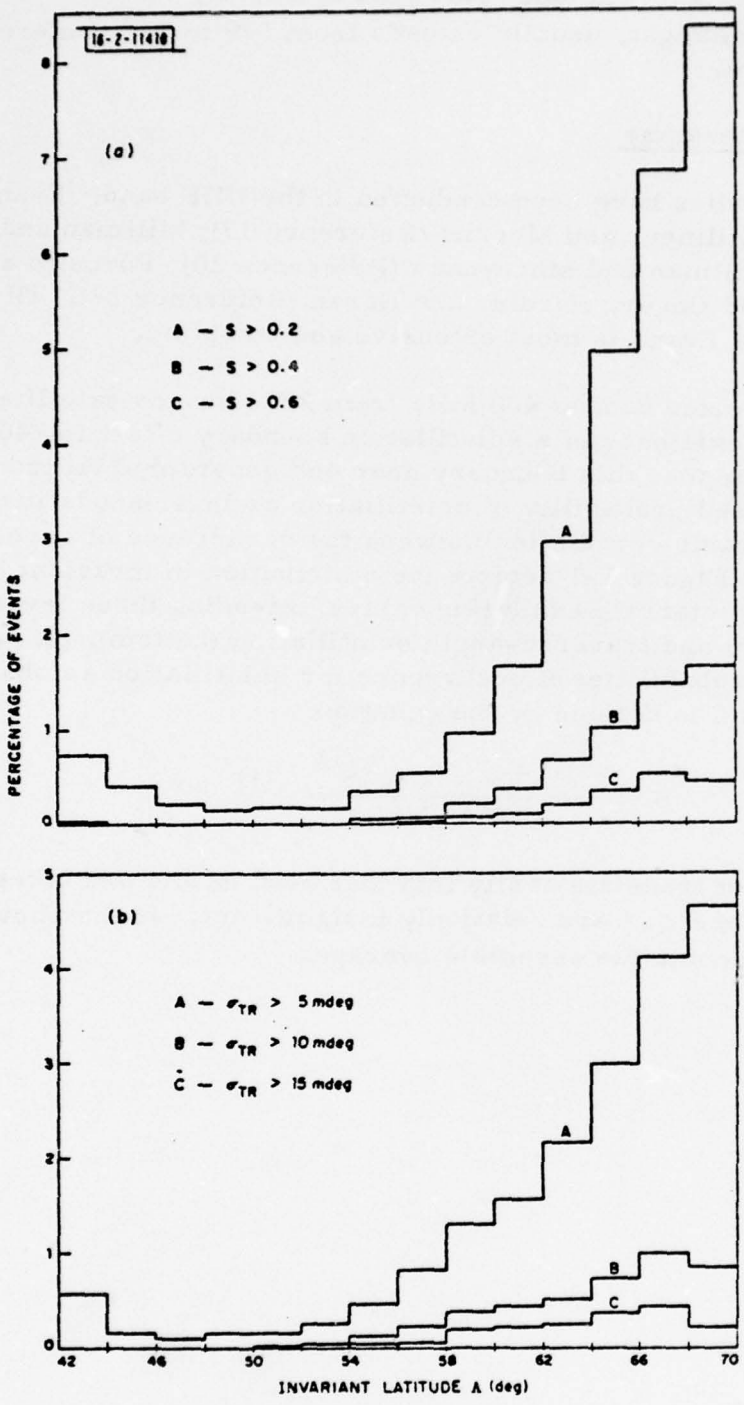

Figure 1-1

2. THE EXPERIMENT AND ANALYSIS TECHNIQUES

The satellite track data was collected with the SAFEGUARD PAR as a part of the larger Auroral data gathering mission. The PAR, located near Cavalier, North Dakota, is a pulse-compression (chirp) radar, transmitting a circularly polarized wave from a phase-steered, phased-array antenna and operating in the UHF band near 450 MHz. The PAR has a beam width of less than 1.5^{o}, a range resolution of better than 1.5 km, and range measurement granularity of under 50 feet. High transmit power and low noise levels combine to allow very long range coverage (well over 2000 km) and high sensitivity. The PAR is computer controlled and is equipped with high performance data processing and recording equipment. The selected satellites were acquired and tracked using a special-search-special-track capability. Tracking was done at a data rate of approximately five pulses per second. Satellite track data was gathered simultaneously with auroral backscatter on four separate occasions in 1975 and 1976, September 17-18, September 26-27, March 10-11, and March 26-27. In addition to the tracks in the presence of aurora, several tracks were obtained when the aurora was absent. Over the course of the experiment 39 tracks were made for a total of 10,292 seconds of data. Of these, 17 were spherical satellites and yielded 3,958 seconds of data, and 22 were non-spherical transit satellites yielding a total of 6,334 seconds of data. The quiet track data consisted of eight tracks for a total of 1,175 seconds of data. Of these, two were of non-spherical transit satellites with 251 seconds of data. The objects tracked are tabulated in Table 2-1. All data was recorded on magnetic tape and transferred to M&S Computing in Huntsville for reduction and analysis.

The primary concern of the satellite track study was ionospheric scintillation. The method chosen to study the scintillation effects was to analyze the point-by-point fluctuations. From a sliding window consisting of five consecutive replies, indices of amplitude and angular scintillation are generated using the following equations:

$$SIp = \frac{S_{max} - S_{min}}{S_{max} + S_{min}}, \text{ and} \qquad (2)$$

$$P_{\Theta} = \Theta_{max} - \Theta_{min}, \qquad (3)$$

where S_{max} and S_{min} are the maximum and minimum replies in watts selected from the five points in the window, and Θ_{max} and Θ_{min} are the maximum and minimum angle in degrees of either azimuth or elevation. To emphasize the different mathematical form of the equations, the amplitude index will be referred to as a scintillation index and the angle indices as perturbation indices. Plots of these indices versus elapsed time are then generated and examined for scintillation effects. In addition to the above indices, a composite plot showing curves of azimuth, elevation, range, and raw reply power is generated for each track.

SATELLITE CHARACTERISTICS

OBJECT	TYPE		NUMBER OF TRACKS
0902	Sphere	14 inches diameter	3
1512	Sphere	14 inches diameter	2
1520	Sphere	14 inches diameter	1
2754	Transit		4
2807	Transit		4
2826	Sphere	20 inches diameter	1
2909	Sphere	18 inches diameter	1
2965	Transit		4
3133	Transit		1
4507	Transit		3
4957	Sphere	.26m Aluminum	5
4958	Sphere	.26m Aluminum	3
4963	Transit		2
5398	Sphere	$1m^2$ Optical Area	1
6909	Transit		4

Table 2-1

In generating the angular scintillation plots, baseline removal was necessary and was accomplished using Kalman smoothed trajectory data supplied by the PAR data processing programs. The Kalman smoothed data was used as a linear predictor of the satellite's position. This method proved adequate in the majority of cases. Ground track data was also generated for each satellite and hand-plotted on time-correlated, top-down plots of auroral backscatter to allow comparison of backscatter location and the indices.

For the first two groups of tracks ephemeris data was available and was used to confirm that the proper object was acquired. This was not possible for Groups three and four, and a possibility of error does exist.

3. RESULTS

The available data is summarized in the following tables. Tables 3-1 and 3-2 present the results for satellites tracked in the aurorally active environment, differentiating between spheres and transits, respectively. Table 3-3 presents the data for the quiet non-auroral tracks. Each track is identified by object number, track number, and duration. The tracks are numbered according to arbitrary tape format order, and missing numbers indicate redundant track data. As a measure of amplitude scintillation the third peak of the index is given, rounded to the nearest tenth. For the angle perturbation indices the maximum, rounded to the nearest tenth of a degree, is given. To provide a rough measure of the relative magnetic activity, the mean number of auroral backscatter replies per scan (29 seconds) is also given.

As can be readily seen from Table 3-1, the transit satellites provide uniformly high indices. This is due to the natural variations in their cross section as their aspect angle varies. Some of these are probably further perturbed by ionospheric scintillations; however, separation of the aspect and ionospheric effects is not possible with the amount of data available. For this reason the transit satellites will not be considered in the following discussion.

Of the spheres only one satellite track, 2/25, from Groups one and two shows strong and distinct scintillation. Track 2/37 shows a deep fade which may be due to ionospheric irregularities. All of the spheres from Group four show very high scintillation. As mentioned in Section 2, we are unfortunately unable to confirm that the correct object was tracked.

Composite plots for the bulk of the satellites are included in the Appendix. Those of special interest will be included elsewhere.

TRACK SUMMARY FOR SPHERICAL SATELLITES IN AN AURORAL ENVIRONMENT

			Rounded Off to Nearest .1			
Track No.	Object	Time In Track Sec.	Third Maximum SI_P	Maximum PI_{AZ}	Maximum PI_{EL}	Mean # Auroral Replies
1/02	2826-SS	406	.4	.2	.1	5974
1/04	0902-SS	354	.5	.7	.8	6527
1/12	0902-SS	153	.7	.6	.4	5740
1/24	4957-SS	232	.2	.2	.1	117
1/32	4963-SS	282	.3	.5	.2	793
1/40	4958-SS	190	.3	.2	.1	973
1/44	4957-SS	117	.3	.3	.2	2230
1/48	5398-SS	292	.4	.1	.1	3721
1/60	1512-SS	220	.4	.5	.3	4573
1/64	1520-SS	220	.5	.5	.5	5531
2/14	4963-SS	225	.3	.2	.1	1066
2/18	4957-SS	277	.3	.4	.3	6611
2/25	0902-SS	220	.9	.5	.4	6178
2/37	1512-SS	327	.5	.4	.3	6510
2/40	4958-SS	153	.3	.8	.3	8898
4/06	4957-SS	241	.6	.4	.3	8950
4/10	4958-SS	339	1.0	1.0	1.4	16318
4/14	4957-SS	195	1.0	1.6	1.6	34545
4/26	2909-SS	303	1.0	1.2	1.5	33831

Table 3-1

TRACK SUMMARY FOR TRANSIT SATELLITES IN AN AURORAL ENVIRONMENT

			Rounded Off to Nearest .1			
Track No.	Object	Time In Track Sec.	Third Maximum SI_P	Maximum PI_{AZ}	Maximum PI_{EL}	Mean # Auroral Replies
1/08	3133-TP	327	1.0	.4	.7	10673
1/16	6909-TP	284	.9	.3	.3	1407
1/20	2807-TP	323	.9	.7	1.0	240
1/28	2965-TP	348	.7	.3	.3	363
1/36	2807-TP	251	1.0	.5	.9	1167
1/52	2965-TP	174	.5	.4	.3	3568
1/56	2754-TP	344	1.0	.5	.5	6988
1/68	2754-TP	205	.9	.9	.8	4443
1/72	4507-TP	354	.9	.6	.2	280
2/02	6909-TP	333	.7	.3	.2	12736
2/06	2807-TP	349	1.0	.9	.7	16684
2/10	6909-TP	210	.7	.4	.3	3636
2/22	2754-TP	292	.6	.3	.9	10450
2/29	2754-TP	297	.7	.2	.2	17000
2/33	2965-TP	349	.6	.2	.1	3235
2/43	4507-TP	221	.9	1.5	1.2	20313
3/02	2807-TP	330	.9	1.6	1.0	17955
4/02	6909-TP	231	1.0	1.4	1.0	8147
4/18	2965-TP	200	1.0	1.9	1.0	46943
4/30	4507-TP	124	1.0	.7	.6	65106

Table 3-2

TRACK SUMMARY FOR SATELLITES IN A NON-AURORAL (QUIET) ENVIRONMENT

			Rounded Off to Nearest .1		
Track No.	Object	Elapsed Time Sec.	Third Maximum SI_P	Maximum PIAZ	Maximum PI_{EL}
Q/01	2907-SS	154	.4	.2	.1
Q/06	2907-SS	154	.5	.3	.2
Q/08	2909-SS	154	.5	.3	.2
Q/10	4957-SS	154	.3	.2	.2
Q/13	4957-SS	154	.4	.2	.2
Q/20	2909-SS	154	.5	.5	.4
Q/23	6909-TP	154	1.0	.8	.6
Q/25	6909-TP	97	1.0	.07	.2

Table 3-3

4. DISCUSSION

As can be seen from Figures 4-1, 4-2, 4-3, and 4-4, track 2/25 displays the type of scintillation characterized by rapid amplitude fluctuations. Since scintillation decreases while the elevation is decreasing and the range is increasing, we can be fairly certain that this is not due to standard atmospheric effects or due to reduced signal level. This track provides a very clear example of ionospheric scintillation of its type.

Possible spatial correlation with auroral backscattering regions is shown by a top-down (see PAR Auroral Study, Volume I) plot in Figure 4-5 which shows auroral backscatter replies and ground tracks of the intercept between the target to radar line-of-sight and constant altitude shells. The altitudes shown are 80 km, 150 km, and 300 km. The auroral backscatter which lies on the radar line-of-sight is bounded by the first two curves. The third, at 300 km, corresponds to the most probable altitude for the scintillation irregularities. As can be seen, there is no obvious direct correlation between the occurrence of scintillation at the beginning of the track and the location of the auroral backscatter. However, the small burst of scintillation occurring near the middle of the track does have a corresponding backscatter reply. For this reason, we feel that there may be two sets of irregularities influencing the scintillation. This is probably analogous to the case of sporadic-E scintillation. However, in the presence of auroral backscatter, E-region irregularities would be the rule rather than the exception and scintillation would be much more common. Ground tracks plotted against auroral backscatter for the remaining spheres showed that none of them were tracked through the E-region auroral irregularity structure with only tracks 1/04, 2/18, and 2/37 allowing for F-region intersection above the auroral backscatter region. Tracks 1/04 (Figures 4-6, 4-7, 4-8, and 4-9) and 2/18 (Figures 4-10, 4-11, 4-12, and 4-13) show a gradual increase in scintillation as their 300 km intercept crosses the auroral backscatter region. This could conceivably be due to normal decrease in elevation but is more likely due to enhanced electron densities above the aurora. Track 2/37 (Figures 4-14, 4-15, 4-16, 4-17, and 4-18) shows a more dramatic deep fade effect.

The fourth group of tracks cannot be so easily handled. Due to the lack of ephemeris data it is not possible to verify satellite I. D. 's. This being the case, the observed effects might be attributed to acquiring the wrong objects in track. A comparison of tracks 4/06 (Figure 4-19) and 3/02 (Figure 4-20) shows similar behavior and gives rise to the suspicion that 4/06 may actually be a transit track. From Figure 4-18, which shows a plot of the radar line-of-sight for track 2/37, it is apparent that the E-region auroral backscatter was not intercepted by the line-of-sight between the radar and satellite. There is some correlation, however, between the observed fade and the 300 km intercept curve. The fade could be caused by an irregularity structure above the backscatter regions. This fade is an indication that the fourth group of tracks may indeed be spherical satellites. If spherical, there is no doubt that they are severely perturbed.

TRAJECTORY COMPOSITE 2/25

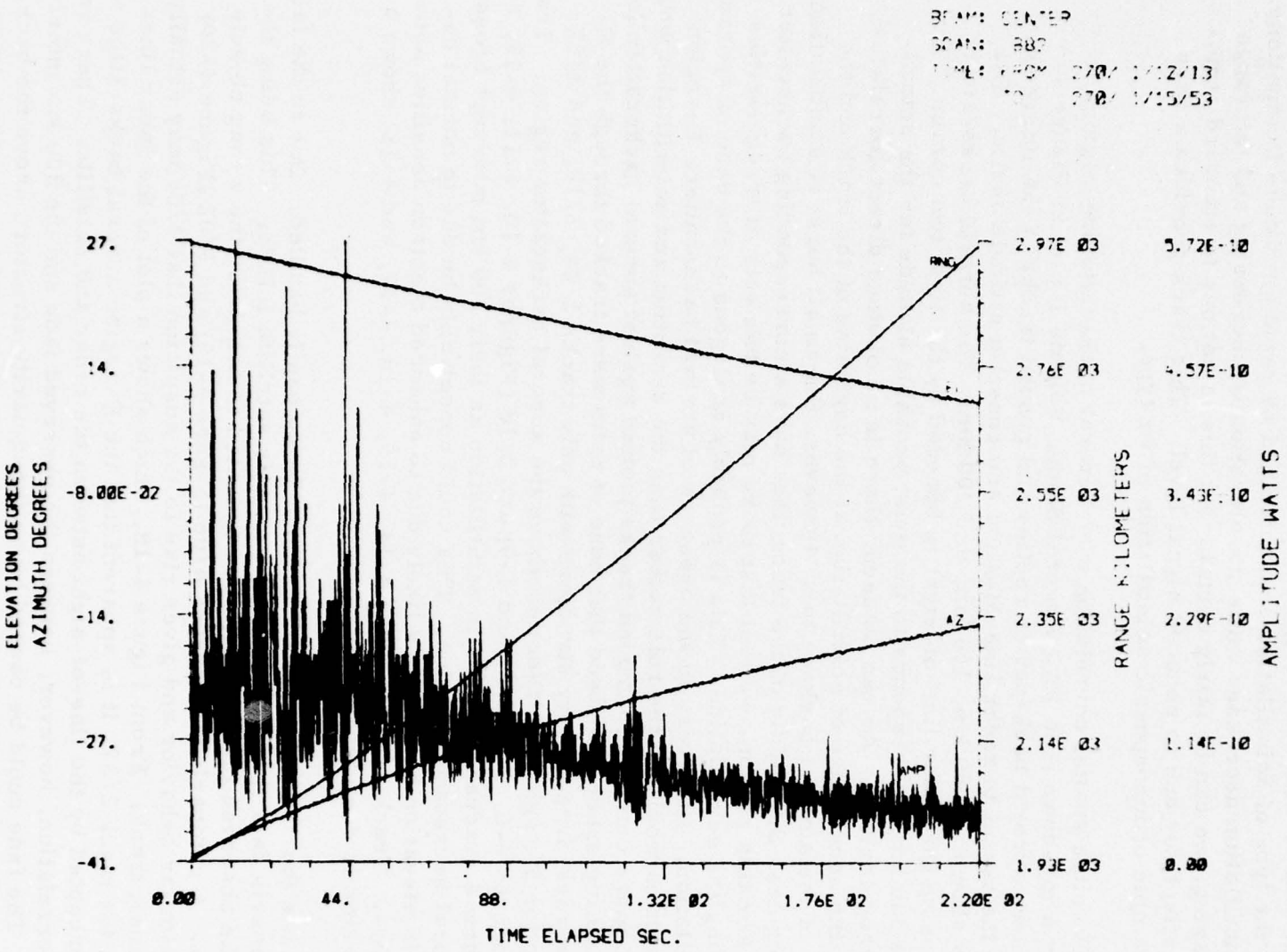

Figure 4-1

AMPLITUDE SCINTILLATION 2/25

BEAM: CENTER
SCAN: 882
TIME: FROM 270/ 1/12/13
TO 270/ 1/15/53

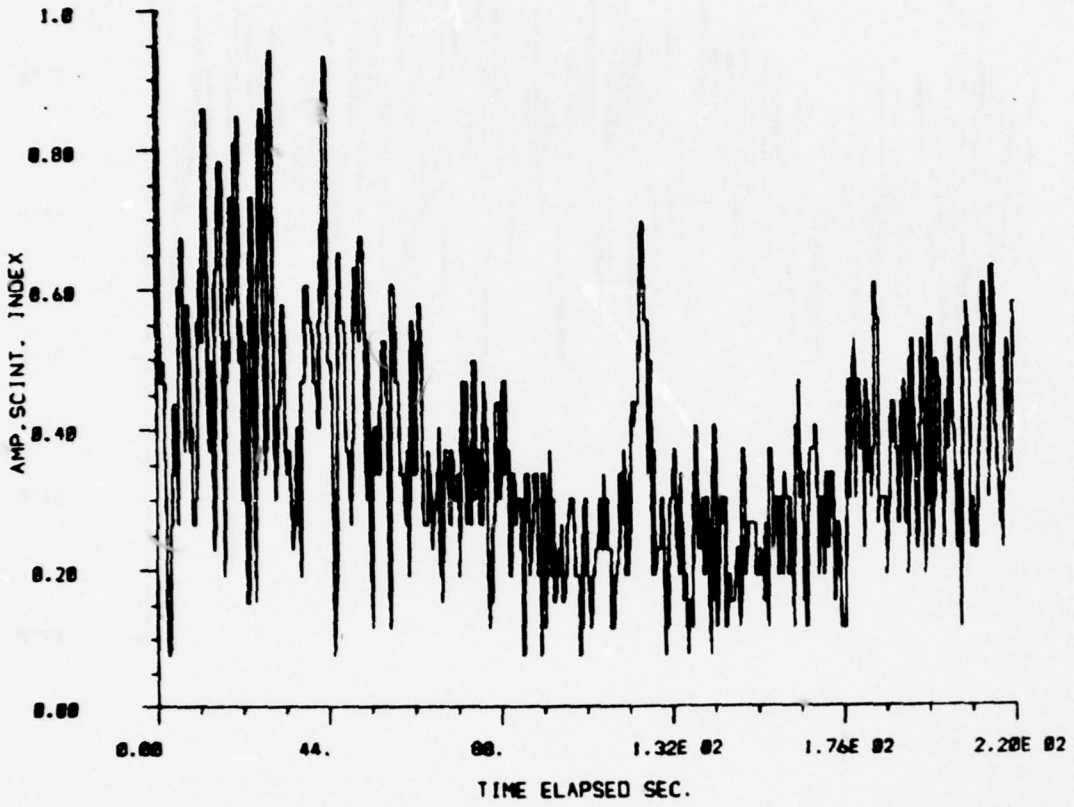

Figure 4-2

AZIMUTH PERTURBATION 2/25

BEAM: CENTER
SCAN: 882
TIME: FROM 2787 1/12/13
TO 2787 1/15/53

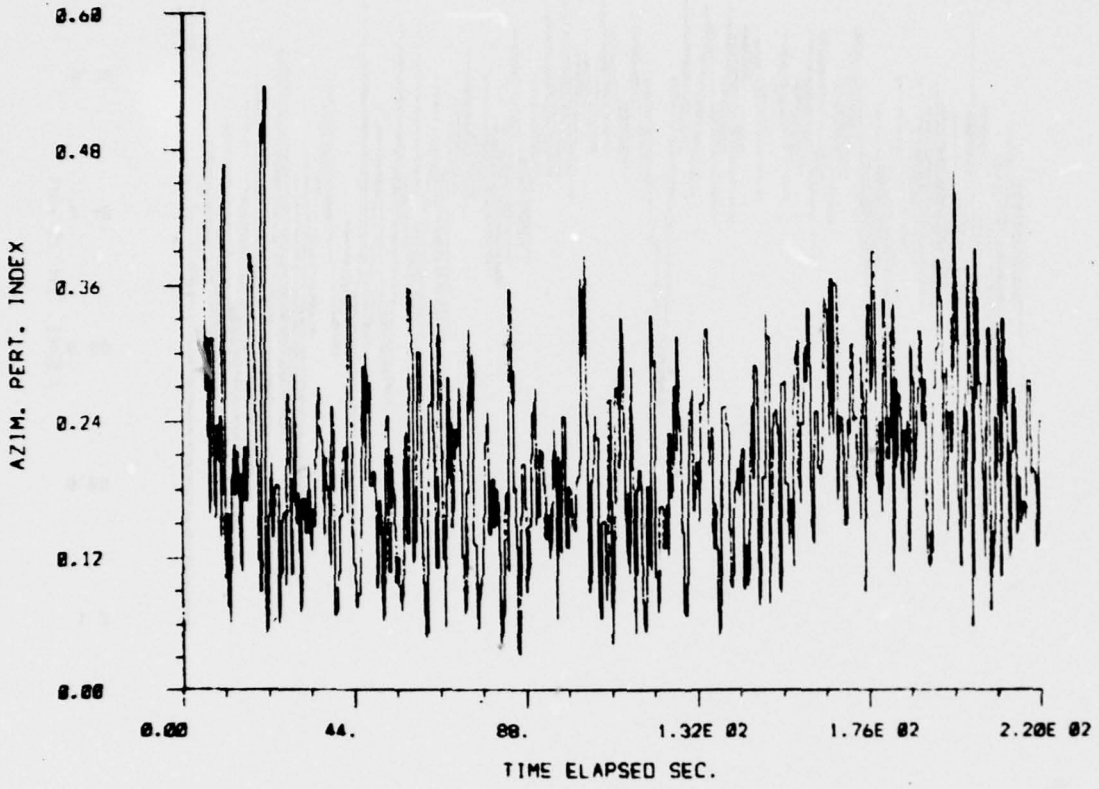

TRACK # 2/25 SAT ID 0902 - SS PRC = SIPT05

Figure 4-3

ELEVATION PERTURBATION 2/25

BEAM: CENTER
SCAN: 882
TIME: FROM 270/ 1/12/13
TO 270/ 1/15/53

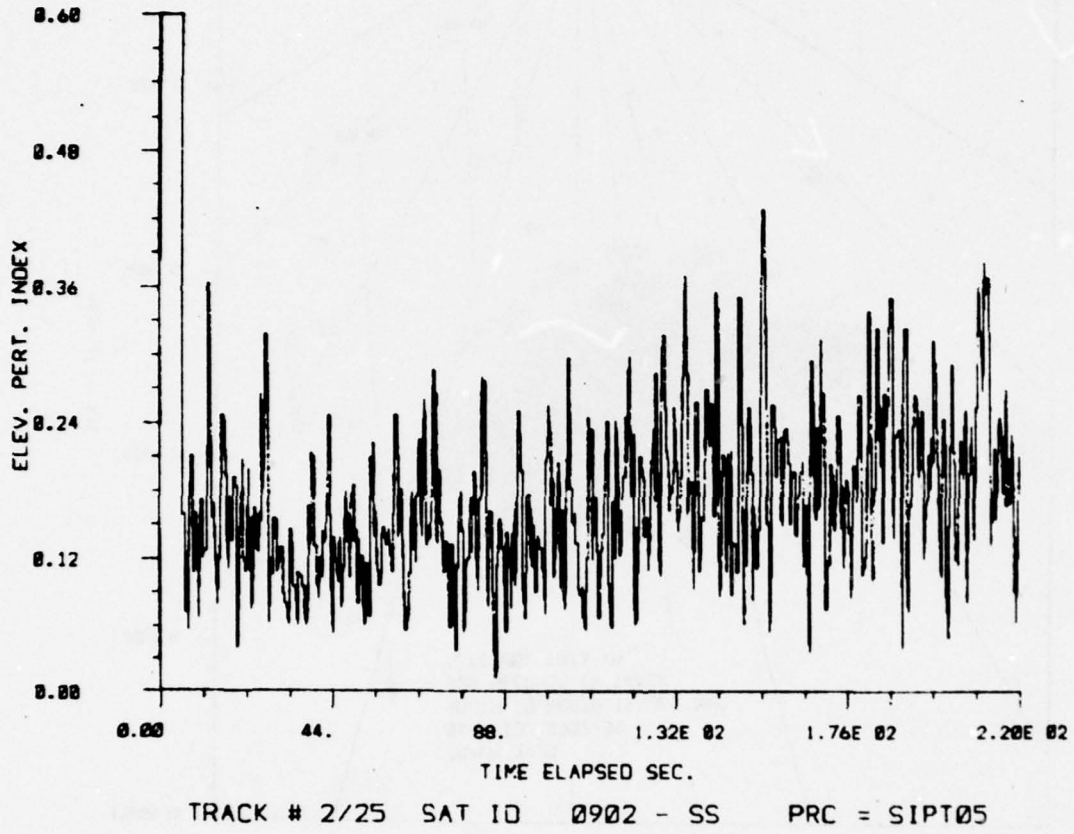

TRACK # 2/25 SAT ID 0902 - SS PRC = SIPT05

Figure 4-4

AURORAL BACKSCATTER WITH GROUND TRACKS 2/25

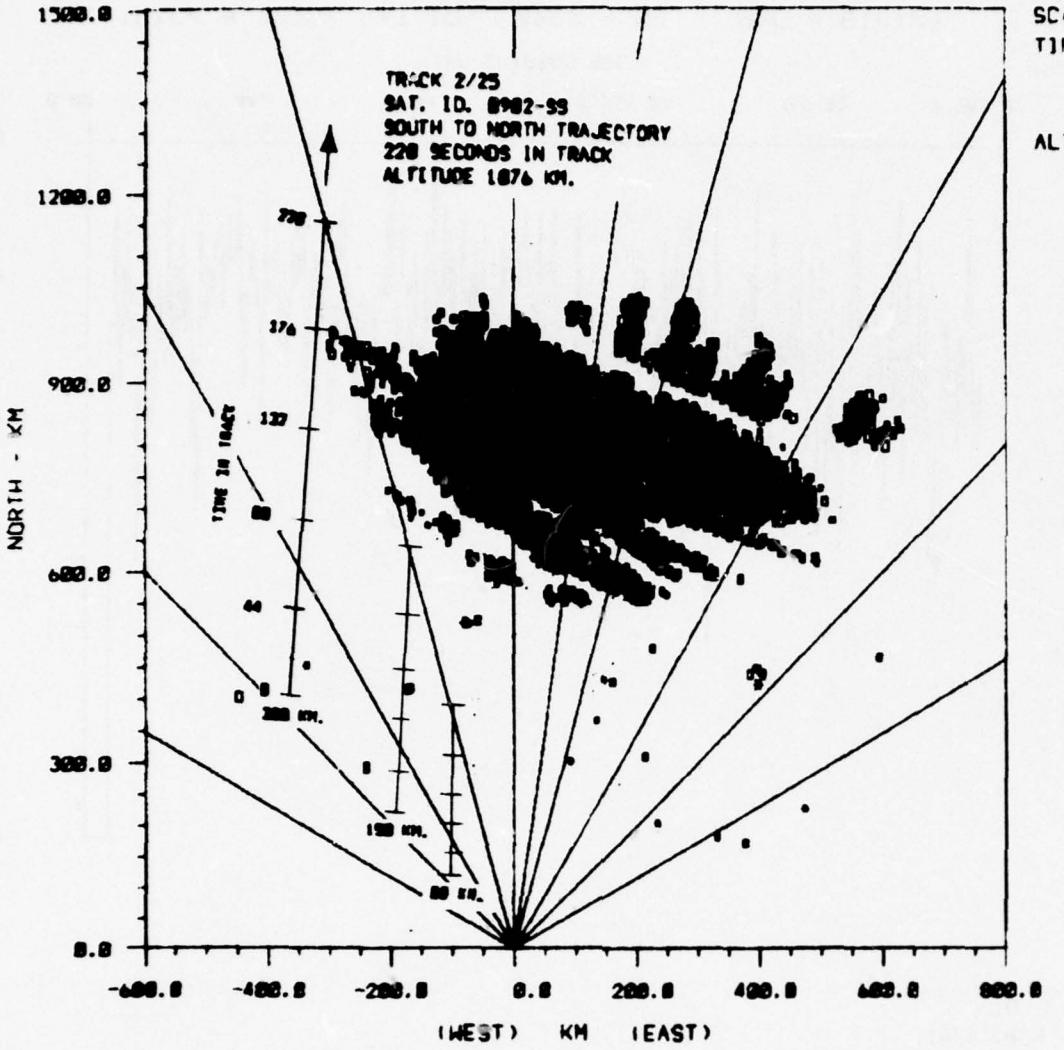

BEAM: BOTH
SCAN: 882
TIME: FROM 270/ 1/12/16
TO 270/ 1/12/36

ALT (KM): 70.0 TO 170.0

ALTITUDES				DN LEVEL
70.0	TO	80.0	KM	5
80.0	TO	90.0	KM	6
90.0	TO	100.0	KM	7
100.0	TO	110.0	KM	8
110.0	TO	120.0	KM	9
120.0	TO	130.0	KM	10
130.0	TO	140.0	KM	11
140.0	TO	150.0	KM	12
150.0	TO	160.0	KM	13
160.0	TO	170.0	KM	14

TOP DOWN VIEW SHOWING AURORAL REFLECTIVITY

Figure 4-5

TRAJECTORY COMPOSITE 1/04

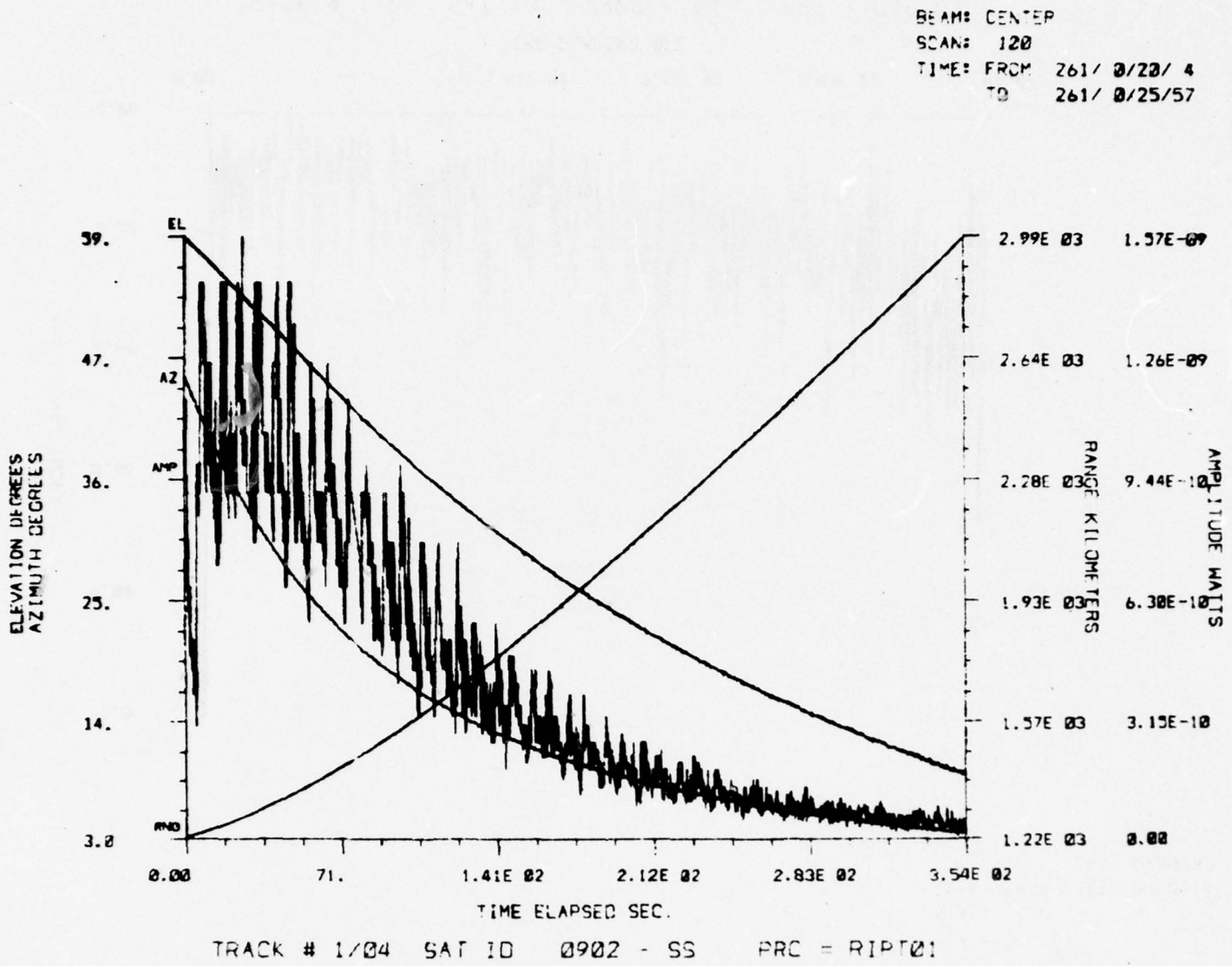

Figure 4-6

AMPLITUDE SCINTILLATION 1/04

BEAM: CENTER
SCAN: 122
TIME: FROM 261 0/20/ 4
TO 261 0/25/57

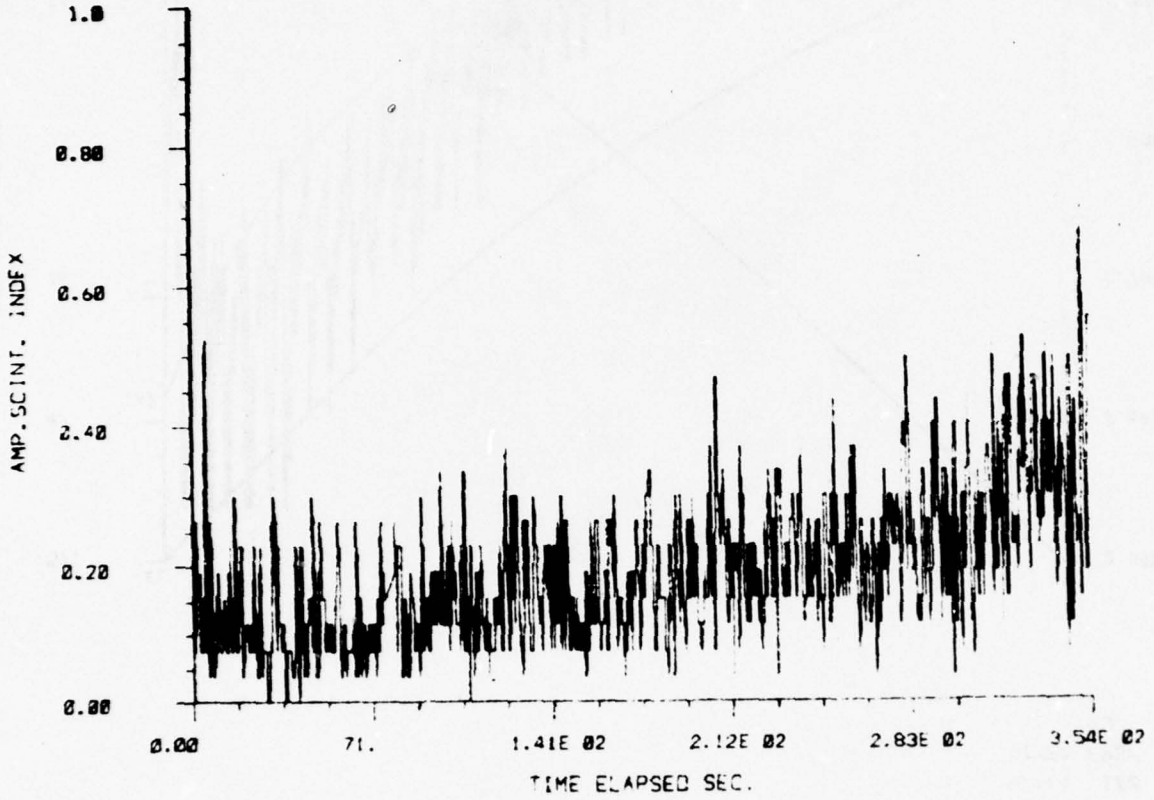

TRACK # 1/04 SAT ID 0902 - SS PRC = RIP 05

Figure 4-7

AZIMUTH PERTURBATION 1/04

BEAM: CENTER
SCAN: 100
TIME: FROM 261/ 0/20/ 4
TO 261/ 0/25/57

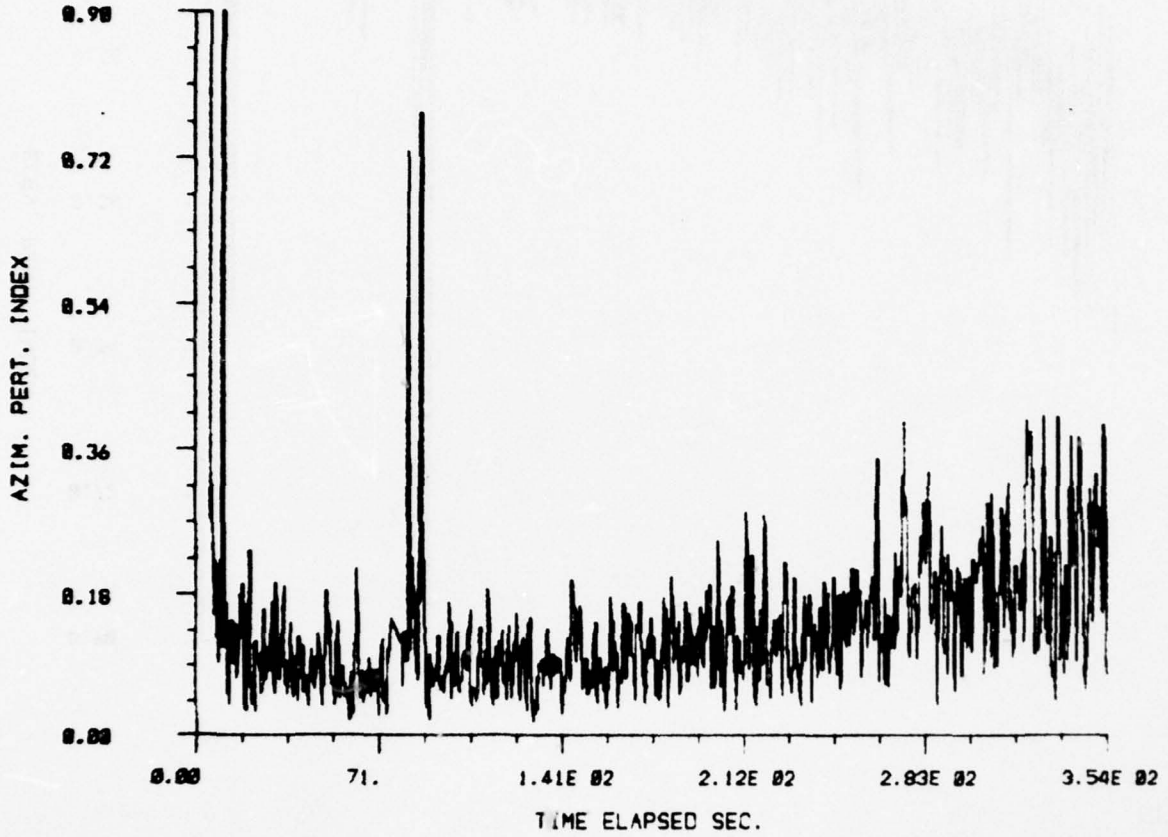

TRACK # 1/04 SAT ID 0902 - SS PRC = RIPT05

Figure 4-8

ELEVATION PERTURBATION 1/04

BEAM: CENTER
SCAN: 100
TIME: FROM 261/ 0/20/ 4
TO 261/ 0/25/57

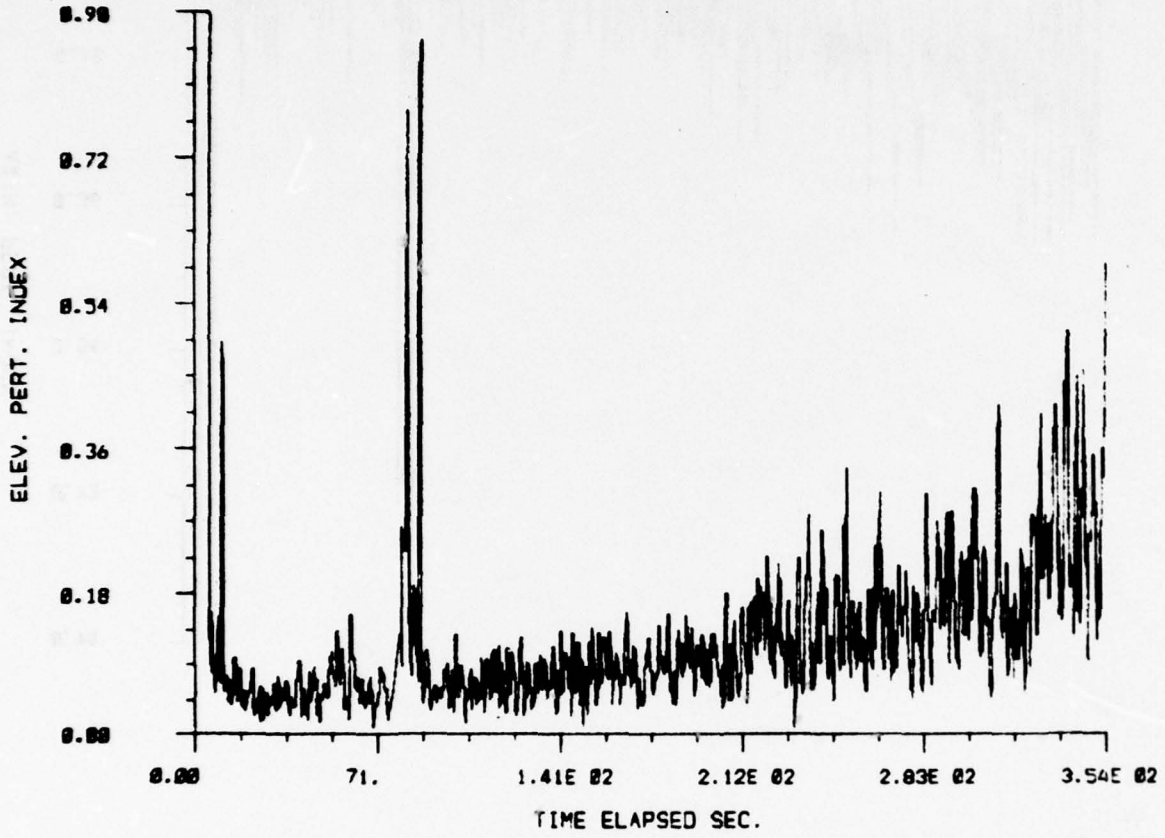

TRACK # 1/04 SAT ID 0902 - SS PRC = RIPT05

Figure 4-9

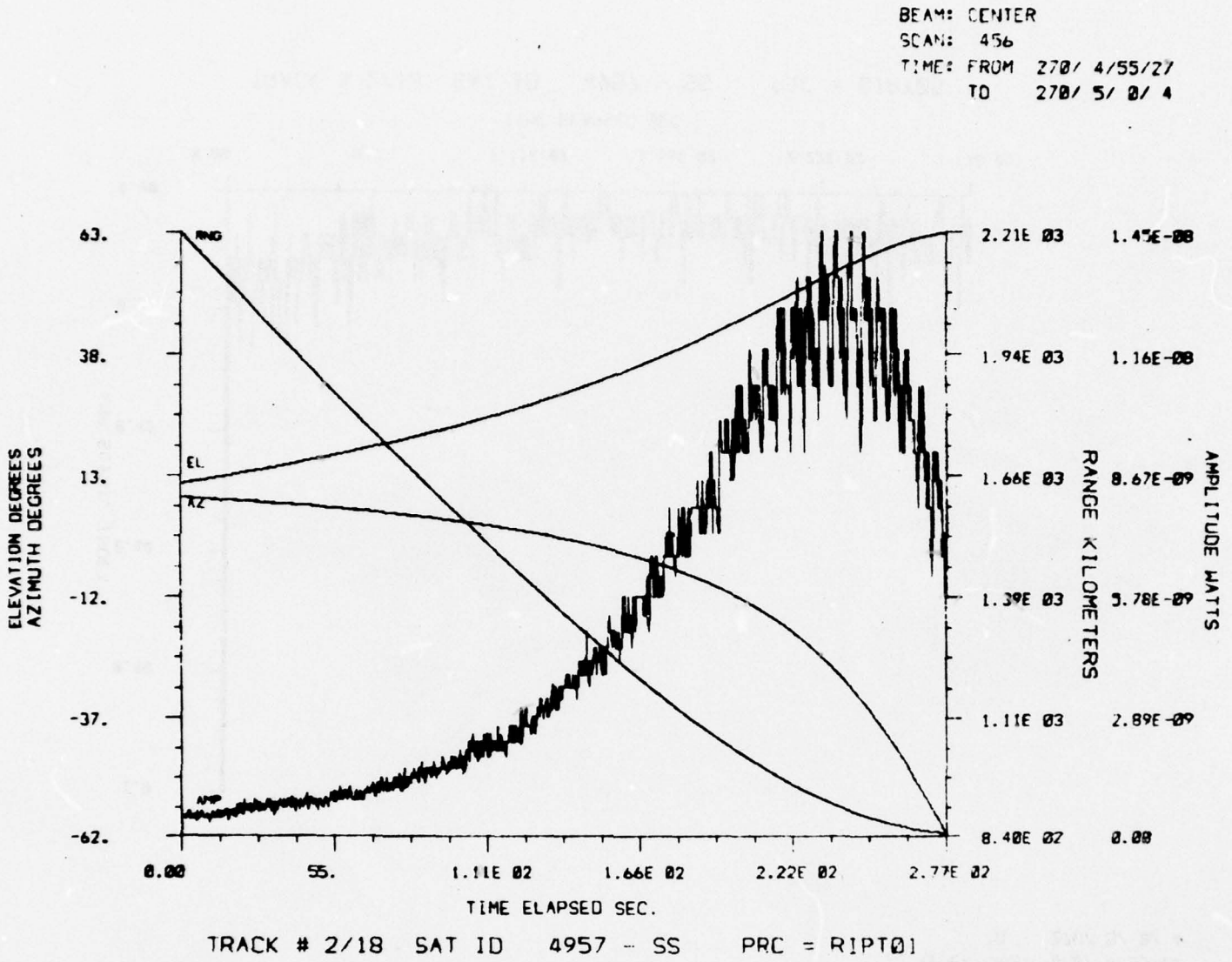
BEAM: CENTER
SCAN: 456
TIME: FROM 270/ 4/55/27
TO 270/ 5/ 0/ 4
63.
38.
13.
-12.
-37.
-62.
RNG
EL
AZ
AMP
2.21E 03
1.94E 03
1.66E 03
1.39E 03
1.11E 03
8.40E 02
1.45E-08
1.16E-08
8.67E-09
5.78E-09
2.89E-09
0.00
0.00
55.
1.11E 02
1.66E 02
2.22E 02
2.77E 02
TIME ELAPSED SEC.
ELEVATION DEGREES
AZIMUTH DEGREES
RANGE KILOMETERS
AMPLITUDE WATTS
TRACK # 2/18 SAT ID 4957 - SS PRC = RIPT01

Figure 4-10

AMPLITUDE SCINTILLATION 2/18

BEAM: CENTER
SCAN: 456
TIME: FROM 270/ 4/55/27
TO 270/ 5/ 9/ 4

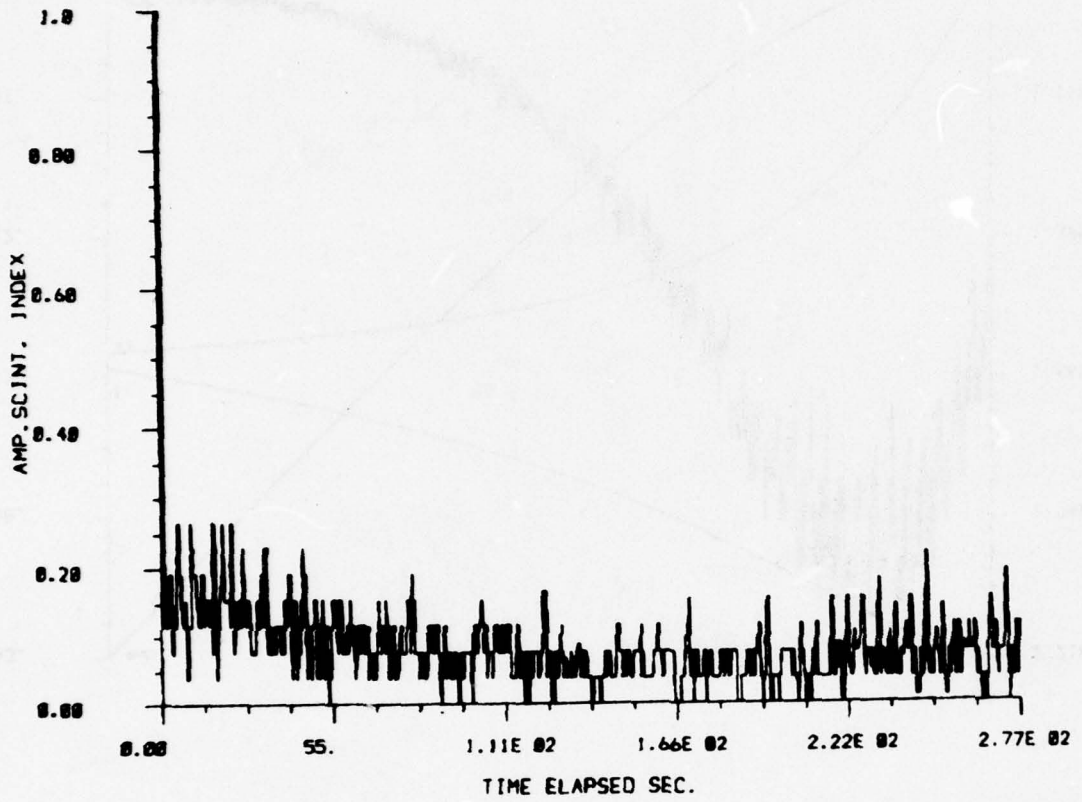

Figure 4-11

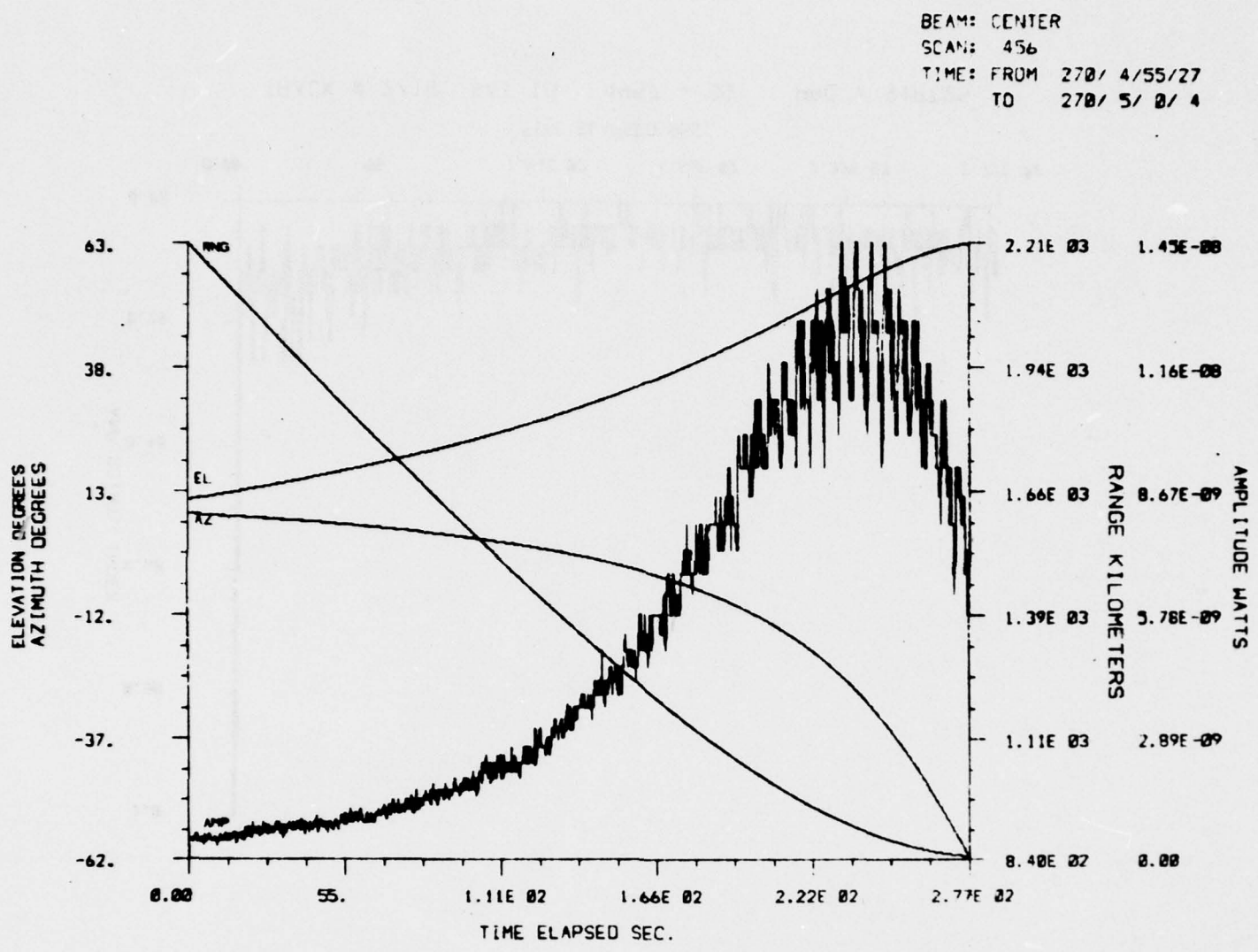
BEAM: CENTER
SCAN: 456
TIME: FROM 270/ 4/55/27
TO 270/ 5/ 0/ 4
63.
38.
13.
-12.
-37.
-62.
RNG
EL
AZ
AMP
ELEVATION DEGREES
AZIMUTH DEGREES
2.21E 03
1.94E 03
1.66E 03
1.39E 03
1.11E 03
8.40E 02
RANGE KILOMETERS
1.45E-08
1.16E-08
8.67E-09
5.78E-09
2.89E-09
0.00
AMPLITUDE WATTS
0.00
55.
1.11E 02
1.66E 02
2.22E 02
2.77E 02
TIME ELAPSED SEC.
TRACK # 2/18 SAT ID 4957 - SS PRC = RIPT01

Figure 4-10

AMPLITUDE SCINTILLATION 2/18

BEAM: CENTER
SCAN: 456
TIME: FROM 270/ 4/55/27
TO 270/ 5/ 0/ 4

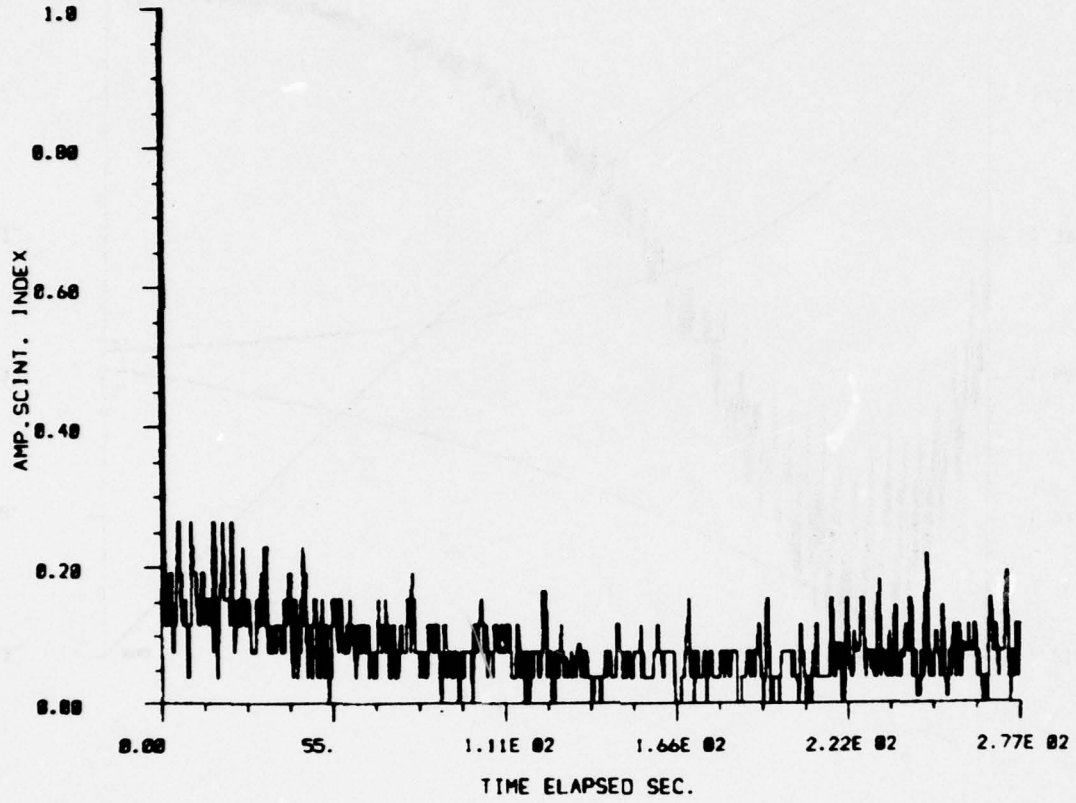

TRACK # 2/18 SAT ID 4957 - SS PRC = SIPT05

Figure 4-11

AZIMUTH PERTURBATION 2/18

BEAM: CENTER
SCAN: 456
TIME: FROM 270/ 4/55/27
TO 270/ 5/ 0/ 4

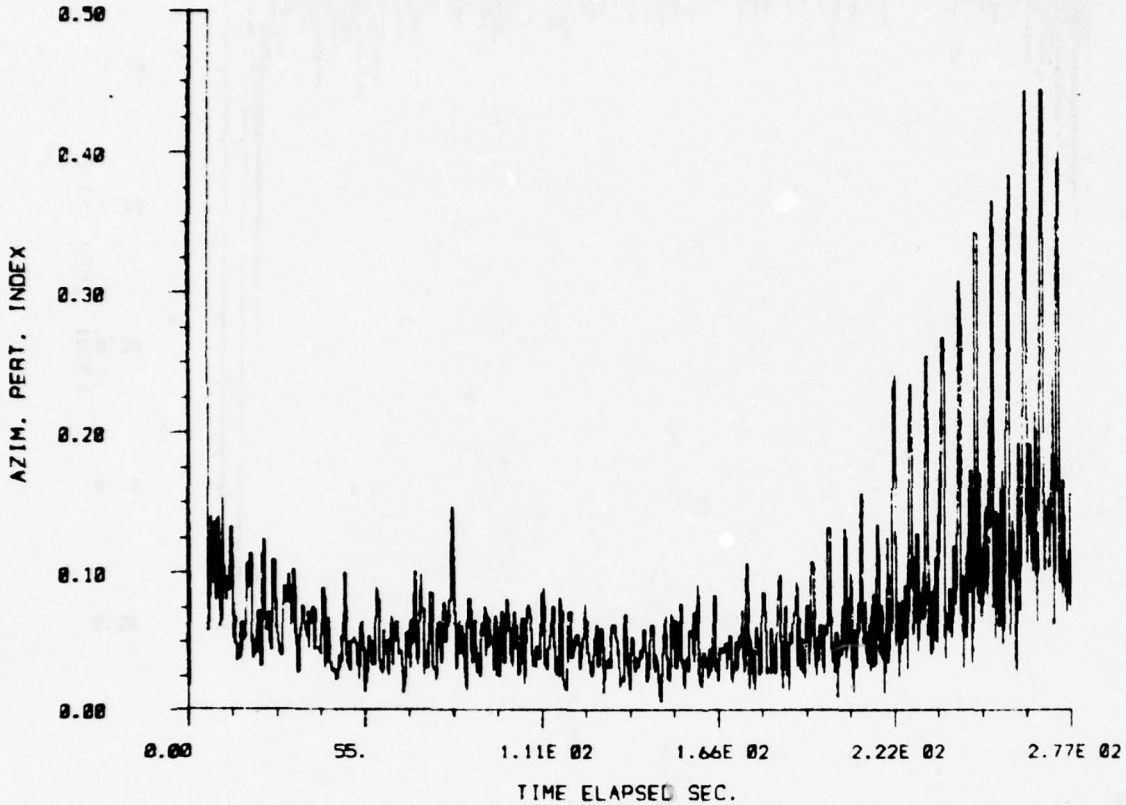

TRACK # 2/18 SAT ID 4957 - SS PRC = SIPT05

Figure 4-12

ELEVATION PERTURBATION 2/18

BEAM: CENTER
SCAN: 456
TIME: FROM 270/ 4/55/27
TO 270/ 5/ 0/ 4

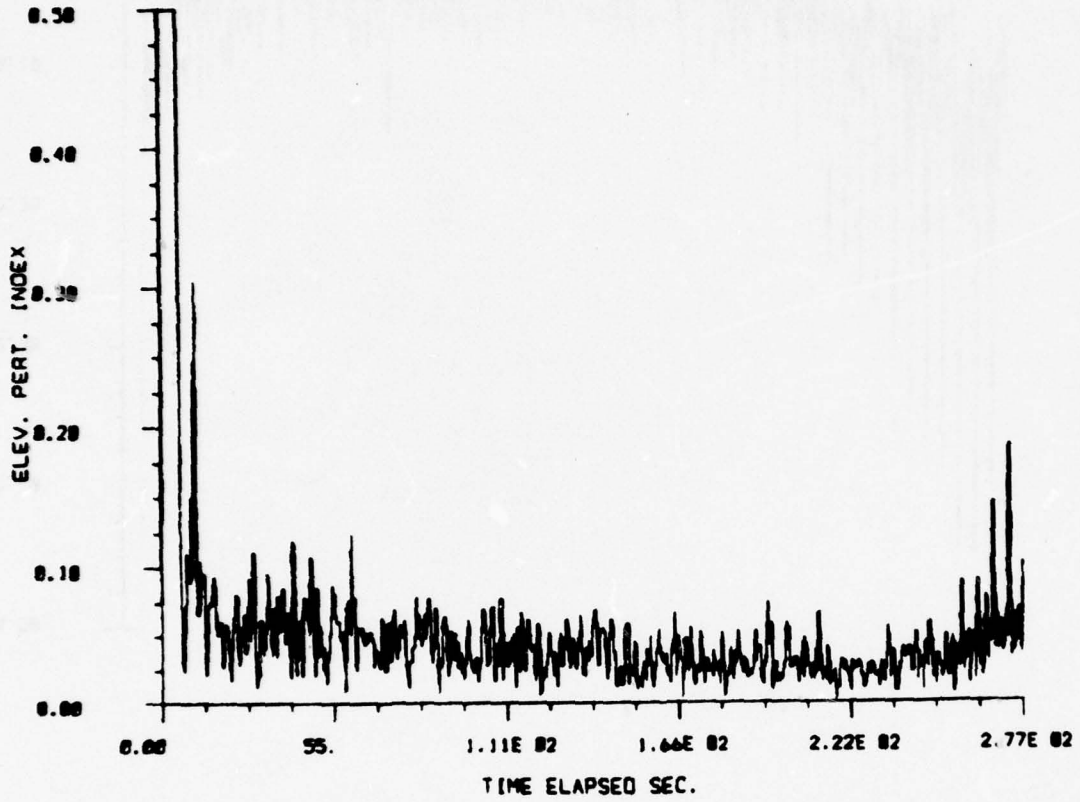

TRACK # 2/18 SAT ID 4957 - SS PRC = SIPT05

Figure 4-13

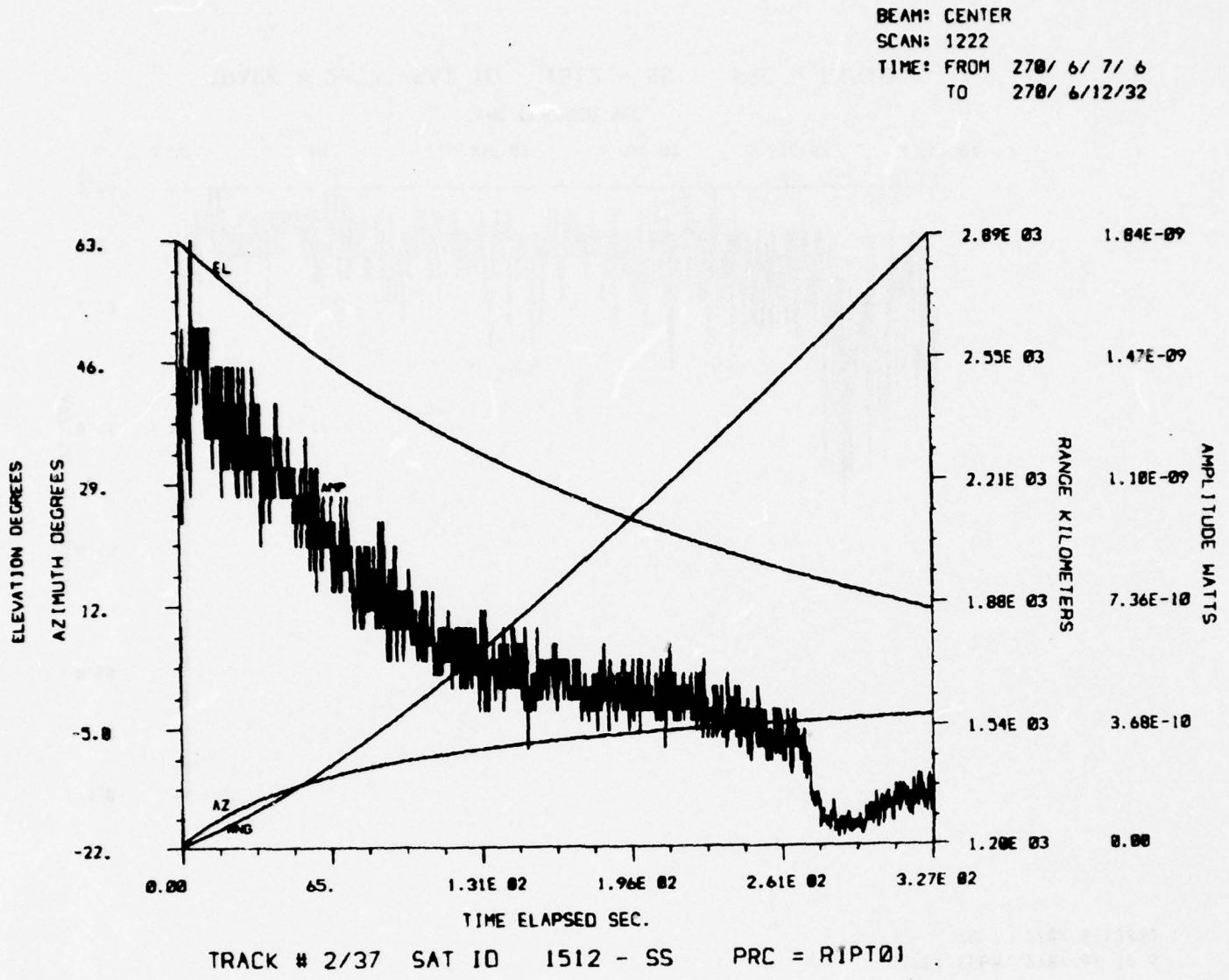
BEAM: CENTER
SCAN: 1222
TIME: FROM 270/ 6/ 7/ 6
TO 270/ 6/12/32
63.
46.
29.
12.
-5.0
-22.
EL
AMP
AZ
RNG
ELEVATION DEGREES
AZIMUTH DEGREES
2.89E 03
2.55E 03
2.21E 03
1.88E 03
1.54E 03
1.20E 03
RANGE KILOMETERS
1.84E-09
1.47E-09
1.10E-09
7.36E-10
3.68E-10
0.00
AMPLITUDE WATTS
0.00
65.
1.31E 02
1.96E 02
2.61E 02
3.27E 02
TIME ELAPSED SEC.
TRACK # 2/37 SAT ID 1512 - SS PRC = RIPT01

Figure 4-14

AMPLITUDE SCINTILLATION 2/37

BEAM: CENTER
SCAN: 1222
TIME: FROM 270/ 6/ 7/ 6
TO 270/ 6/12/32

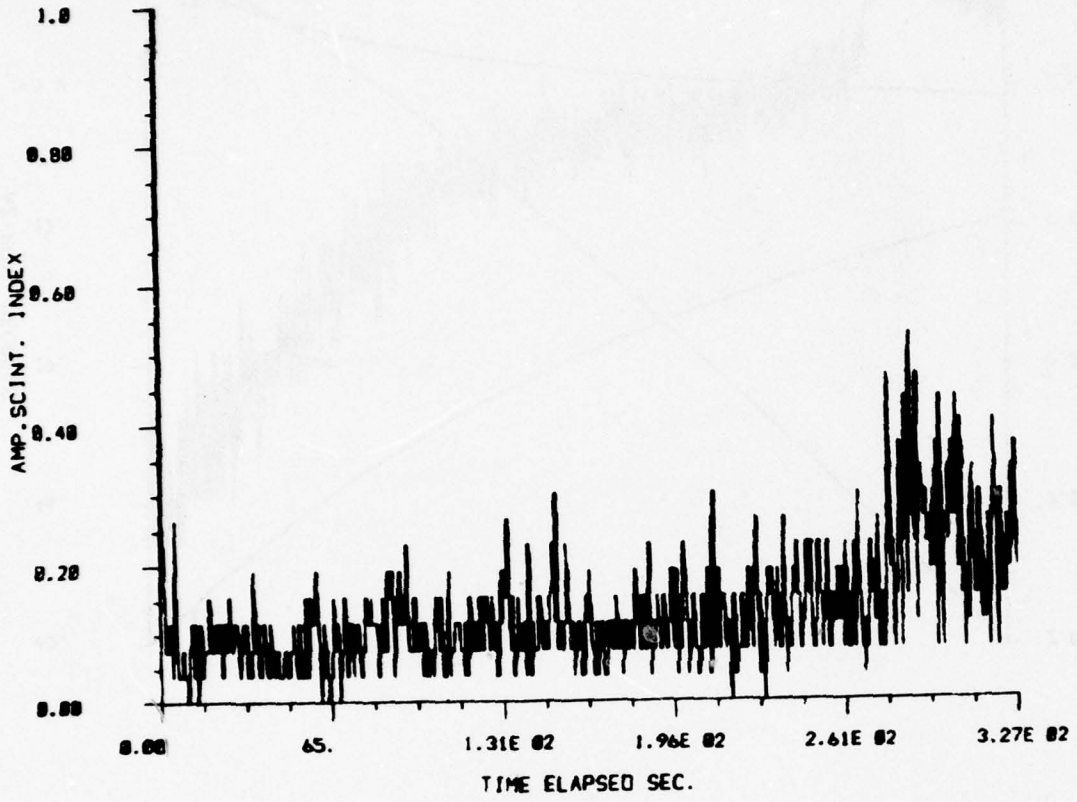

TRACK # 2/37 SAT ID 1512 - SS PRC = RIPT05

Figure 4-15

AZIMUTH PERTURBATION 2/37

BEAM: CENTER
SCAN: 1222
TIME: FROM 270/ 6/ 7/ 6
TO 270/ 6/12/32

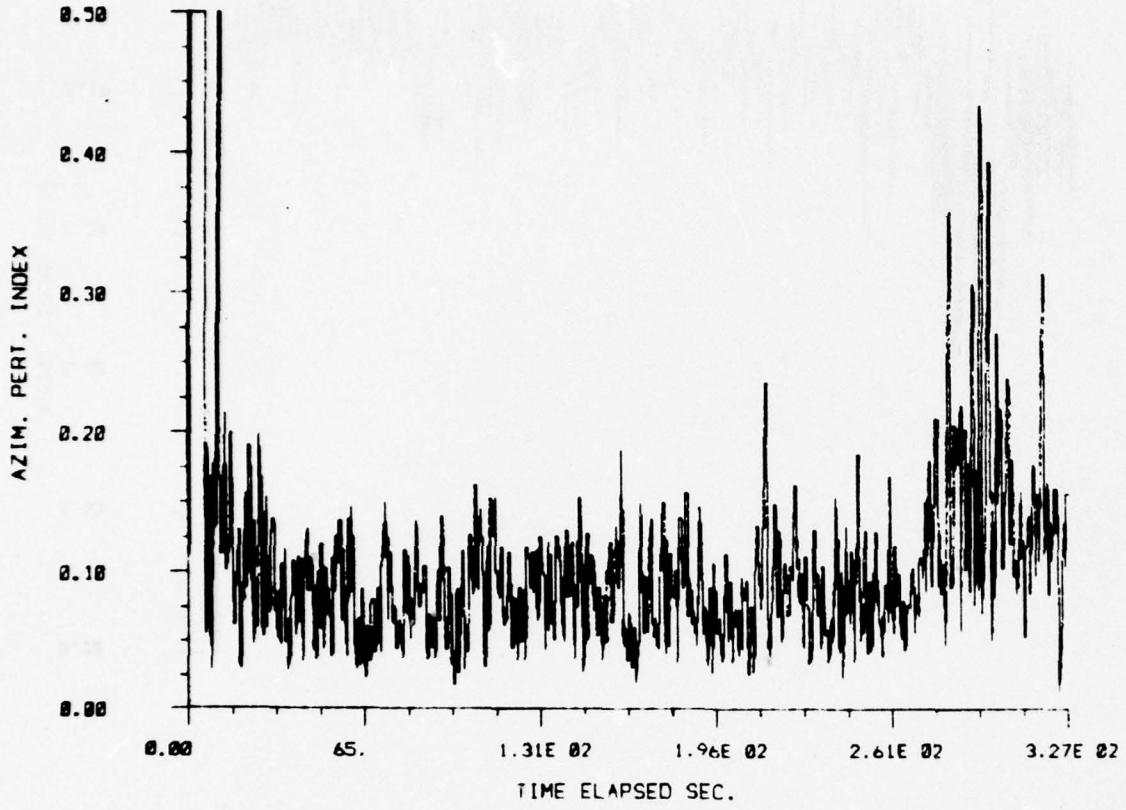

TRACK # 2/37 SAT ID 1512 - SS PRC = RIPT05

Figure 4-16

ELEVATION PERTURBATION 2/37

BEAM: CENTER
SCAN: 1222
TIME: FROM 270/ 6/ 7/ 6
TO 270/ 6/12/32

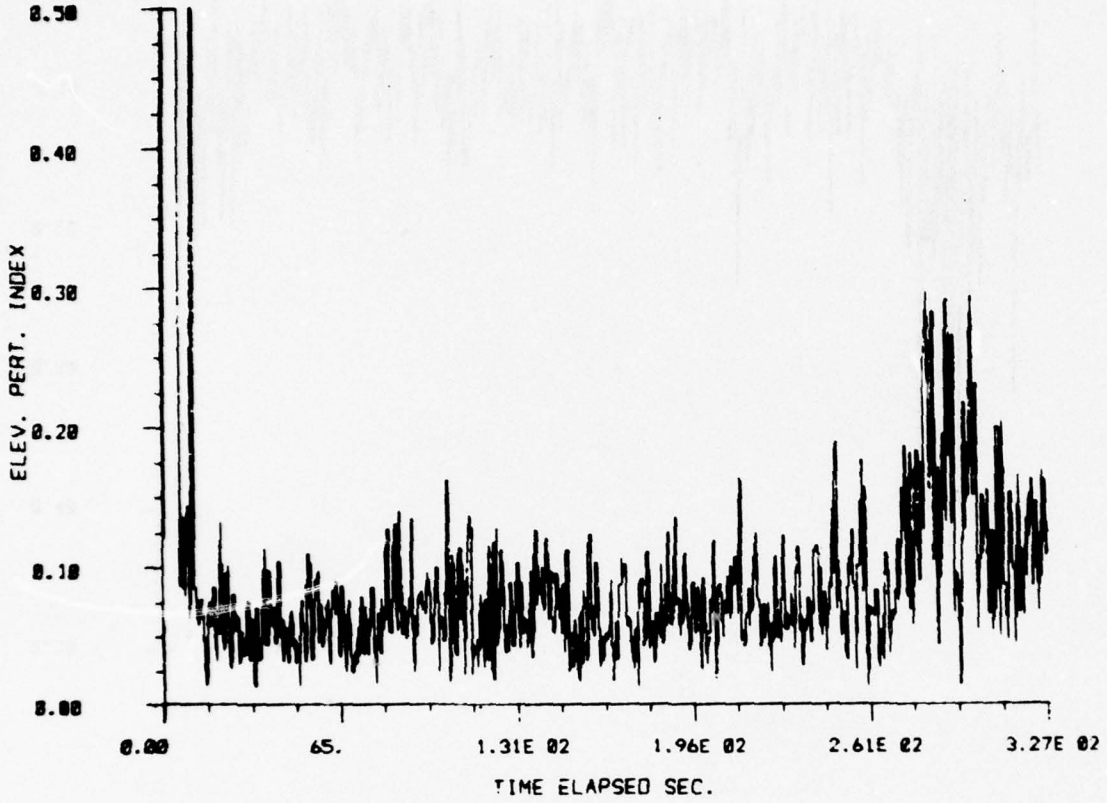

TRACK # 2/37 SAT ID 1512 - SS PRC = RIPT05

Figure 4-17

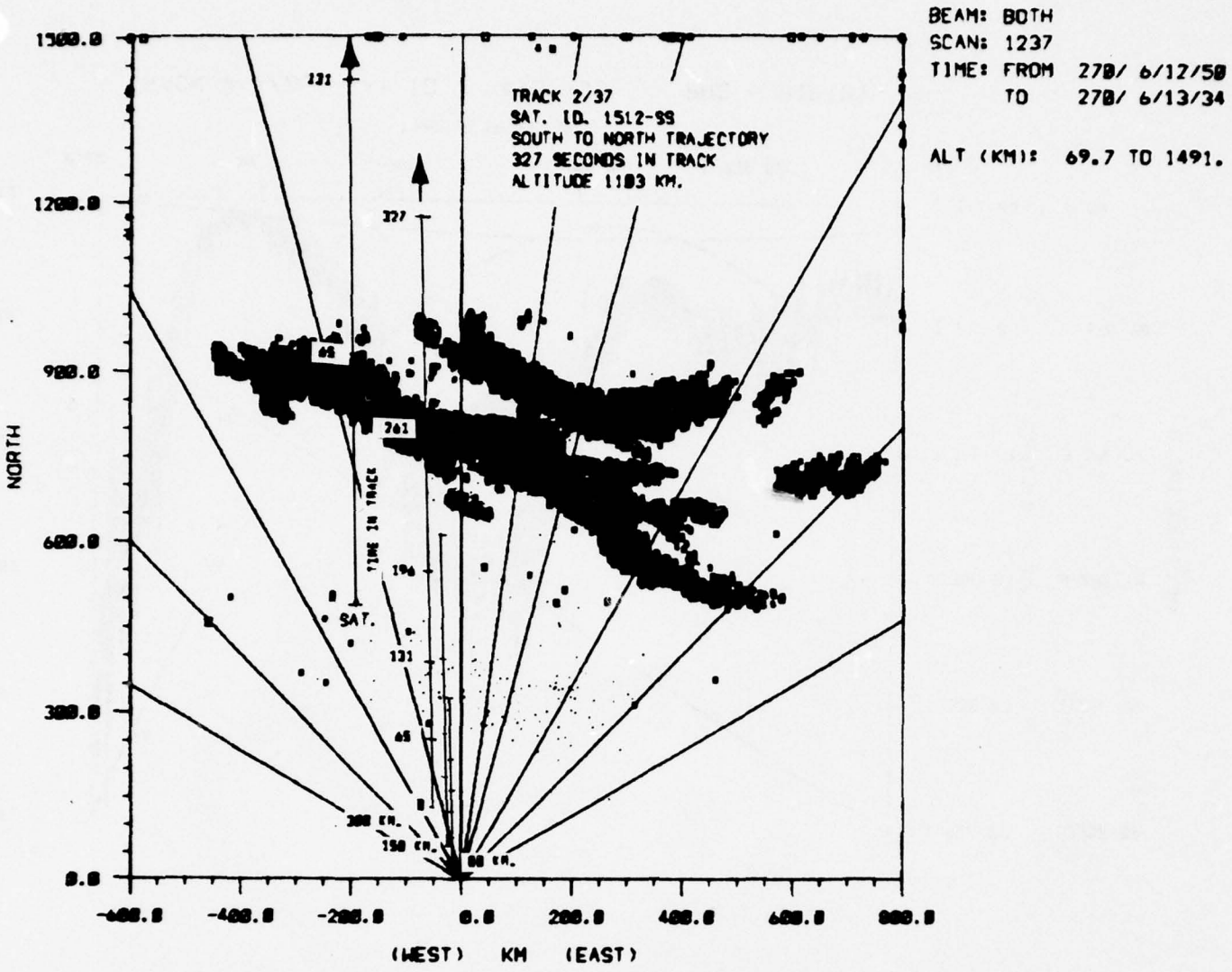

TOP DOWN VIEW OF AURORAL PHENOMENA AT PAR

Figure 4-18

TRAJECTORY COMPOSITE 4/06

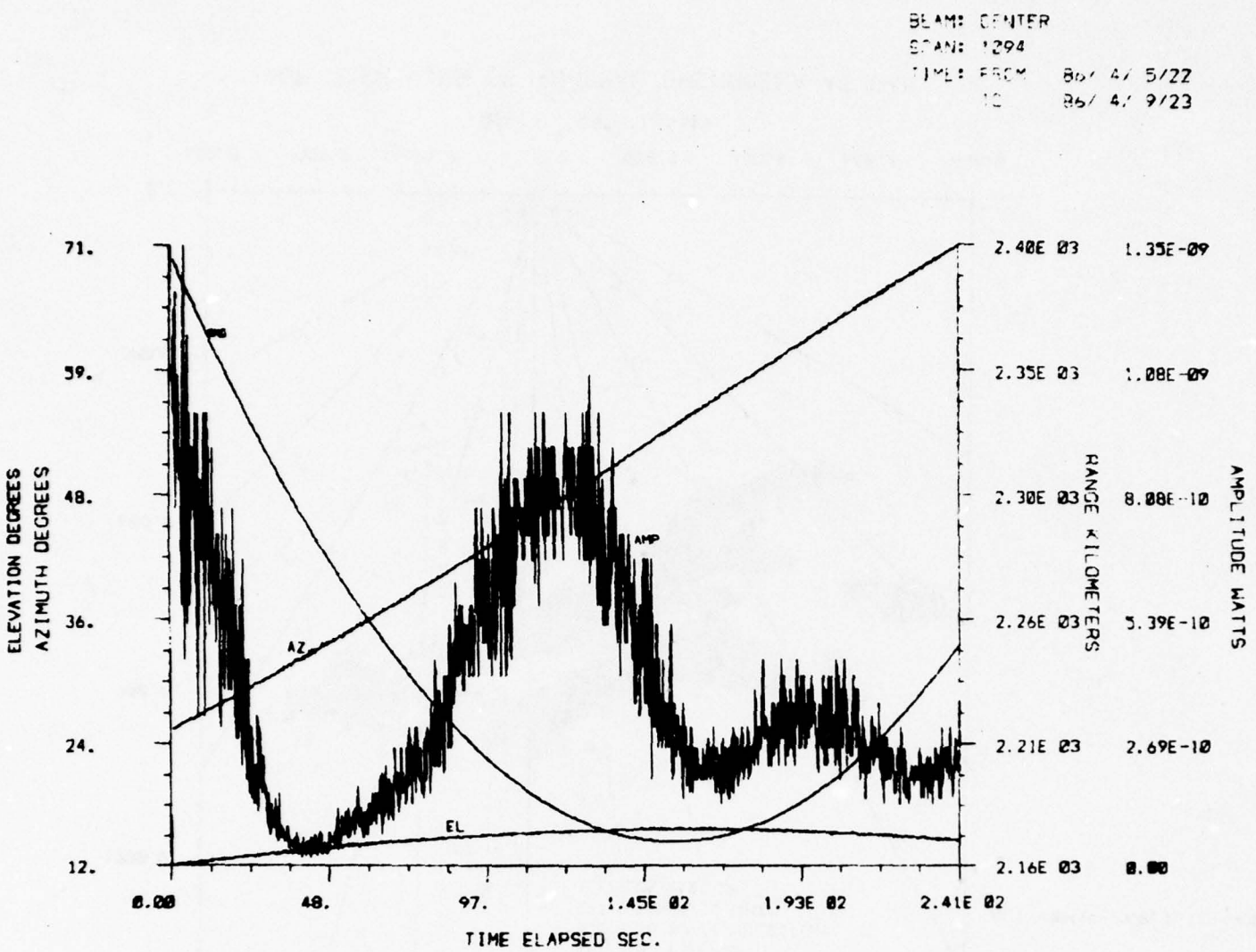

Figure 4-19

BEAM: CENTER
SCAN: 1496
TIME: FROM 70/ 2/21/40
TO 70/ 2/27/10

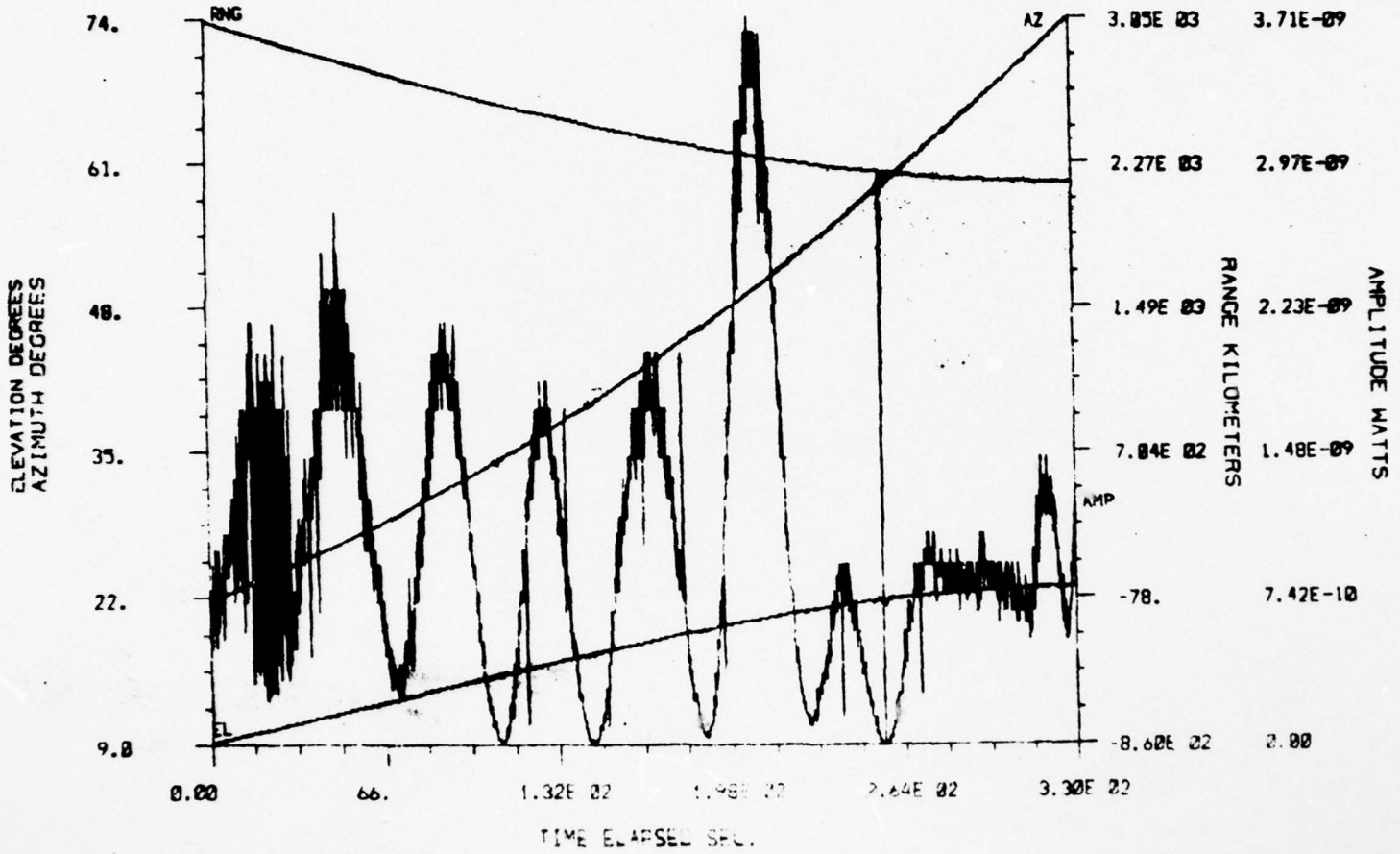

TRACK # 3/02 SAT ID 2827 TP PRC = R1PT01

Figure 4-20

5. CONCLUSIONS

From the results of the experiment we confirm that the PAR can be significantly influenced by scintillations. Furthermore, there appears to be some correlation betweens the auroral backscatter zone and the occurrence of scintillation. In the case of the tracks of Group 4, the scintillation effects were such as to render their signatures unrecognizable. Thus we were unable to confidently determine the identity of the objects tracked. Furthermore, we could not confirm that the PAR tracked the intended satellites. This raises the possibility that during intense auroral events the target discrimination mission of the PAR may be seriously impaired or even rendered useless. The detection of multiple targets in close proximity will certainly be impaired. To determine the extent of the total impact on the PAR mission, further study is required.

Future studies would utilize the multiple-object track capabilities of the PAR to map the extent of the irregularity structures responsible for scintillation. The use of mainly spherical satellites with known ephemeris would allow a measure of the scintillation intensities and their relative probabilities to be obtained. Auroral backscatter data should be taken concurrently to allow investigation of E-region scintillations and establish the degree of correlation between auroral backscatter zones and ionospheric scintillation. In addition, the experiment should include magnetometer and riometer data as well as normal planetary magnetic indices. The experiment should then be of sufficient duration to allow determination of the correlation between probability and intensity of scintillation and the geophysical parameters. With this information the track and discrimination capabilities of the PAR in an aurorally perturbed environment can be determined precisely.

REFERENCES

1. Aarons, J., R. S. Allen, and H. E. Whitney, "Observations of Scintillations of Two Satellite Beacons Near the Boundary of the Irregularity Region," Planet, Space Sci., 1972, Volume 20, pp. 965-972.

2. Aarons, Jules, "High-Latitude Irregularities During the Magnetic Storm of October 31 to November 1, 1972," Journal of Geophysical Research, Volume 81, No. 4, February 1, 1976, pp. 661-670.

3. Aarons, Jules, H. E. Whitney, and R. S. Alley, "Global Morphology of Ionospheric Scintillations." Proceedings of the IEEE, Volume 59, No. 2, February 1971, pp. 159-172.

4. Clark, D. H., "Radio-Satellite Scintillation:" Irregularity Height Variation, and Its Association with Magnetic Activity," Planet, Space Sci., 1971, Volume 19, pp. 1588-1590.

5. Clark, D. H., J. Mawdsley, and W. Ireland, "Mid-Latitude Radio Satellite Scintillation: The Height of the Irregularities," Planet, Space Sci., 1970, Volume 18, pp. 1785-1791.

6. Clark D. H., and W. J. Raitt, "Characteristics of the High-Latitude Ionospheric Irregularity Boundary, as Monitored by the Total Ion Current Probe on ESRO-4, "Planet, Space Sci., Volume 23, 1975, pp. 1643-1647.

7. Dyson, P. L., "Direct Measurements of the See and Amplitude of Irregularities in the Topside Ionosphere," Journal of Geophysical Research, Volume 74, No. 26, December 1, 1969, pp. 6291-6303.

8. Evans, J. V., Millstone Hill Radar Propagation Study Report prepared jointly by Lincoln Laboratory under Army Contract F19628-73-CL0002 and Bell Laboratories for the U. S. Army SAFEGUARD System Command under Contract DAHC60-71-C-0005.

9. Feinblum, D. A., R. J. Horan, HILION - A Model of the High-Latitude Ionospheric F2-Layer Statistics of Regular Ionospheric Effects at Ft. Churchill, 1968. Report prepared by Bell Laboratories on behalf of Western Electric for the U. S. Army SAFEGUARD System Command under Contract DAHC60-71-C-0005.

10. Francis, S. H., Theory and Models of Atmospheric Acoustic - Gravity Waves and Traveling Ionospheric Disturbances Report prepared by Bell Laboratories on behalf on Western Electric for the U. S. Army

SAFEGUARD System Command under Contract DAHC60-71-C-0005, October 1973.

11. Hajkowicz, L. A., "The Effects of the Satellite Position on the Spacial Occurrence of Angular Scintillations," Planet, Space Sci., 1974, Volume 22, pp. 617-621.

12. Hardin, R. H., and F. D. Tappert, Analysis, Simulation, and Models of Ionospheric Scintillation report prepared by Bell Laboratories on behalf of Western Electric for the U. S. Army SAFEGUARD System Command under Contract DAHC60-710C-0005, March 1974.

13. Hargreaves, J. K., "Auroral Absorption of HF Radio Waves in the Ionosphere: A Review of Results from the First Decade of Riometry." Proceedings of the IEEE, Volume 57, No. 8, August 1969, pp. 1348-1373.

14. Jones, K. L., "Variation in the Properties of Scintillation Activity with the Latitude of the Observer," Planet, Space Sci., 1969, Volume 17, pp. 585-593.

15. Jones, M., Index of Radar Propagation Study Literature, Talks, and Reports, prepared by Bell Laboratories on behalf of Western Electric for the U. S. Army SAFEGUARD System Command under Contract DAHC60-71-C-0005, March 1974.

16. Lawrence, R. S., C. G. Little, H. J. A. Chivers "A Survey of Ionospheric Effects Upon Earth-Space Radio Propagation" Proceedings IEEE, Volume 52, No. 1, January 1964, pp. 4-27.

17. Little, C. G., G. C. Reid, E. Stiltner, and R. P. Merritt, "An Experimental Investigation of the Scintillation of Radio Stars Observed at Frequencies of 223 and 456 Megacycles per Second from a Location Close to the Auroral Zone," Journal of Geophysical Reseach Volume 67, No. 5, May 1962, pp. 1763-1784.

18. Millman, G. H., Tropospheric Effects on Space Communications, General Electric Technical Information Series Report No. R70EMH28, September 1970.

19. Millman, G. H., and R. E. Anderson, "Ionospheric Phase Fluctuations of Satellite Transmissions" Journal of Geophysical Research Volume 73, No. 13, July 1, 1968, pp. 4434-4438.

20. Millman, G. H., and A. J. Moceyunas, "Observations of Ionospheric Scintillations by Ultra High Frequency Radar Reflections from Earth's Satellites, "Journal of Geophysical Research Volume 70, No. 1, January 1, 1965, pp. 81-88.

21. Peterson, A. M., O. G. Villard, Jr., R. L. Leadabrand, and P. B. Gallagher, "Regularly-Observable Aspect-Sensitive Radio Reflections from Ionization Aligned with the Earth's Magnetic Field and Located within the Ionospheric Layers at Middle Latitudes." Journal of Geophysical Research Volume 60, No. 4, December 1955, pp. 497-512.

22. Porcello, L. J., and L. R. Hughes, "Observed Fine Structure of a Phase Perturbation Induced during Transauroral Propagation," Journal of Geophysical Research, Volume 73, No. 19, October 1, 1963, pp. 6337-6346.

23. Preddey, G. F., "Mid-Latitude Radio Satellite Scintillation: The Variation with Latitude," Planet, Space Sci., 1969, Volume 17, pp. 1557-1561.

24. Preddey, G. F., J. Mawdsley and W. Ireland, "Mid-Latitude Radio - Satellite Scintillation, the morphology near sunspot minimum." Planet, Space Sci., Volume 17, 1969, pp. 1161-1171.

25. Sailors, D. B., "Effects of Scintillation on Syncronous Satellite Communication at 250 MHz in the Equatorial Region." Paper No. 72-178 AIAA 10th Aerospace Sciences Meeting, January 1972, pp. 1-7.

26. Titheridge, J. E., G. F. Stuart, "The Distribution of Irregularities in the Antarctic Ionospheric - I," Journal of Atmospherical and Terrestrial Physics, 1968, Volume 30, pp. 85-98.

27. Unger, J. H. W., R. H. Hardin, and R. J. Horan, Auroral Clutter in UHF Radar, A Report Prepared by Bell Laboratories on Behalf of Western Electric for the Advanced Ballistic Missile Defense Agency under Contract DAHC60-60-0008, 1975.

APPENDIX

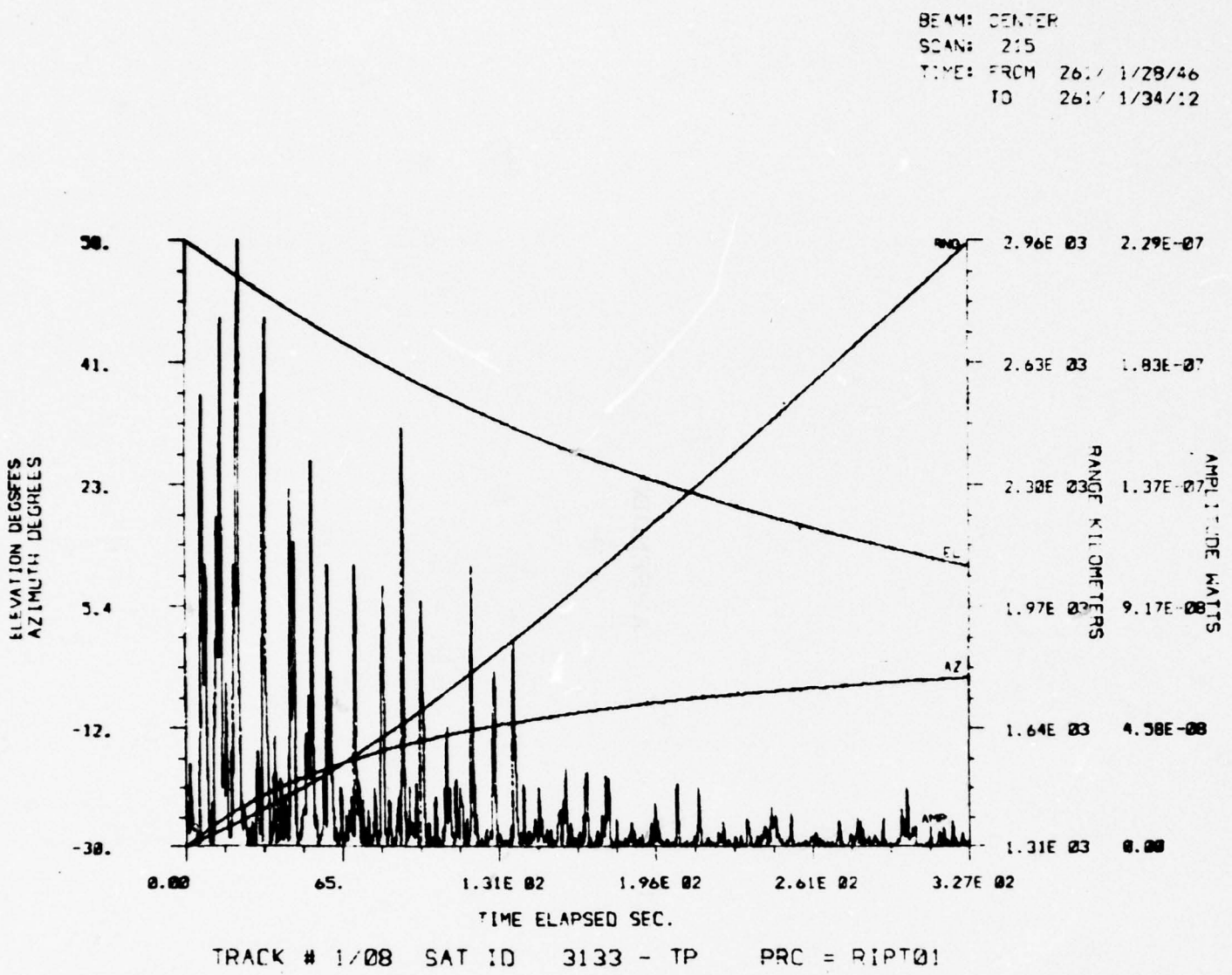
BEAM: CENTER
SCAN: 215
TIME: FROM 261/ 1/28/46
TO 261/ 1/34/12
30.
41.
23.
5.4
-12.
-30.
ELEVATION DEGREES
AZIMUTH DEGREES
RNG
EL
AZ
AMP
2.96E 03
2.63E 03
2.30E 03
1.97E 03
1.64E 03
1.31E 03
2.29E-07
1.83E-07
1.37E-07
9.17E-08
4.58E-08
0.00
RANGE KILOMETERS
AMPLITUDE WATTS
0.00
65.
1.31E 02
1.96E 02
2.61E 02
3.27E 02
TIME ELAPSED SEC.
TRACK # 1/08 SAT ID 3133 - TP PRC = RIPT01

Figure A-1

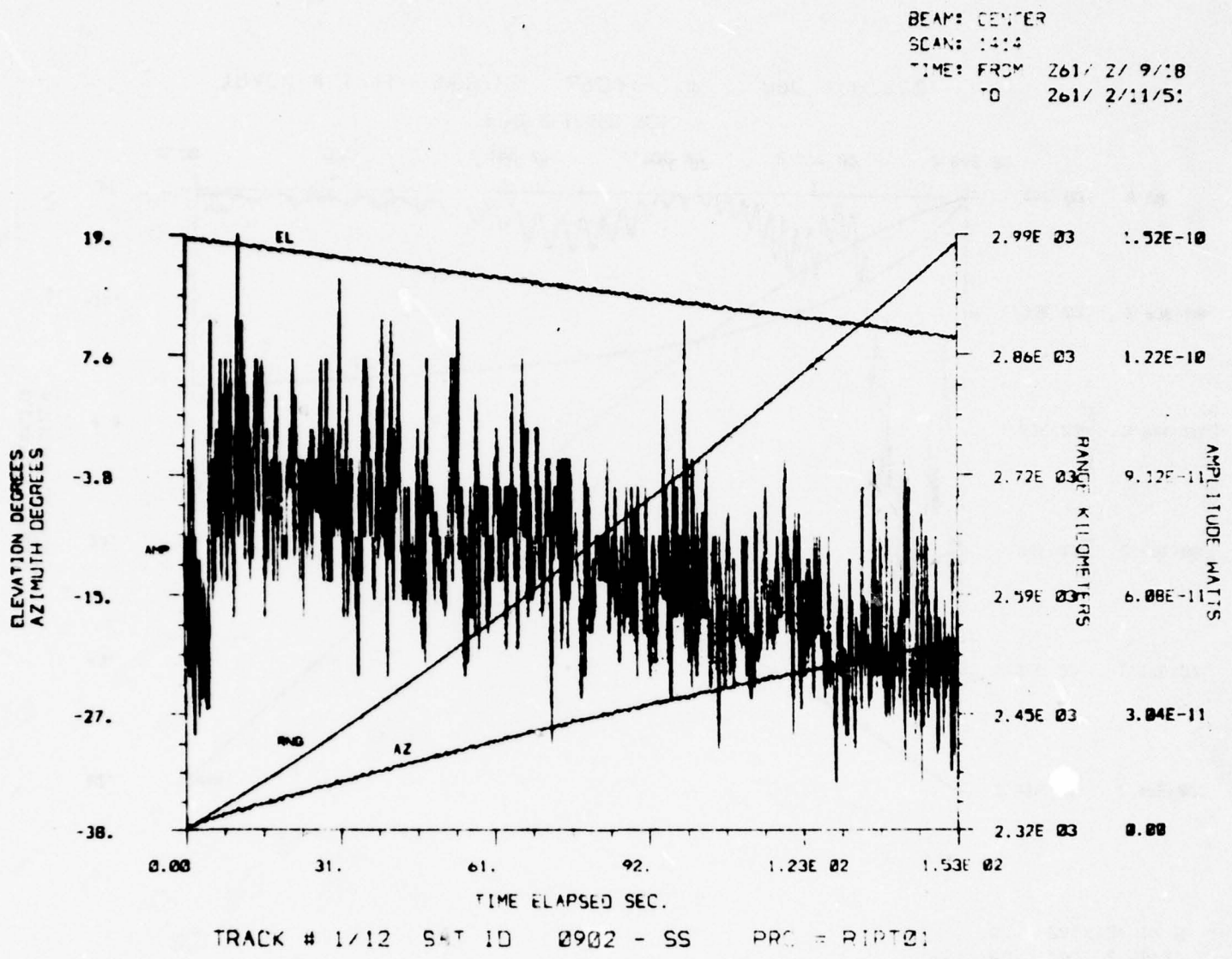
BEAM: CENTER
SCAN: 1414
TIME: FROM 261/ 2/ 9/18
TO 261/ 2/11/51
19.
7.6
-3.8
-15.
-27.
-38.
EL
RNG
AZ
2.99E 03
2.86E 03
2.72E 03
2.59E 03
2.45E 03
2.32E 03
1.52E-10
1.22E-10
9.12E-11
6.08E-11
3.04E-11
0.00
RANGE KILOMETERS
AMPLITUDE WATTS
ELEVATION DEGREES
AZIMUTH DEGREES
0.00
31.
61.
92.
1.23E 02
1.53E 02
TIME ELAPSED SEC.
TRACK # 1/12 SAT ID 0902 - SS PRG = RIPT01

Figure A-2

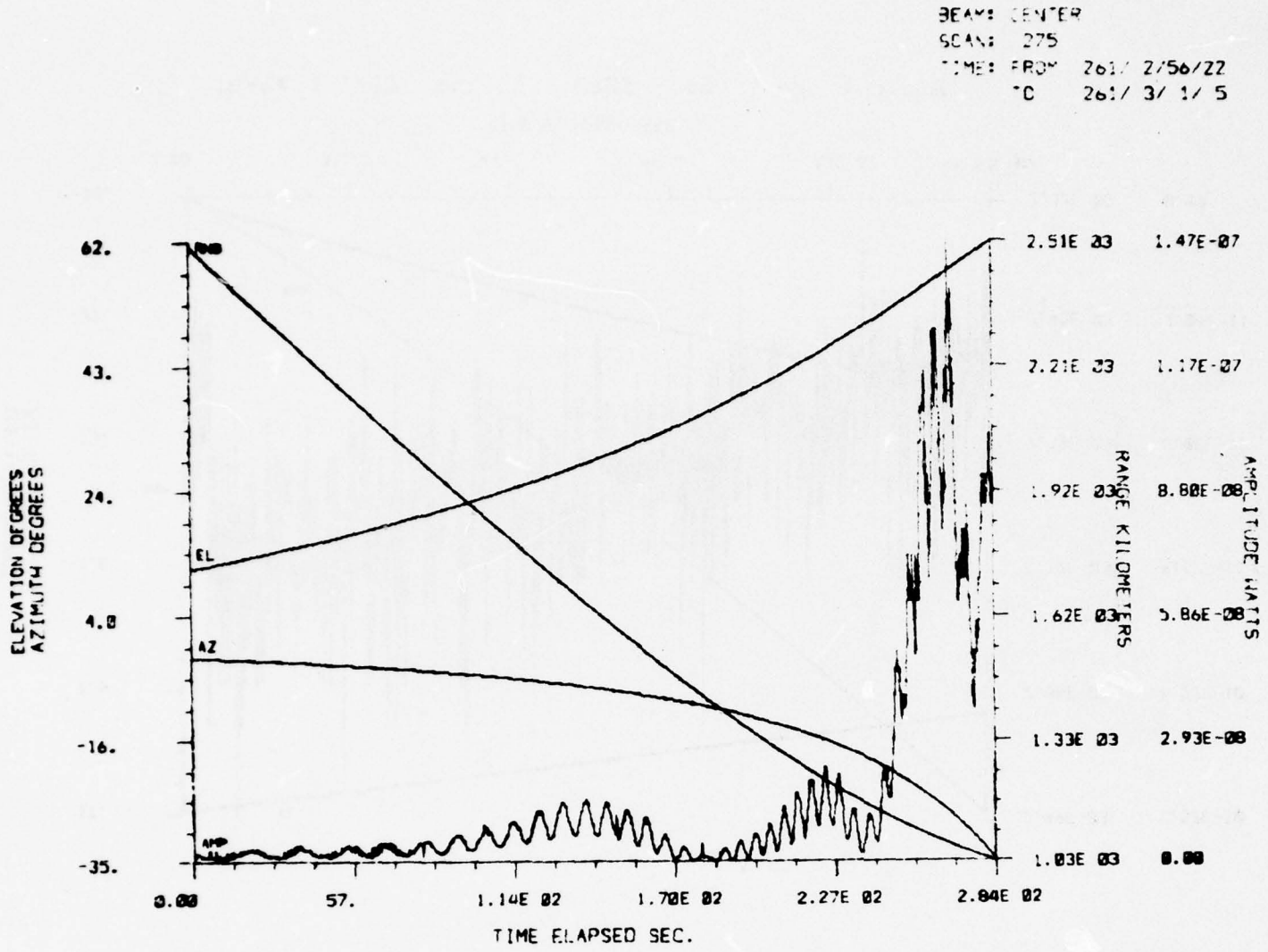
BEAM: CENTER
SCAN: 275
TIME: FROM 261/ 2/56/22
TO 261/ 3/ 1/ 5
62.
43.
24.
4.0
-16.
-35.
EL
AZ
0.00
57.
1.14E 02
1.70E 02
2.27E 02
2.84E 02
TIME ELAPSED SEC.
2.51E 03
2.21E 03
1.92E 03
1.62E 03
1.33E 03
1.03E 03
RANGE KILOMETERS
1.47E-07
1.17E-07
8.80E-08
5.86E-08
2.93E-08
0.00
AMPLITUDE UNITS
ELEVATION DEGREES
AZIMUTH DEGREES
TRACK # 1/16 SAT ID 6909 - TP PRC = RIPT01

Figure A-3

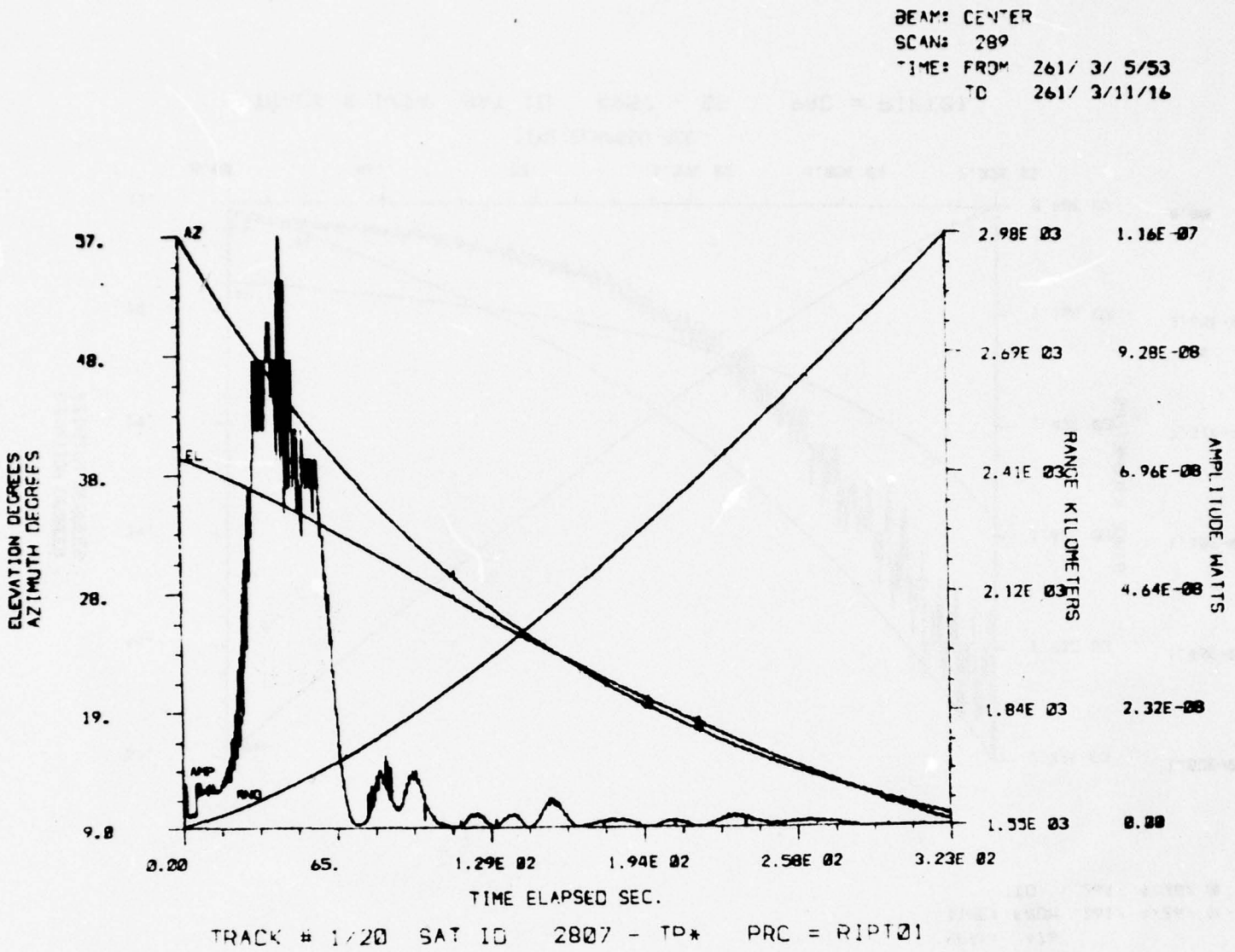
BEAM: CENTER
SCAN: 289
TIME: FROM 261/ 3/ 5/53
TO 261/ 3/11/16
57.
48.
38.
28.
19.
9.8
AZ
EL
AMP
RNG
ELEVATION DEGREES
AZIMUTH DEGREES
2.98E 03
2.69E 03
2.41E 03
2.12E 03
1.84E 03
1.55E 03
RANGE KILOMETERS
1.16E-07
9.28E-08
6.96E-08
4.64E-08
2.32E-08
0.00
AMPLITUDE WATTS
0.00
65.
1.29E 02
1.94E 02
2.58E 02
3.23E 02
TIME ELAPSED SEC.
TRACK # 1/20 SAT ID 2807 - TP* PRC = RIPT01

Figure A-4

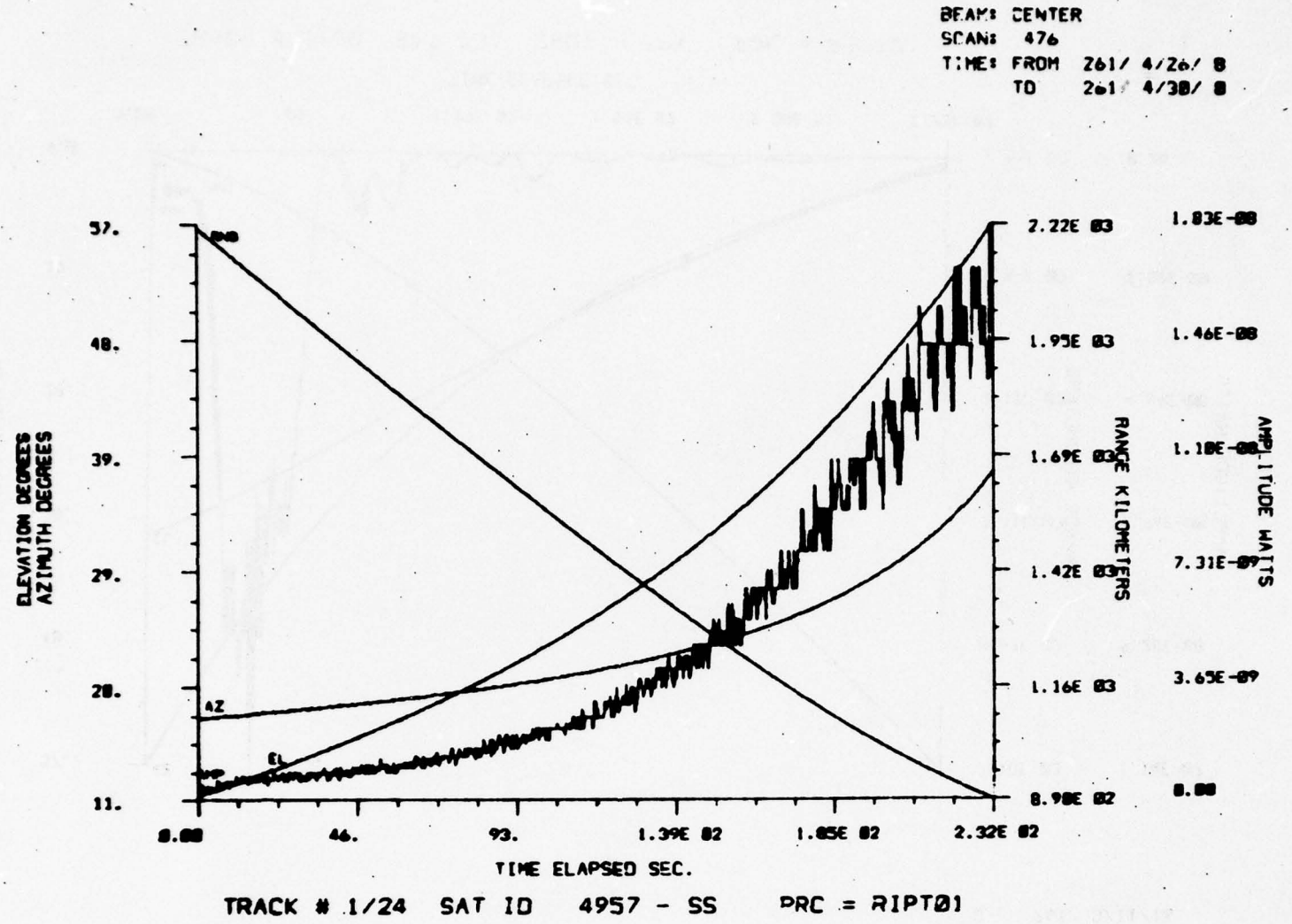
BEAM: CENTER
SCAN: 476
TIME: FROM 261/ 4/26/ 8
TO 261/ 4/30/ 8
57.
48.
39.
29.
20.
11.
ELEVATION DEGREES
AZIMUTH DEGREES
AZ
EL
2.22E 03
1.95E 03
1.69E 03
1.42E 03
1.16E 03
8.98E 02
RANGE KILOMETERS
1.83E-08
1.46E-08
1.10E-08
7.31E-09
3.65E-09
0.00
AMPLITUDE WATTS
0.00
46.
93.
1.39E 02
1.85E 02
2.32E 02
TIME ELAPSED SEC.
TRACK # 1/24 SAT ID 4957 - SS PRC = RIPT01

Figure A-5

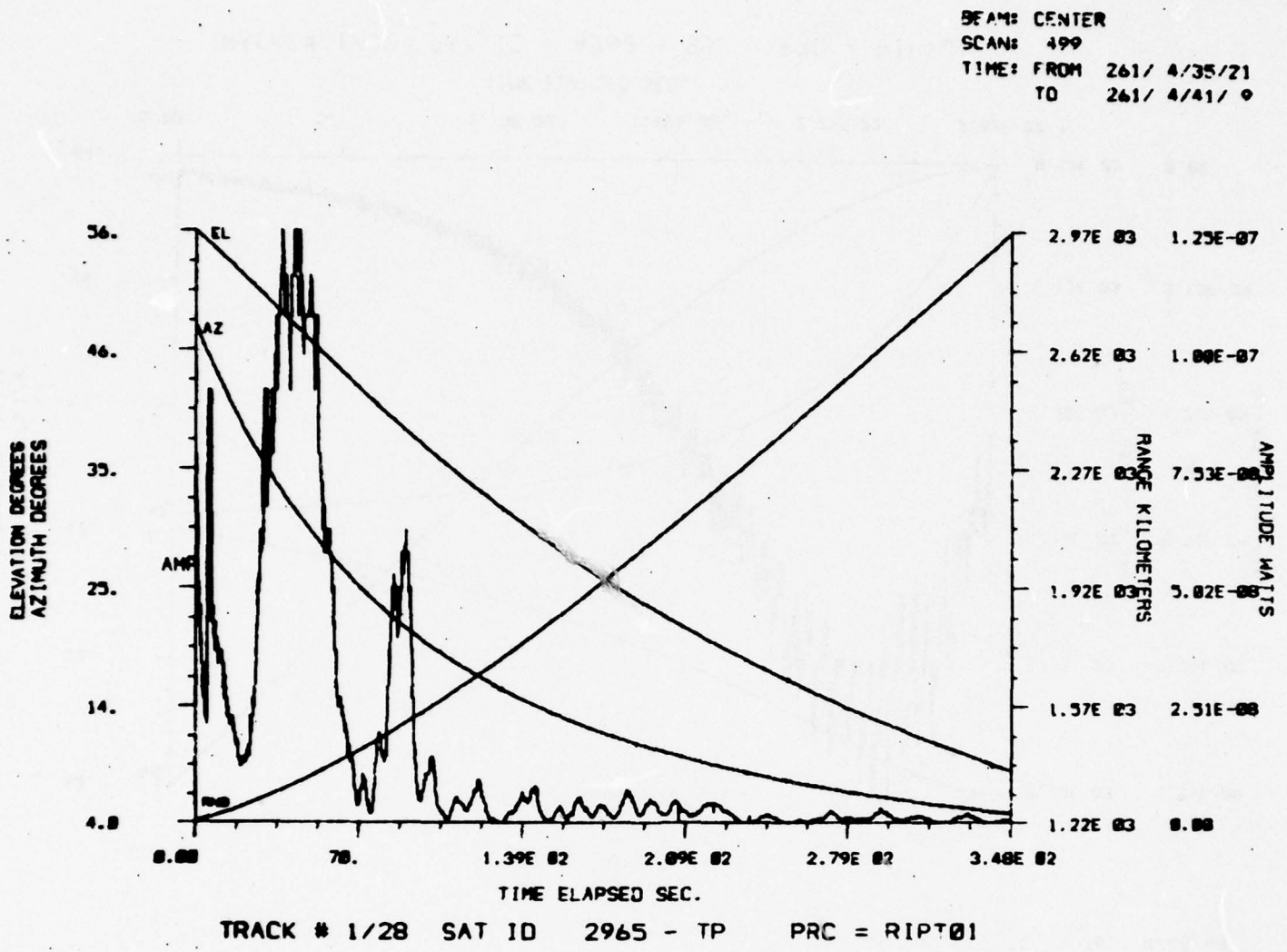
BEAM: CENTER
SCAN: 499
TIME: FROM 261/ 4/35/21
TO 261/ 4/41/ 0
ELEVATION DEGREES
AZIMUTH DEGREES
RANGE KILOMETERS
AMPLITUDE WATTS
EL
AZ
AMP
RNG
56.
46.
35.
25.
14.
4.8
2.97E 03
2.62E 03
2.27E 03
1.92E 03
1.57E 03
1.22E 03
1.25E-07
1.00E-07
7.53E-08
5.02E-08
2.51E-08
0.00
0.00
70.
1.39E 02
2.09E 02
2.79E 02
3.48E 02
TIME ELAPSED SEC.
TRACK # 1/28 SAT ID 2965 - TP PRC = RIPT01

Figure A-6

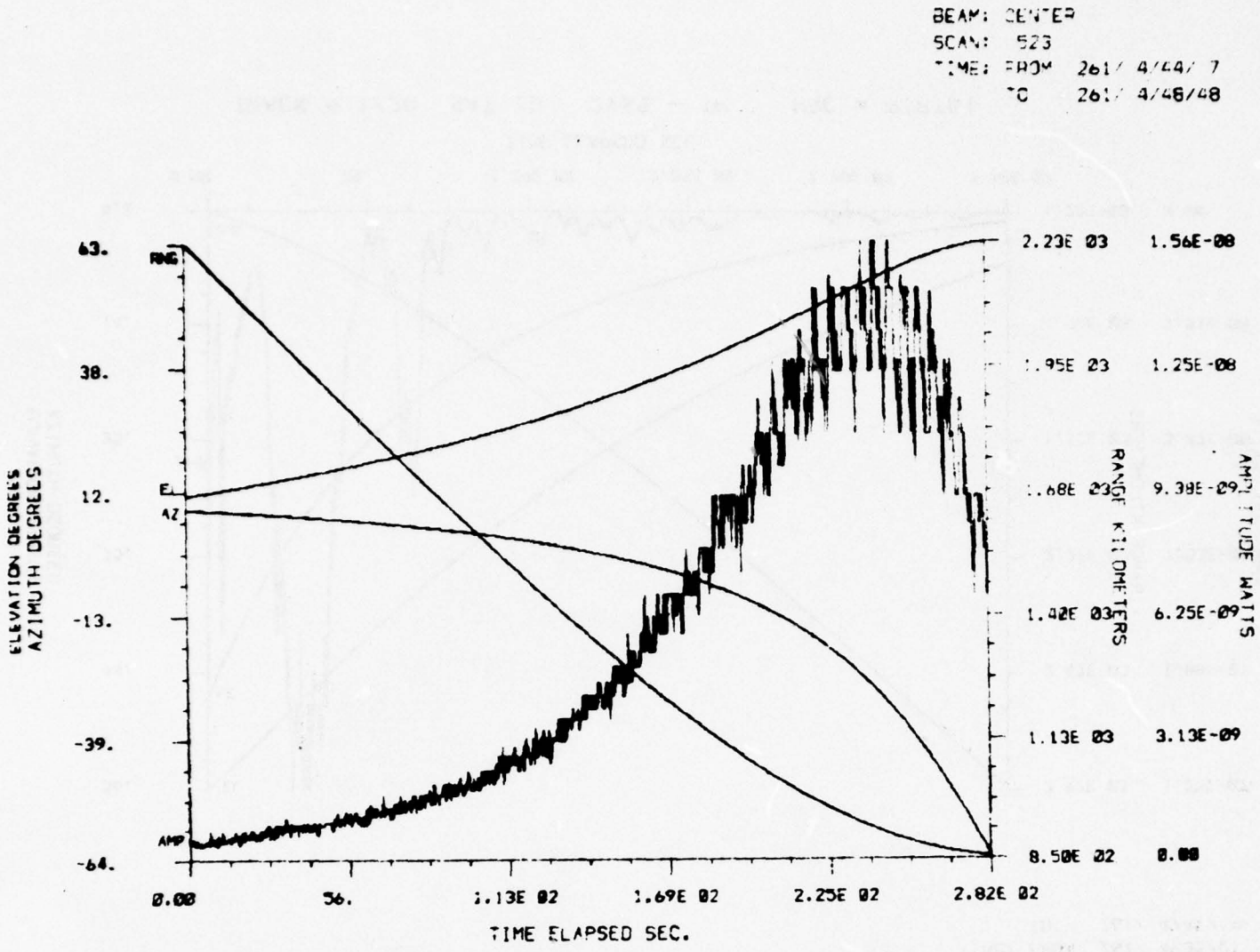
BEAM: CENTER
SCAN: 523
TIME: FROM 261/ 4/44/ 7
TO 261/ 4/46/48
63.
38.
12.
-13.
-39.
-64.
RNG
EL
AZ
AMP
ELEVATION DEGREES
AZIMUTH DEGRELLS
2.23E 03
1.95E 03
1.68E 03
1.40E 03
1.13E 03
8.50E 02
RANGE KILOMETERS
1.56E-08
1.25E-08
9.38E-09
6.25E-09
3.13E-09
0.00
AMPLITUDE WATTS
0.00
56.
1.13E 02
1.69E 02
2.25E 02
2.82E 02
TIME ELAPSED SEC.
TRACK # 1/32 SAT ID 4963 - SS PRC = RIPT0!

Figure A-7

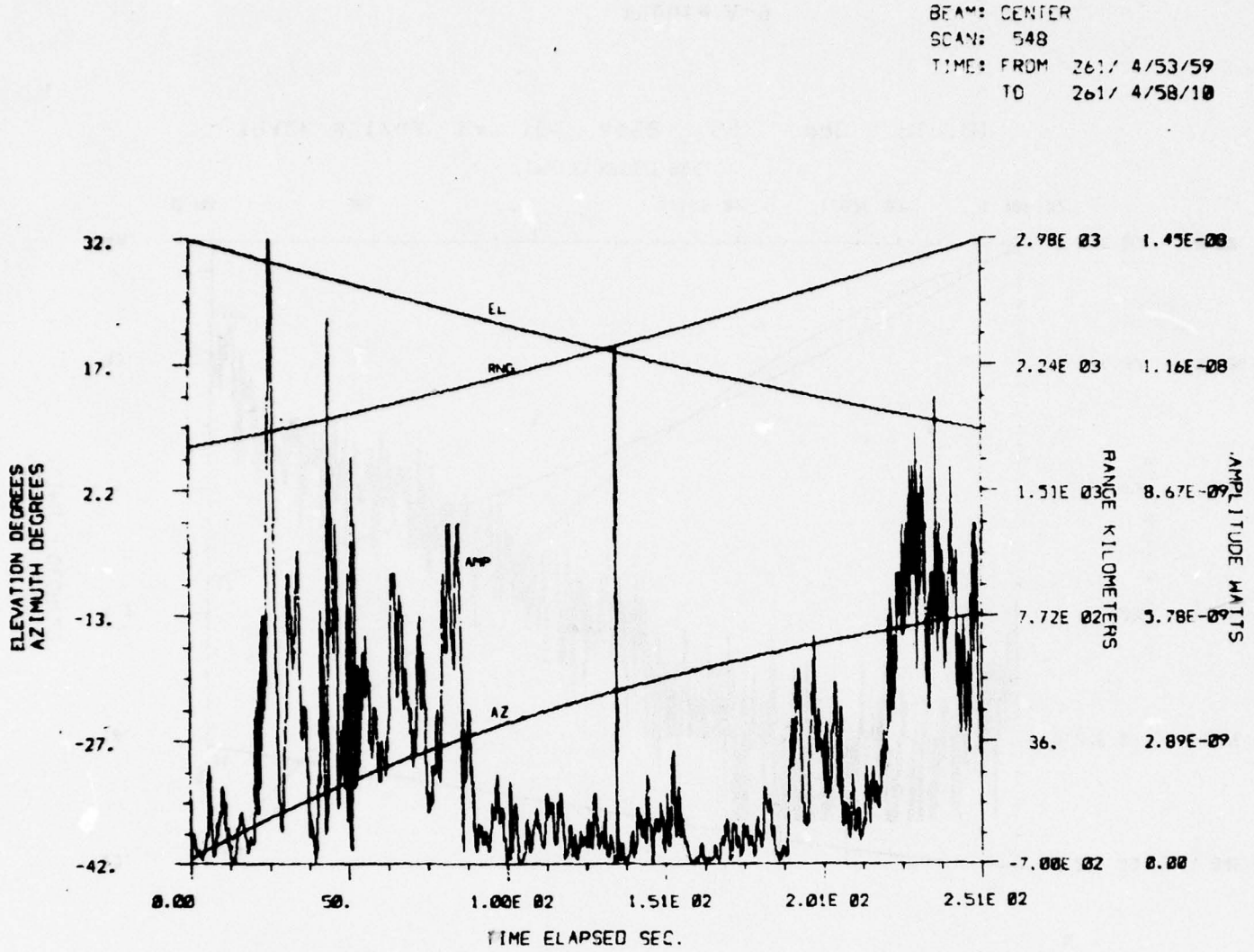
BEAM: CENTER
SCAN: 548
TIME: FROM 261/ 4/53/59
TO 261/ 4/58/10
32.
17.
2.2
-13.
-27.
-42.
ELEVATION DEGREES
AZIMUTH DEGREES
EL
RNG
AMP
AZ
2.98E 03
2.24E 03
1.51E 03
7.72E 02
36.
-7.00E 02
RANGE KILOMETERS
1.45E-08
1.16E-08
8.67E-09
5.78E-09
2.89E-09
0.00
AMPLITUDE WATTS
0.00
50.
1.00E 02
1.51E 02
2.01E 02
2.51E 02
TIME ELAPSED SEC.
TRACK # 1/36 SAT ID 2807 - TP* PRC = RIPT01

Figure A-8

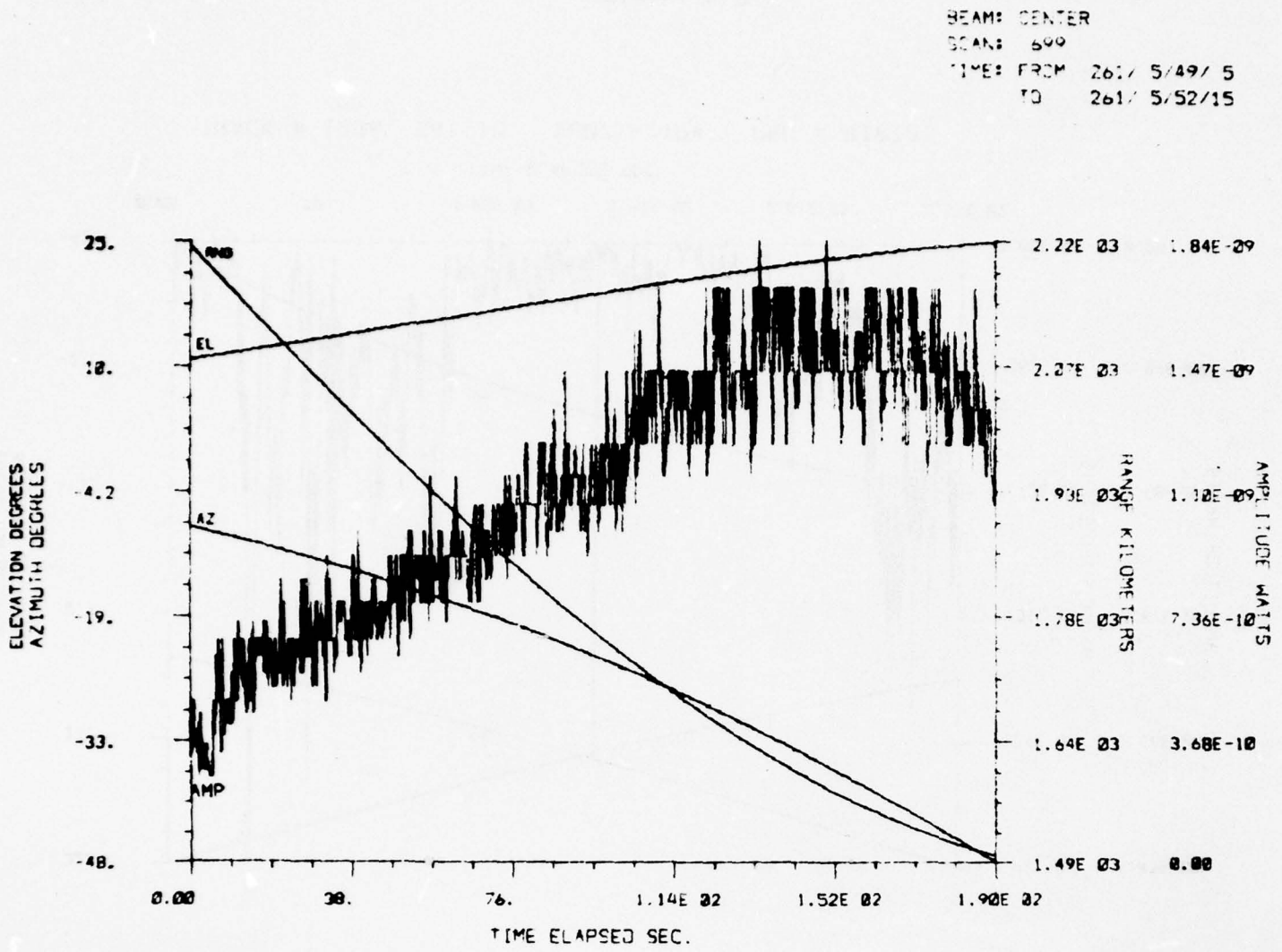
BEAM: CENTER
SCAN: 600
TIME: FROM 261/ 5/49/ 5
TO 261/ 5/52/15
25.
10.
-4.2
-19.
-33.
-48.
ELEVATION DEGREES
AZIMUTH DEGHLLS
EL
AZ
AMP
2.22E 03
2.27E 03
1.93E 03
1.78E 03
1.64E 03
1.49E 03
RANGE KILOMETERS
1.84E-09
1.47E-09
1.10E-09
7.36E-10
3.68E-10
0.00
AMPLITUDE WATTS
0.00
38.
76.
1.14E 02
1.52E 02
1.90E 02
TIME ELAPSED SEC.
TRACK # 1/40 SAT ID 4958 - SS PRC = RIPT01

Figure A-9

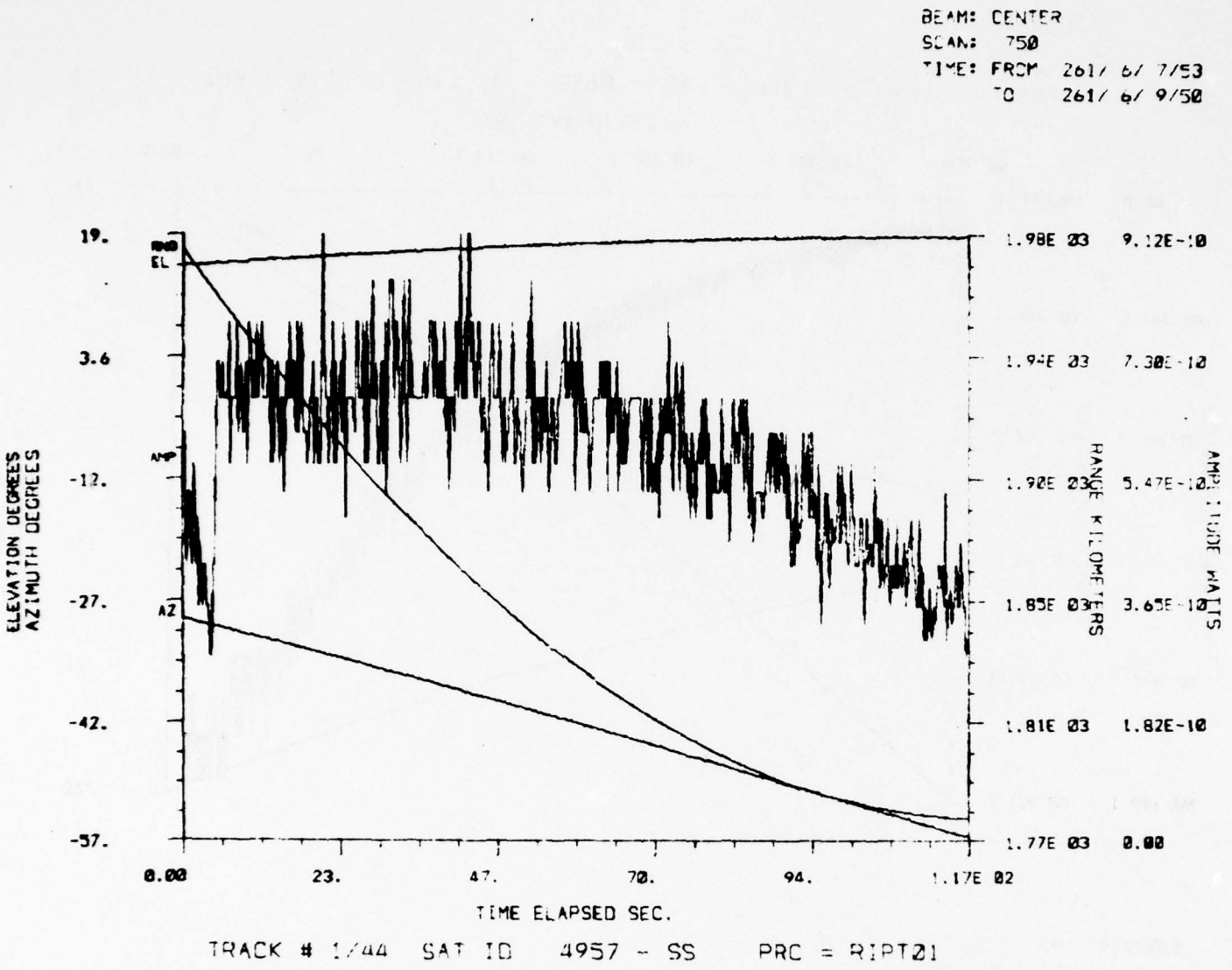
BEAM: CENTER
SCAN: 750
TIME: FROM 261/ 6/ 7/53
TO 261/ 6/ 9/50
19.
3.6
-12.
-27.
-42.
-57.
EL
AZ
ELEVATION DEGREES
AZIMUTH DEGREES
1.98E 03 9.12E-10
1.94E 03 7.30E-10
1.90E 03 5.47E-10
1.85E 03 3.65E-10
1.81E 03 1.82E-10
1.77E 03 0.00
RANGE KILOMETERS
AMPLITUDE WATTS
0.00
23.
47.
70.
94.
1.17E 02
TIME ELAPSED SEC.
TRACK # 1744 SAT ID 4957 - SS PRC = RIPT21

Figure A-10

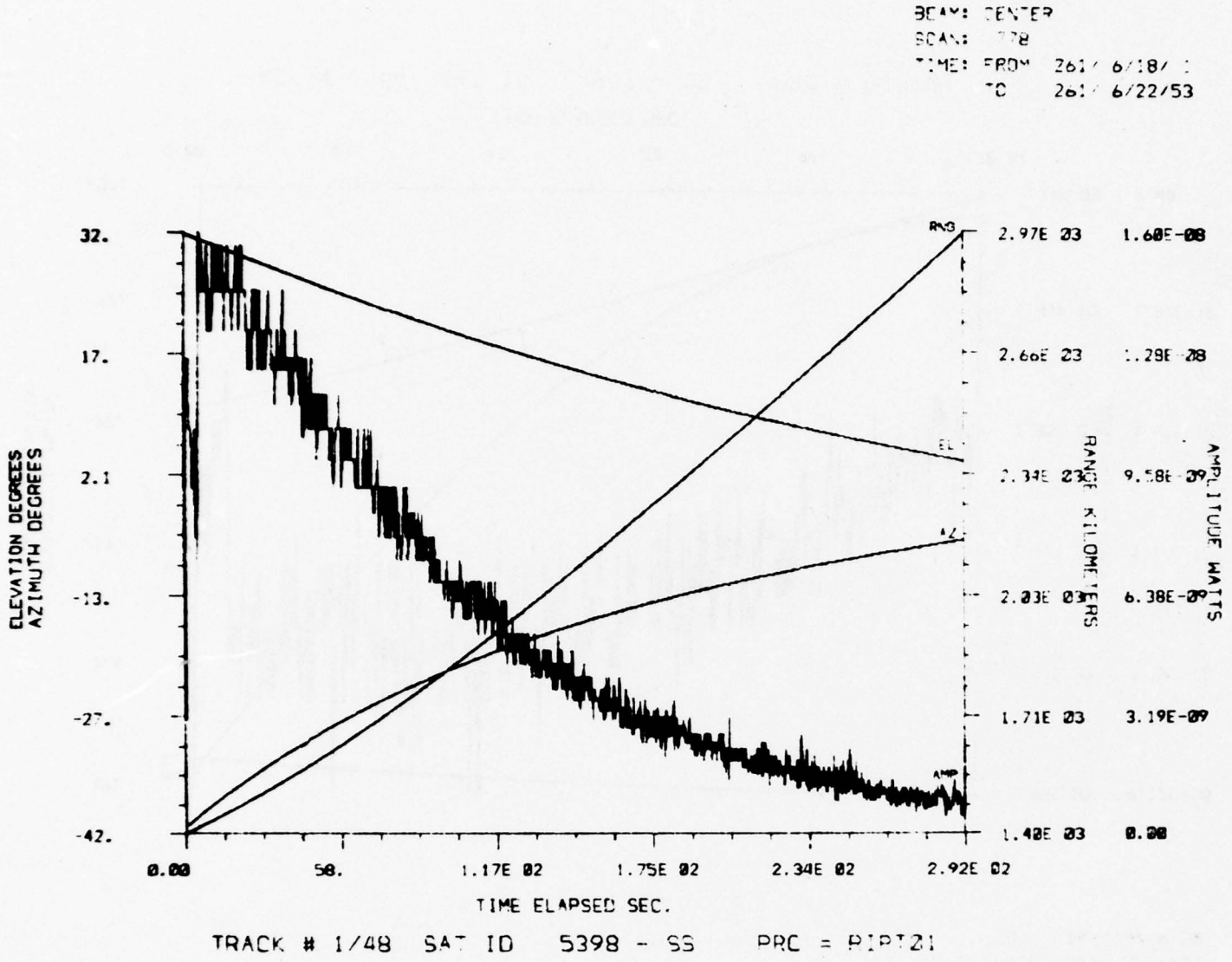
BEAM: CENTER
SCAN: 278
TIME: FROM 261/ 6/18/ 1
TO 261/ 6/22/53
32.
17.
2.1
-13.
-27.
-42.
ELEVATION DEGREES
AZIMUTH DEGREES
RNG
EL
AZ
AMP
2.97E 03
2.60E 03
2.34E 03
2.03E 03
1.71E 03
1.40E 03
1.60E-08
1.29E-08
9.58E-09
6.38E-09
3.19E-09
0.00
RANGE KILOMETERS
AMPLITUDE WATTS
0.00
58.
1.17E 02
1.75E 02
2.34E 02
2.92E 02
TIME ELAPSED SEC.
TRACK # 1/48 SAT ID 5398 - SS PRC = PIPT21

Figure A-11

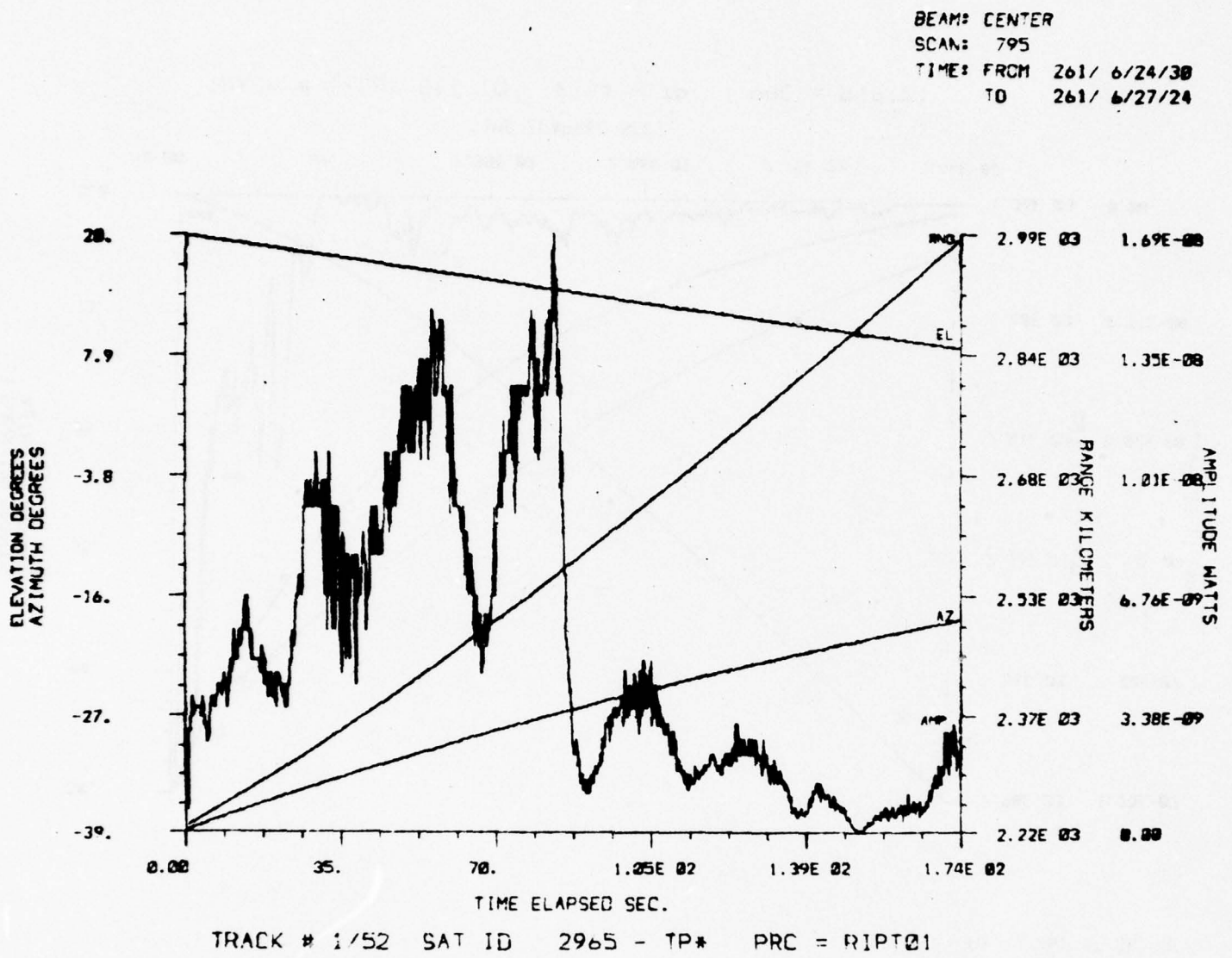
BEAM: CENTER
SCAN: 795
TIME: FROM 261/ 6/24/30
TO 261/ 6/27/24
28.
7.9
-3.8
-16.
-27.
-39.
ELEVATION DEGREES
AZIMUTH DEGREES
RNG
EL
AZ
AMP
2.99E 03
2.84E 03
2.68E 03
2.53E 03
2.37E 03
2.22E 03
1.69E-08
1.35E-08
1.01E-08
6.76E-09
3.38E-09
0.00
RANGE KILOMETERS
AMPLITUDE WATTS
0.00
35.
70.
1.05E 02
1.39E 02
1.74E 02
TIME ELAPSED SEC.
TRACK # 1/52 SAT ID 2965 - TP* PRC = RIPT01

Figure A-12

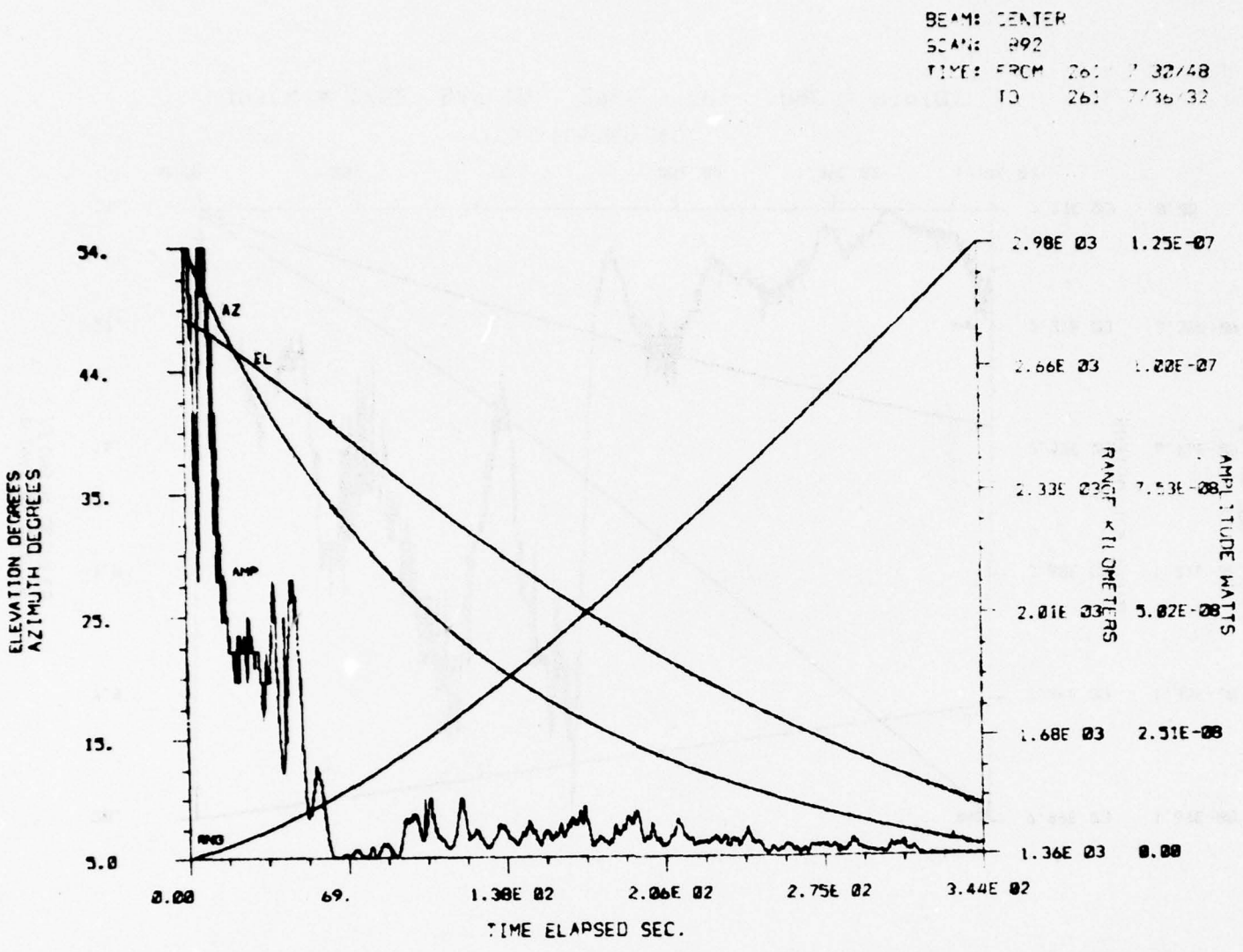
BEAM: CENTER
SCAN: 092
TIME: FROM 261 7 32/48
TO 261 7/36/32
54.
44.
35.
25.
15.
5.0
AZ
EL
AMP
RNG
ELEVATION DEGREES
AZIMUTH DEGREES
2.98E 03
2.66E 03
2.33E 03
2.01E 03
1.68E 03
1.36E 03
1.25E-07
1.00E-07
7.53E-08
5.02E-08
2.51E-08
0.00
RANGE KILOMETERS
AMPLITUDE WATTS
0.00
69.
1.38E 02
2.06E 02
2.75E 02
3.44E 02
TIME ELAPSED SEC.
TRACK # 1/56 SAT ID 2754 - TP PRC = RIPT01

Figure A-13

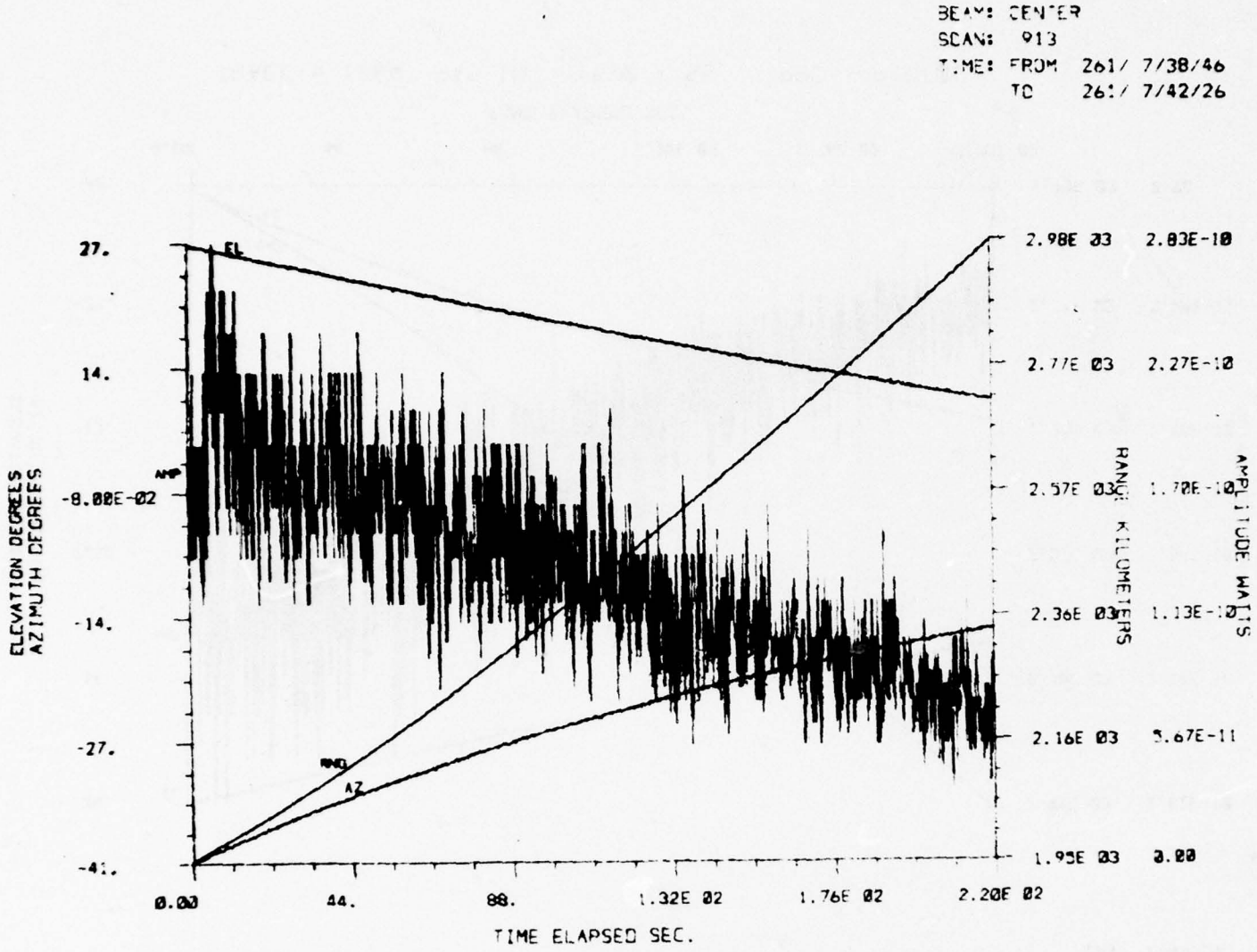
BEAM: CENTER
SCAN: 913
TIME: FROM 261/ 7/38/46
TO 261/ 7/42/26
27.
14.
-8.00E-02
-14.
-27.
-41.
EL
AZ
RNG
AMP
ELEVATION DEGREES
AZIMUTH DEGREES
2.98E 03
2.77E 03
2.57E 03
2.36E 03
2.16E 03
1.95E 03
RANGE KILOMETERS
2.83E-10
2.27E-10
1.70E-10
1.13E-10
5.67E-11
0.00
AMPLITUDE WATTS
0.00
44.
88.
1.32E 02
1.76E 02
2.20E 02
TIME ELAPSED SEC.
TRACK # 1/60 SAT ID 1512 - SS PRC = RIPT01

Figure A-14

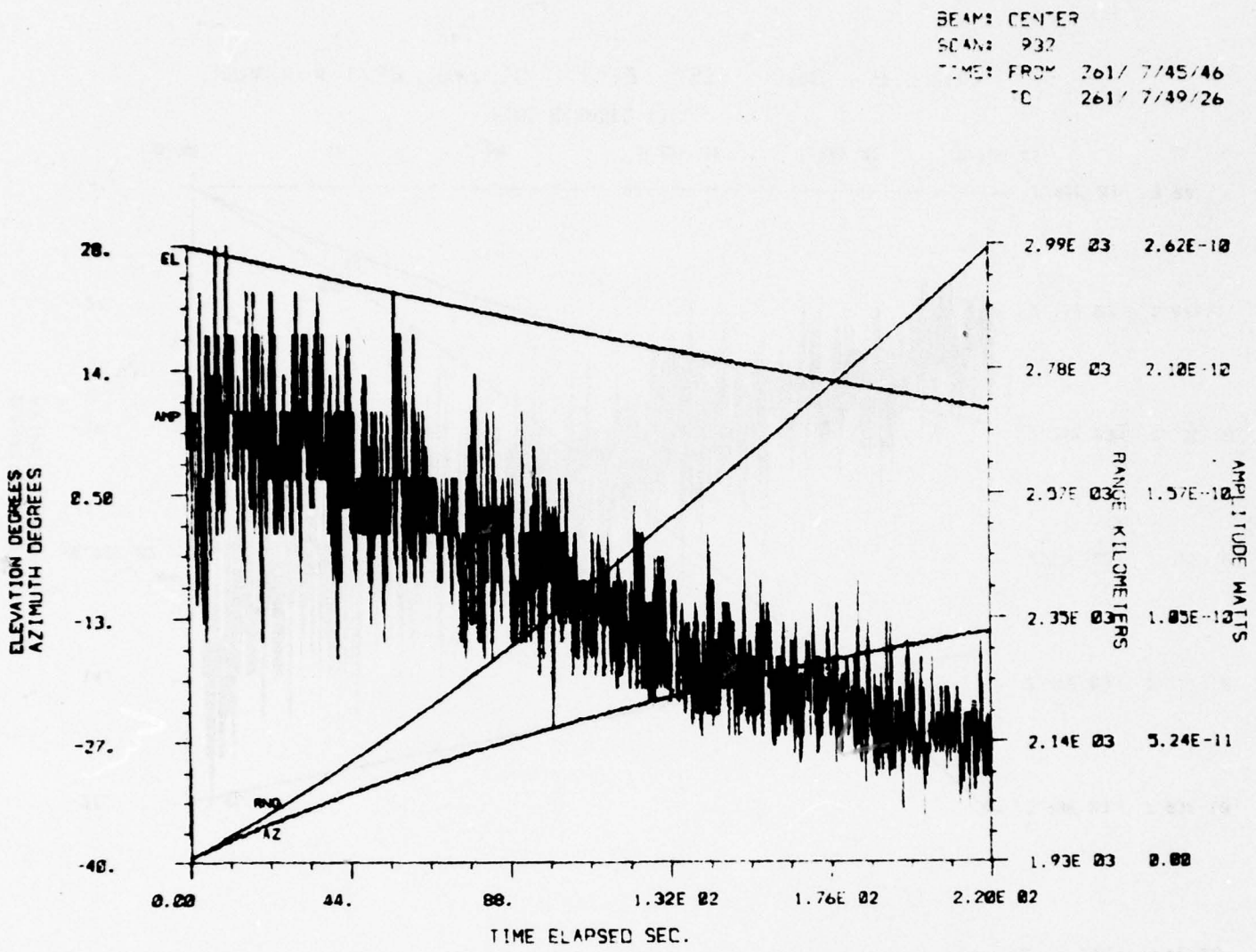
BEAM: CENTER
SCAN: 932
TIME: FROM 261/ 7/45/46
TO 261/ 7/49/26
28.
14.
0.50
-13.
-27.
-40.
EL
AMP
RNG
AZ
ELEVATION DEGREES
AZIMUTH DEGREES
2.99E 03
2.78E 03
2.57E 03
2.35E 03
2.14E 03
1.93E 03
2.62E-10
2.10E-10
1.57E-10
1.05E-10
5.24E-11
0.00
RANGE KILOMETERS
AMPLITUDE WATTS
0.00
44.
88.
1.32E 02
1.76E 02
2.20E 02
TIME ELAPSED SEC.
TRACK # 1/64 SAT ID 1520 - SS PRC = RIPT01

Figure A-15

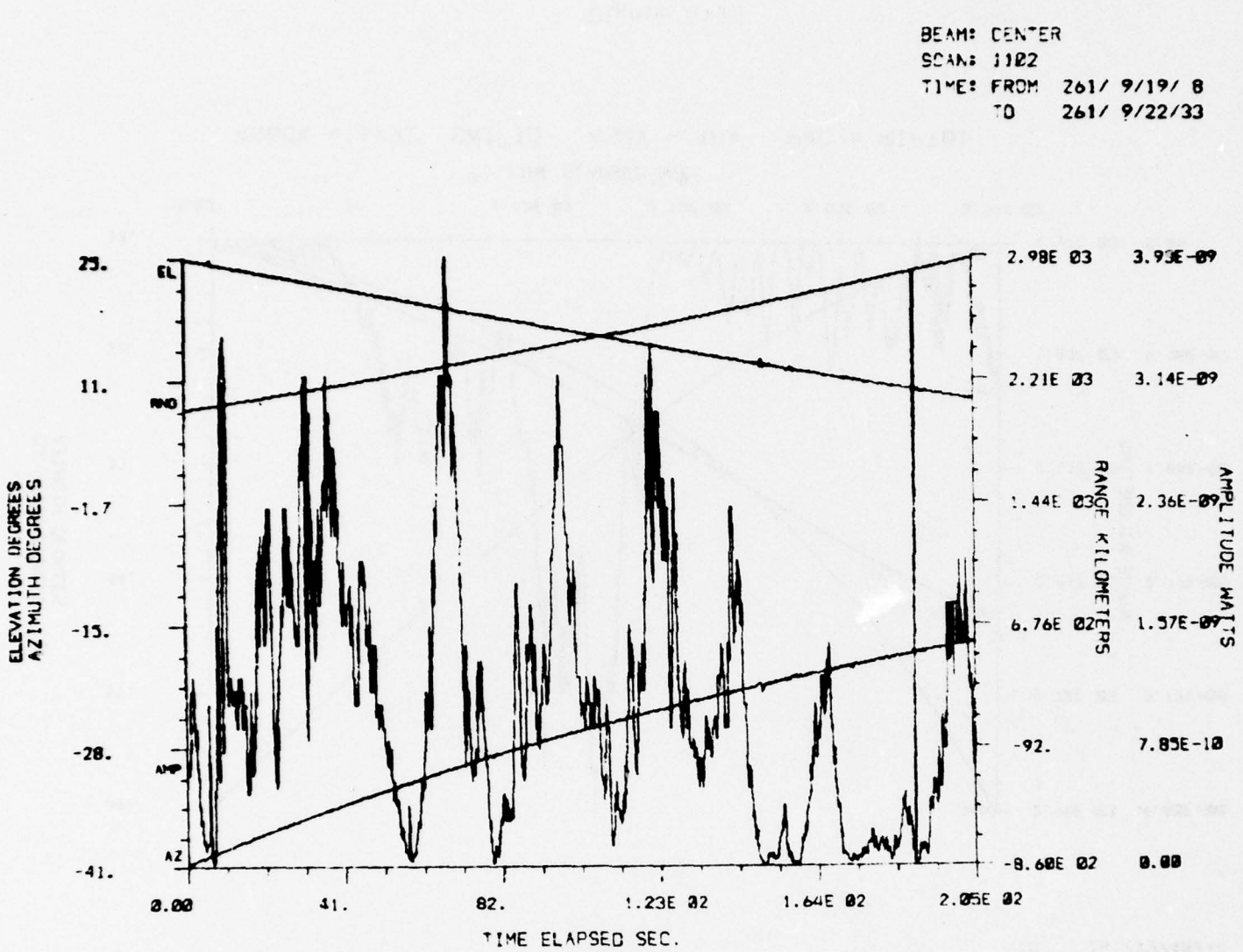
BEAM: CENTER
SCAN: 1102
TIME: FROM 261/ 9/19/ 8
TO 261/ 9/22/33
25.
11.
-1.7
-15.
-28.
-41.
EL
RNG
AMP
AZ
ELEVATION DEGREES
AZIMUTH DEGREES
2.98E 03
2.21E 03
1.44E 03
6.76E 02
-92.
-8.60E 02
3.93E-09
3.14E-09
2.36E-09
1.57E-09
7.85E-10
0.00
RANGE KILOMETERS
AMPLITUDE WATTS
0.00
41.
82.
1.23E 02
1.64E 02
2.05E 02
TIME ELAPSED SEC.
TRACK # 1/68 SAT ID 2754 - TP PRC = RIPT01

Figure A-16

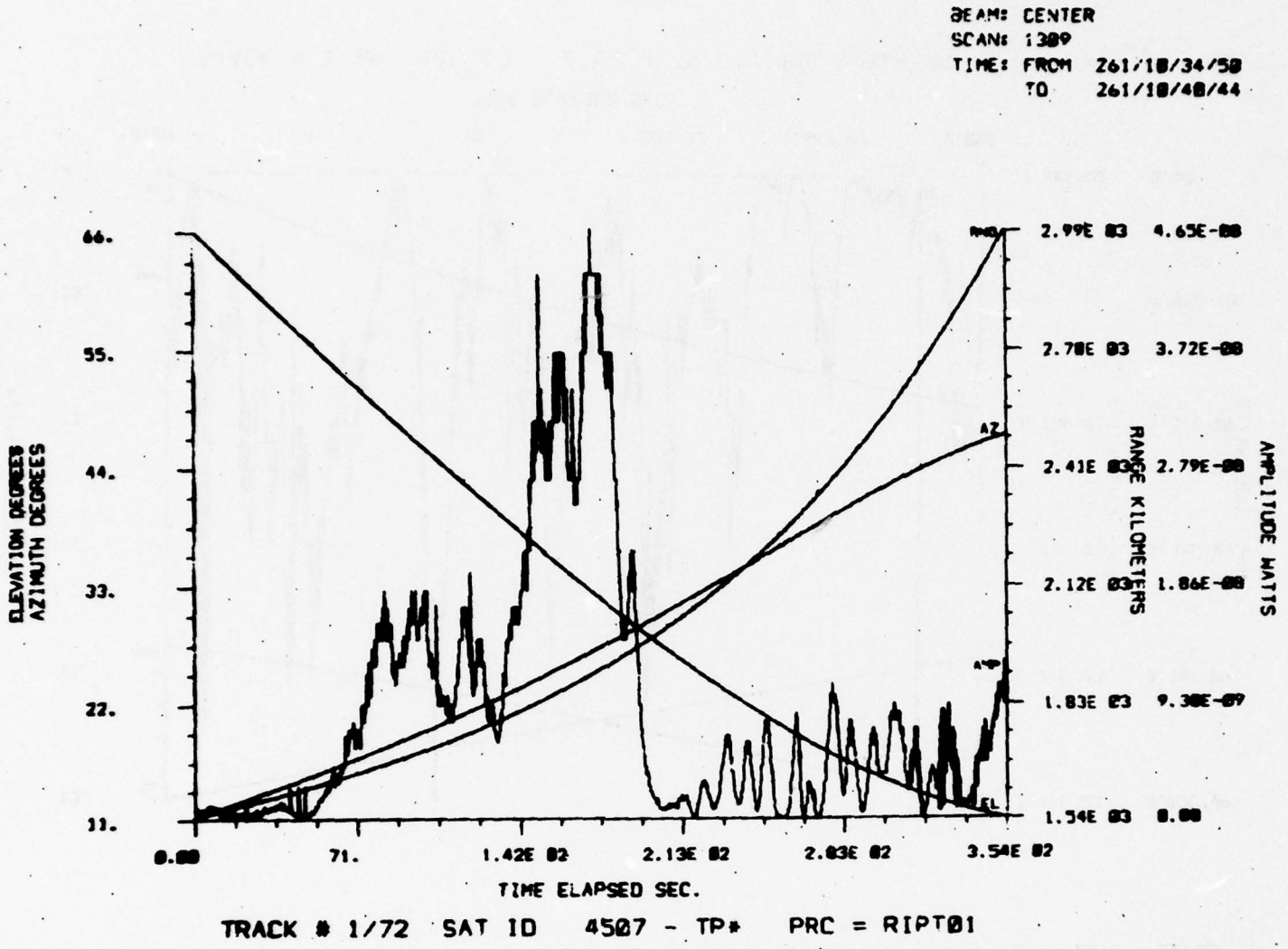
BEAM: CENTER
SCAN: 1389
TIME: FROM 261/18/34/50
TO 261/18/40/44
66.
55.
44.
33.
22.
11.
ELEVATION DEGREES
AZIMUTH DEGREES
2.99E 03
2.78E 03
2.41E 03
2.12E 03
1.83E 03
1.54E 03
RANGE KILOMETERS
AZ
EL
0.00
71.
1.42E 02
2.13E 02
2.83E 02
3.54E 02
TIME ELAPSED SEC.
TRACK # 1/72 SAT ID 4507 - TP# PRC = RIPT01

Figure A-17

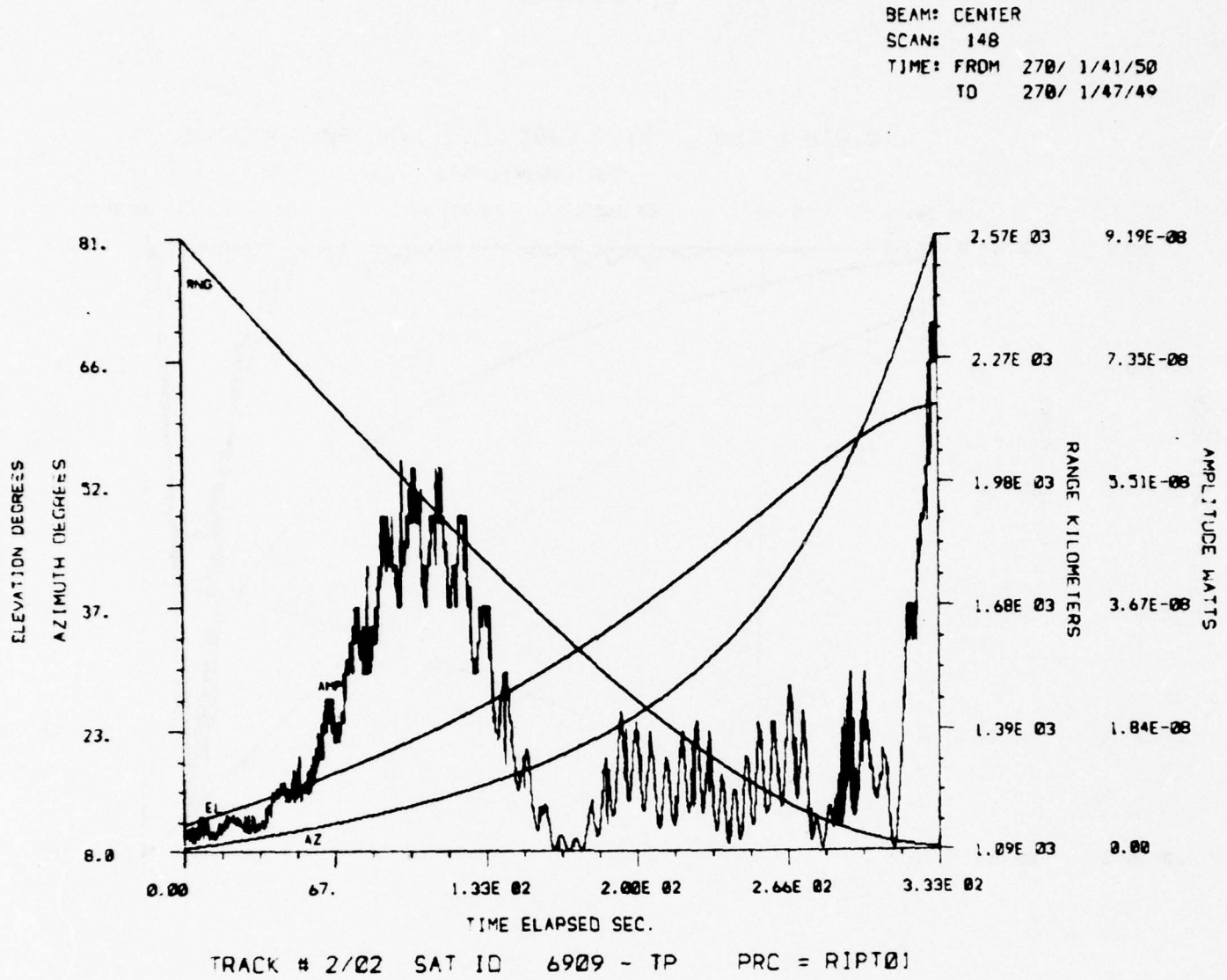
BEAM: CENTER
SCAN: 148
TIME: FROM 270/ 1/41/50
TO 270/ 1/47/49
81.
66.
52.
37.
23.
8.0
ELEVATION DEGREES
AZIMUTH DEGREES
RNG
AMP
EL
AZ
2.57E 03
2.27E 03
1.98E 03
1.68E 03
1.39E 03
1.09E 03
RANGE KILOMETERS
9.19E-08
7.35E-08
5.51E-08
3.67E-08
1.84E-08
0.00
AMPLITUDE WATTS
0.00
67.
1.33E 02
2.00E 02
2.66E 02
3.33E 02
TIME ELAPSED SEC.
TRACK # 2/02 SAT ID 6909 - TP PRC = RIPT01

Figure A-18

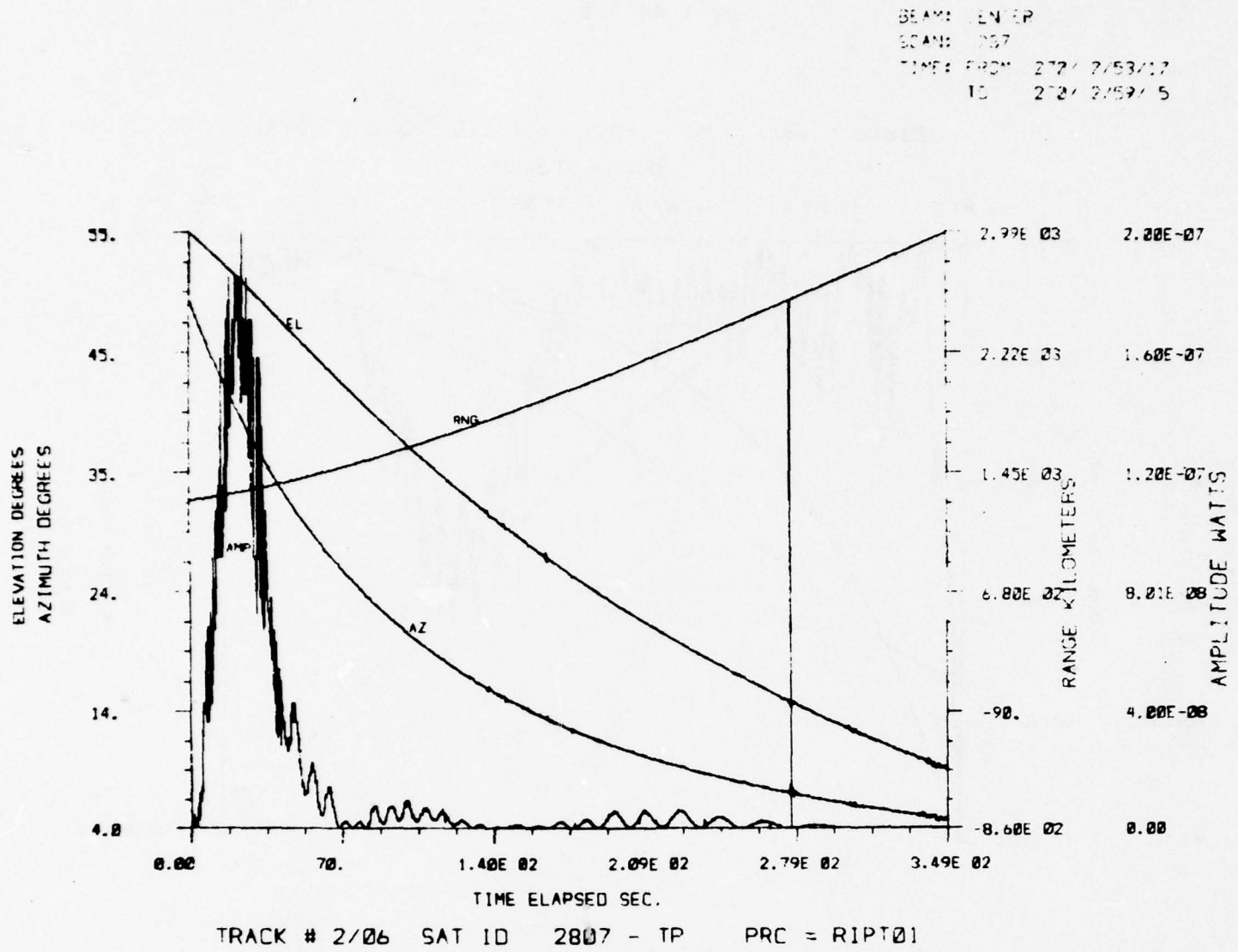
BEAM: EARTH
SCAN: 257
TIME: FROM 272/ 2/53/17
TO 272/ 2/59/ 5
55.
45.
35.
24.
14.
4.0
ELEVATION DEGREES
AZIMUTH DEGREES
EL
RNG
AMP
AZ
2.99E 03
2.22E 03
1.45E 03
6.80E 02
-90.
-8.60E 02
RANGE KILOMETERS
2.00E-07
1.60E-07
1.20E-07
8.01E 08
4.00E-08
0.00
AMPLITUDE WATTS
0.00
70.
1.40E 02
2.09E 02
2.79E 02
3.49E 02
TIME ELAPSED SEC.
TRACK # 2/06 SAT ID 2807 - TP PRC = RIPT01

Figure A-19

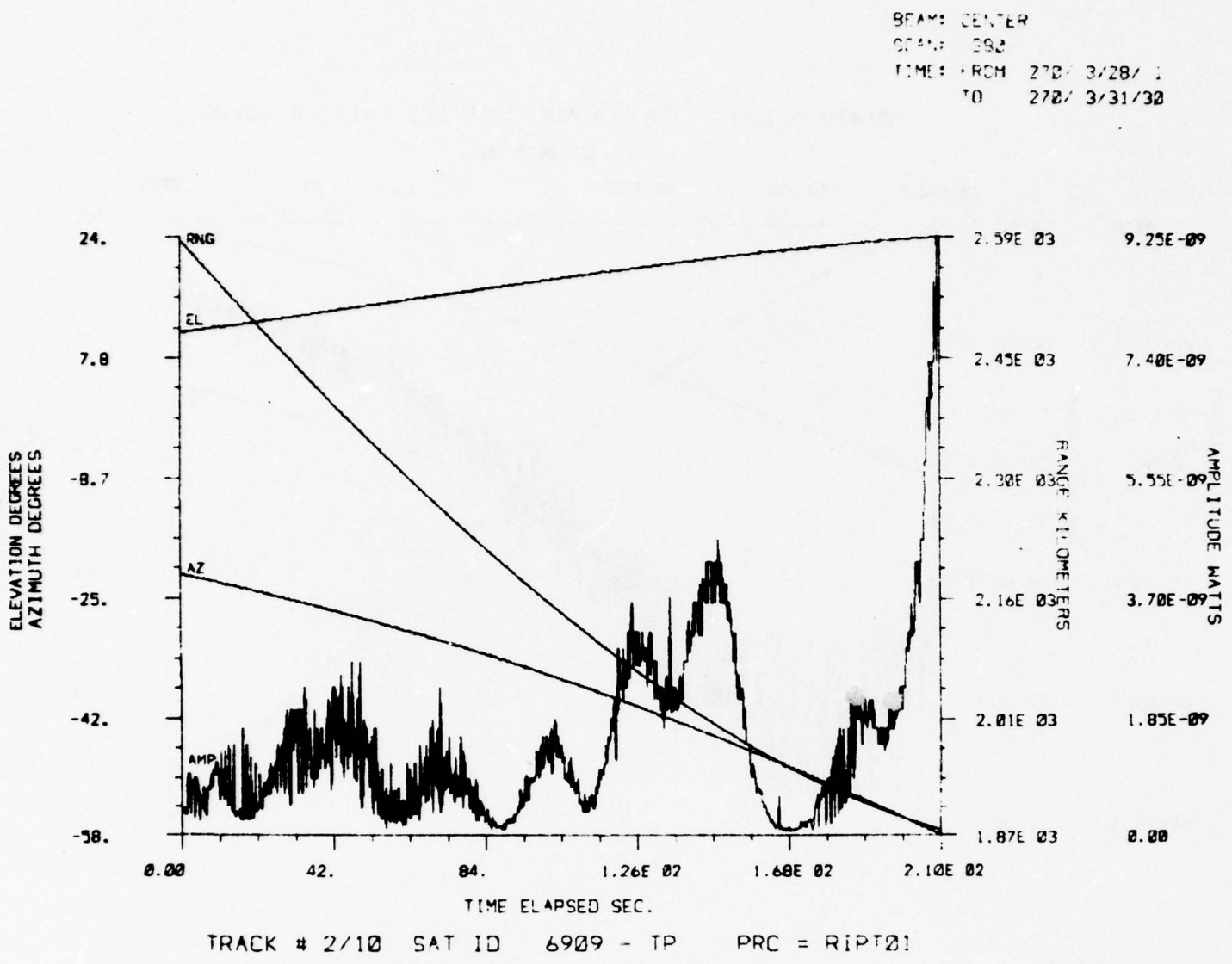
BEAM: CENTER
TIME: FROM 270/ 3/28/ 1
TO 270/ 3/31/30
24.
7.8
-8.7
-25.
-42.
-58.
RNG
EL
AZ
AMP
ELEVATION DEGREES
AZIMUTH DEGREES
2.59E 03
2.45E 03
2.30E 03
2.16E 03
2.01E 03
1.87E 03
RANGE KILOMETERS
9.25E-09
7.40E-09
5.55E-09
3.70E-09
1.85E-09
0.00
AMPLITUDE WATTS
0.00
42.
84.
1.26E 02
1.68E 02
2.10E 02
TIME ELAPSED SEC.
TRACK # 2/10 SAT ID 6909 - TP PRC = RIPT01

Figure A-20

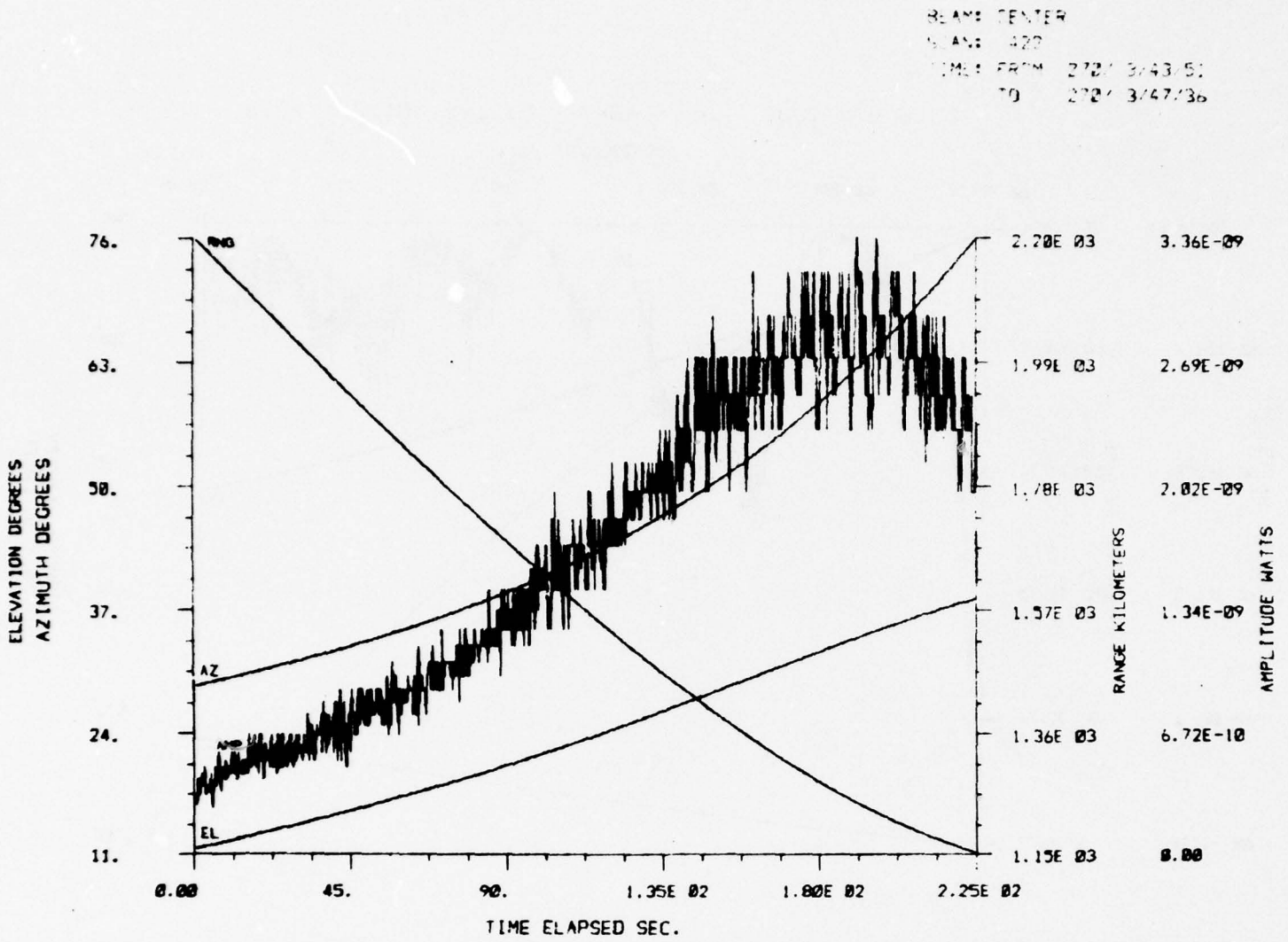
BEAM: CENTER
PLAN: 420
TIME: FROM 272/ 3:43:51
TO 272/ 3:47:36
76.
63.
50.
37.
24.
11.
ELEVATION DEGREES
AZIMUTH DEGREES
RNG
AZ
EL
2.20E 03
1.99E 03
1.78E 03
1.57E 03
1.36E 03
1.15E 03
RANGE KILOMETERS
3.36E-09
2.69E-09
2.02E-09
1.34E-09
6.72E-10
0.00
AMPLITUDE WATTS
0.00
45.
90.
1.35E 02
1.80E 02
2.25E 02
TIME ELAPSED SEC.
TRACK # 2/14 SAT ID 4963 - SS PRC = RIPTØ1

Figure A-21

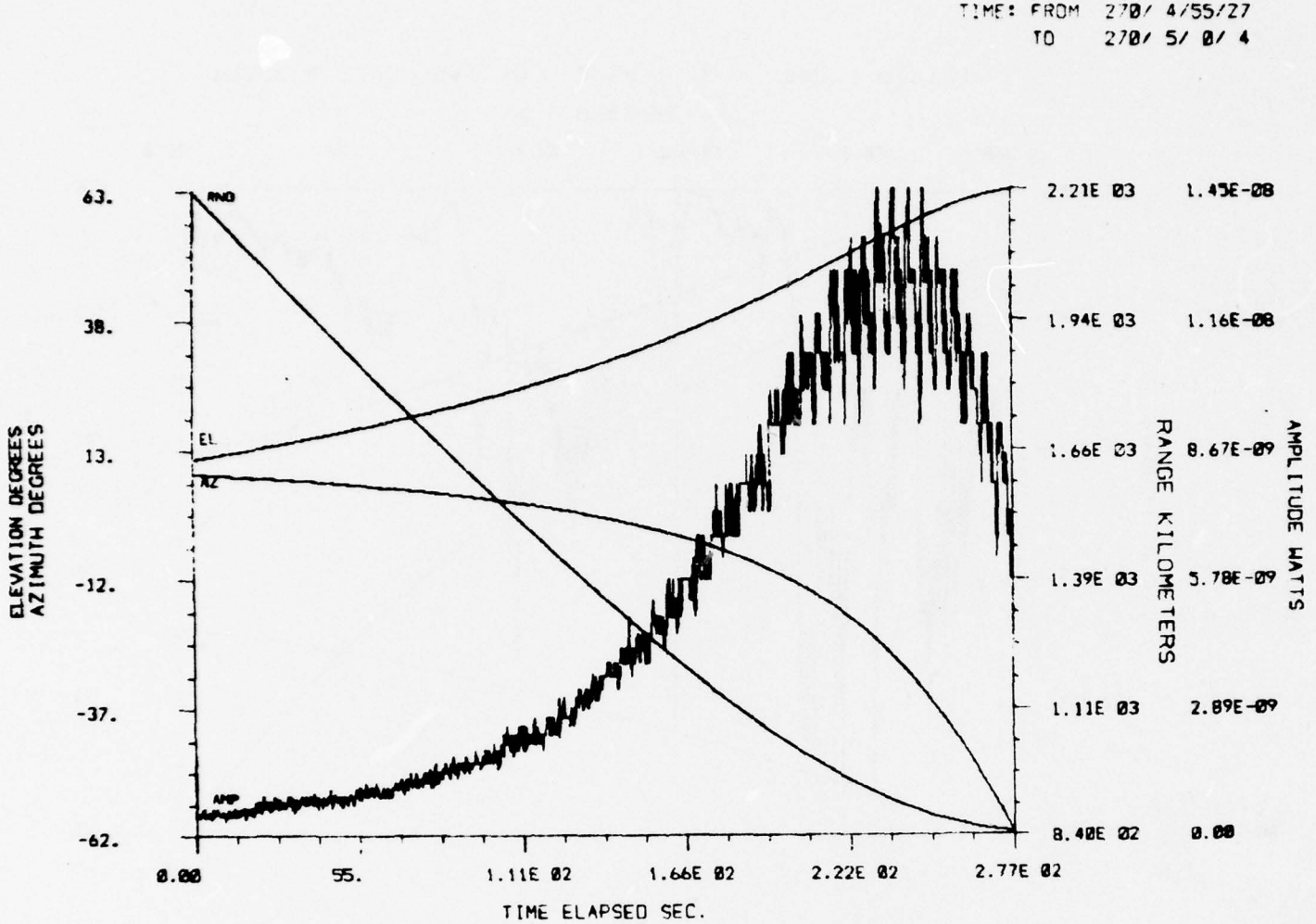
BEAM: CENTER
SCAN: 456
TIME: FROM 270/ 4/55/27
TO 270/ 5/ 0/ 4
63.
38.
13.
-12.
-37.
-62.
RNG
EL
AZ
AMP
ELEVATION DEGREES
AZIMUTH DEGREES
2.21E 03
1.94E 03
1.66E 03
1.39E 03
1.11E 03
8.40E 02
RANGE KILOMETERS
1.45E-08
1.16E-08
8.67E-09
5.78E-09
2.89E-09
0.00
AMPLITUDE WATTS
0.00
55.
1.11E 02
1.66E 02
2.22E 02
2.77E 02
TIME ELAPSED SEC.
TRACK # 2/18 SAT ID 4957 - SS PRC = RIPT01

Figure A-22

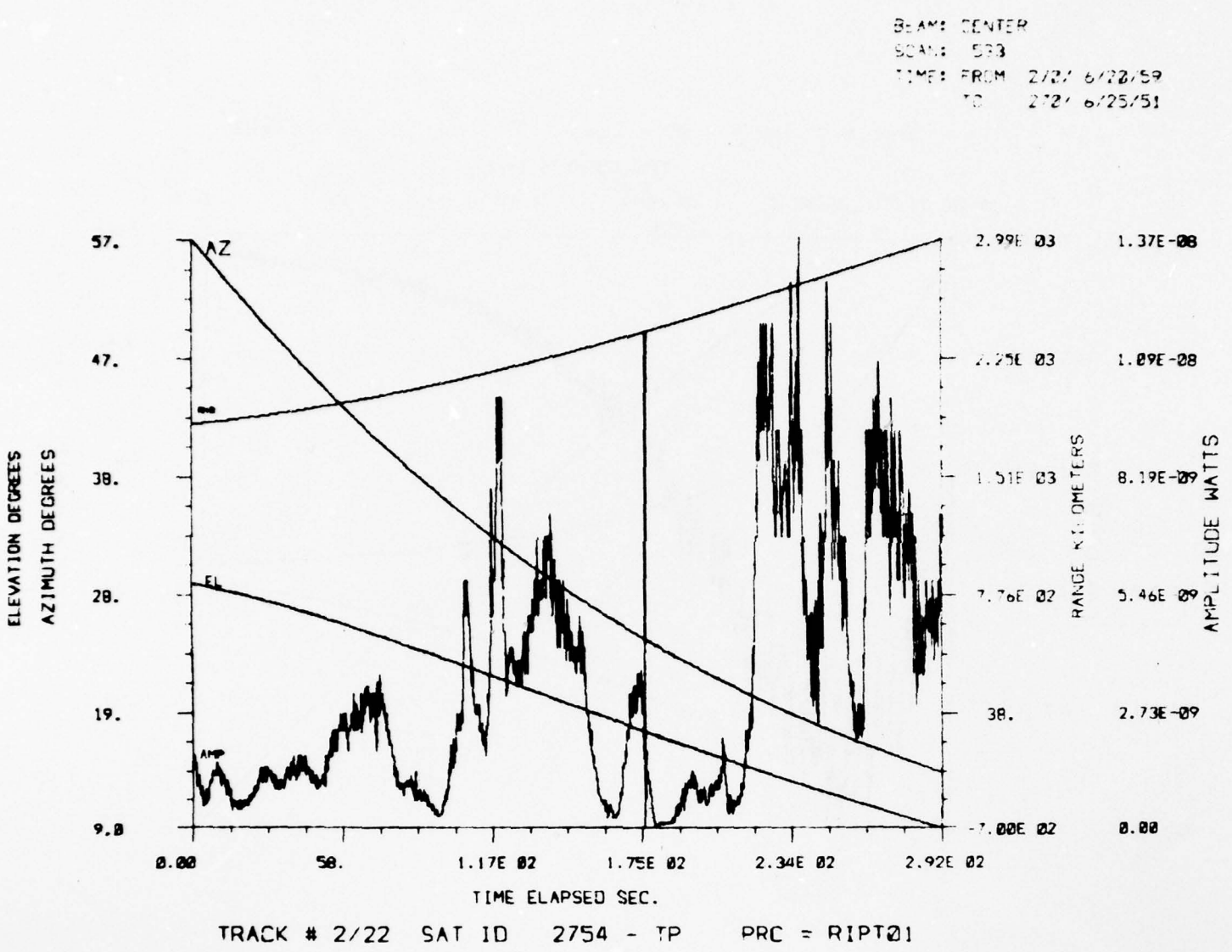
BEAM: CENTER
SCAN: 583
TIME: FROM 272/ 6/22/59
TO 272/ 6/25/51
57.
47.
38.
28.
19.
9.0
AZ
EL
AMP
2.99E 03
2.25E 03
1.51E 03
7.76E 02
38.
-7.00E 02
1.37E-08
1.09E-08
8.19E-09
5.46E-09
2.73E-09
0.00
ELEVATION DEGREES
AZIMUTH DEGREES
RANGE KILOMETERS
AMPLITUDE WATTS
0.00
58.
1.17E 02
1.75E 02
2.34E 02
2.92E 02
TIME ELAPSED SEC.
TRACK # 2/22 SAT ID 2754 - TP PRC = RIPT01

Figure A-23

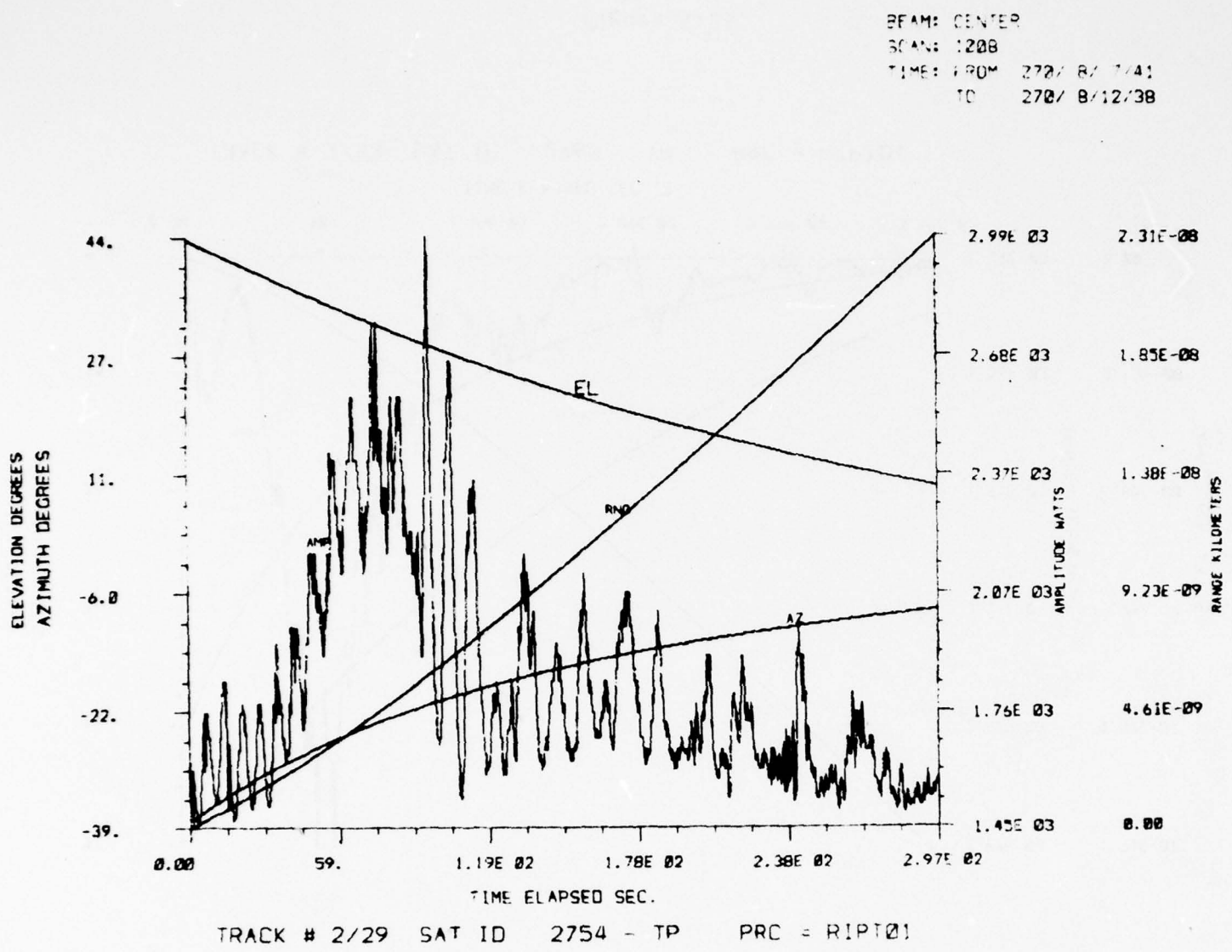
BEAM: CENTER
SCAN: 1208
TIME: FROM 270/ 8/ 7:41
TO 270/ 8/12:38
44.
27.
11.
-6.0
-22.
-39.
ELEVATION DEGREES
AZIMUTH DEGREES
EL
RNG
AMP
AZ
2.99E 03
2.68E 03
2.37E 03
2.07E 03
1.76E 03
1.45E 03
AMPLITUDE WATTS
2.31E-08
1.85E-08
1.38E-08
9.23E-09
4.61E-09
0.00
RANGE KILOMETERS
0.00
59.
1.19E 02
1.78E 02
2.38E 02
2.97E 02
TIME ELAPSED SEC.
TRACK # 2/29 SAT ID 2754 - TP PRC = RIPT01

Figure A-24

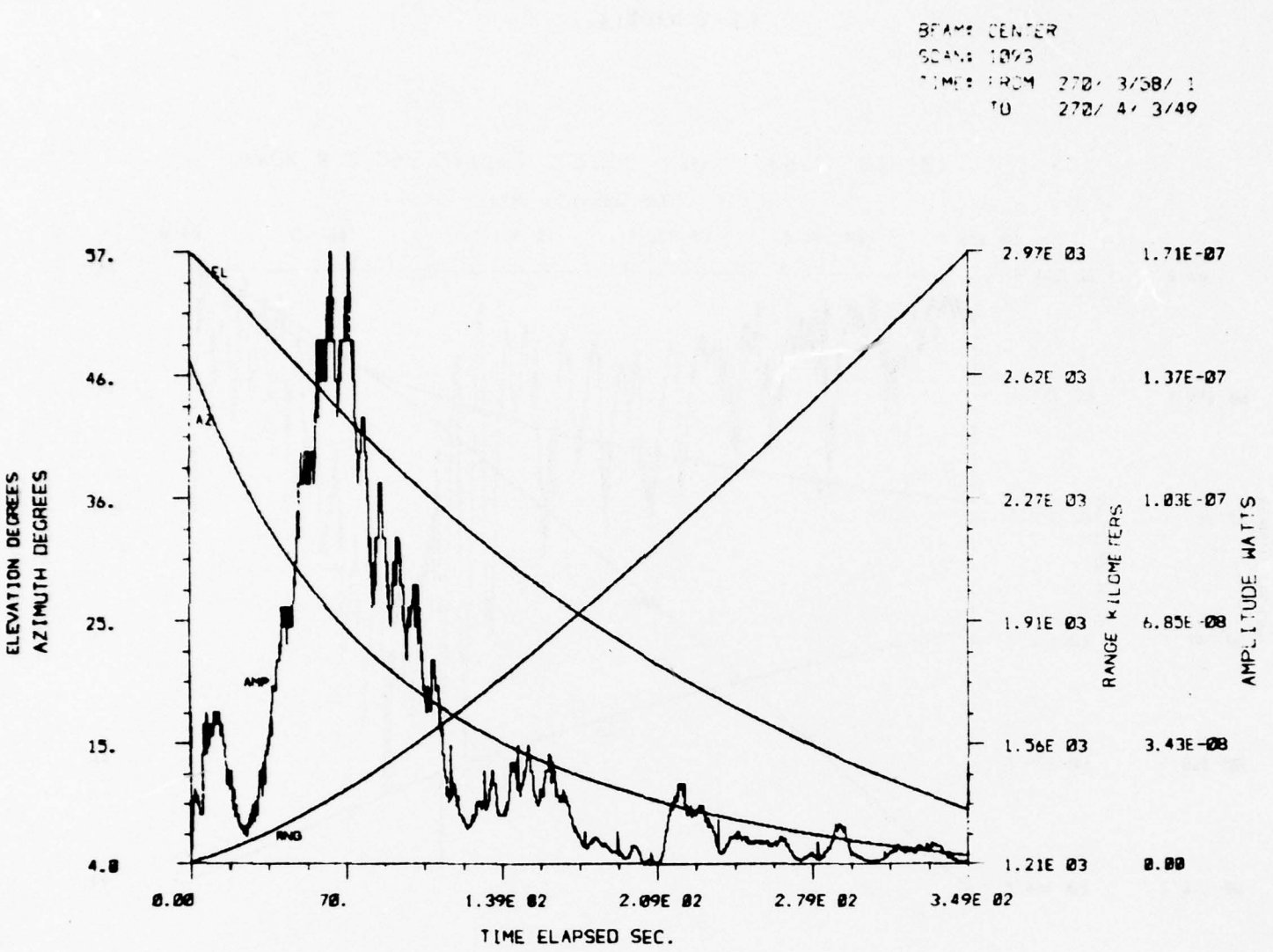
BEAM: CENTER
SCAN: 1063
TIME: FROM 270/ 3/58/ 1
TO 270/ 4/ 3/49
57.
46.
36.
25.
15.
4.8
EL
AZ
AMP
RNG
ELEVATION DEGREES
AZIMUTH DEGREES
2.97E 03
2.62E 03
2.27E 03
1.91E 03
1.56E 03
1.21E 03
RANGE KILOMETERS
1.71E-07
1.37E-07
1.03E-07
6.85E-08
3.43E-08
0.00
AMPLITUDE WATTS
0.00
70.
1.39E 02
2.09E 02
2.79E 02
3.49E 02
TIME ELAPSED SEC.
TRACK # 2/33 SAT ID 2965 - TP PRC = RIPT01

Figure A-25

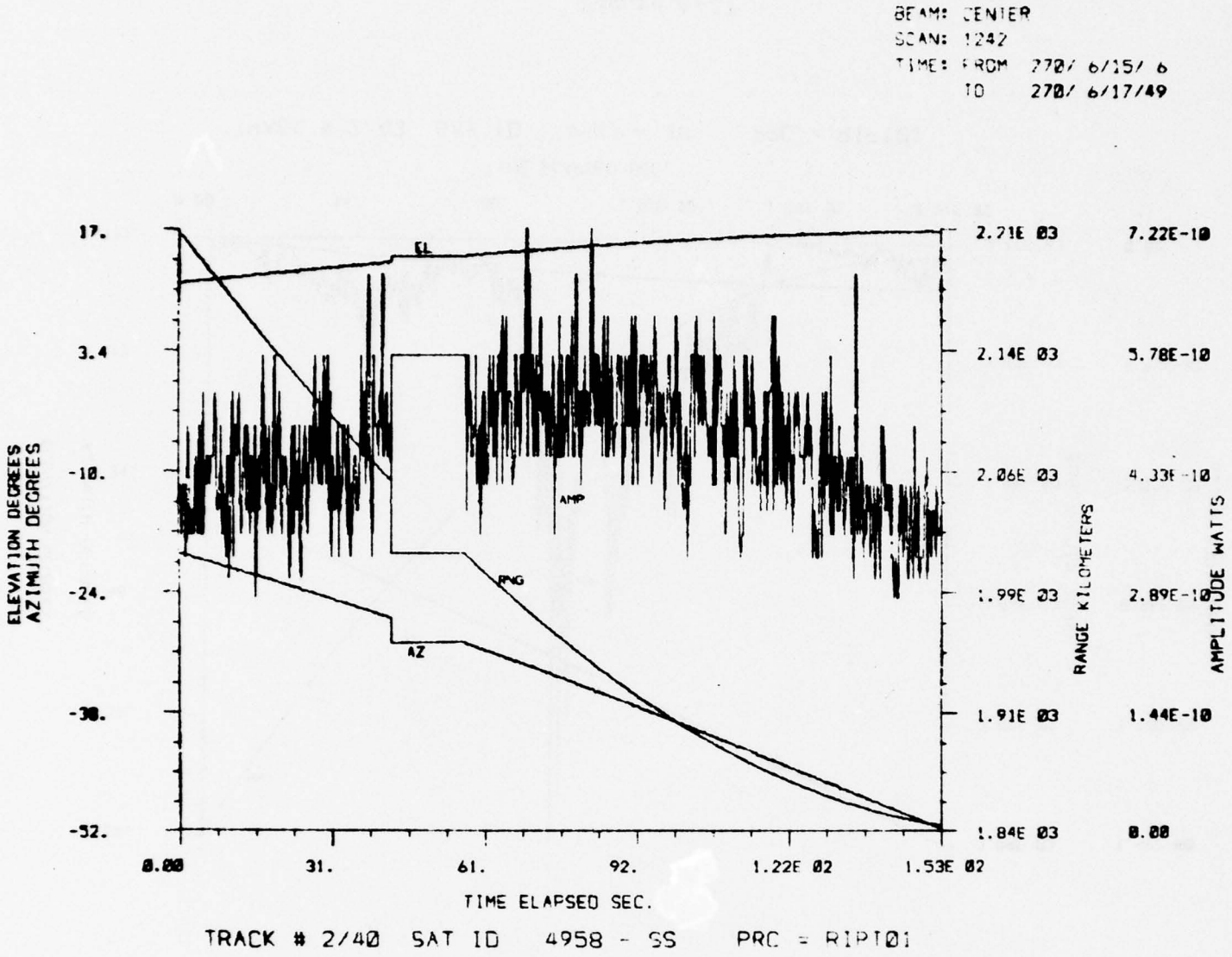
BEAM: CENTER
SCAN: 1242
TIME: FROM 270/ 6/15/ 6
TO 270/ 6/17/49
17.
3.4
-10.
-24.
-38.
-52.
EL
AMP
RNG
AZ
2.21E 03
2.14E 03
2.06E 03
1.99E 03
1.91E 03
1.84E 03
7.22E-10
5.78E-10
4.33E-10
2.89E-10
1.44E-10
0.00
0.00
31.
61.
92.
1.22E 02
1.53E 02
ELEVATION DEGREES
AZIMUTH DEGREES
RANGE KILOMETERS
AMPLITUDE WATTS
TIME ELAPSED SEC.
TRACK # 2/40 SAT ID 4958 - SS PRC = RIPI01

Figure A-26

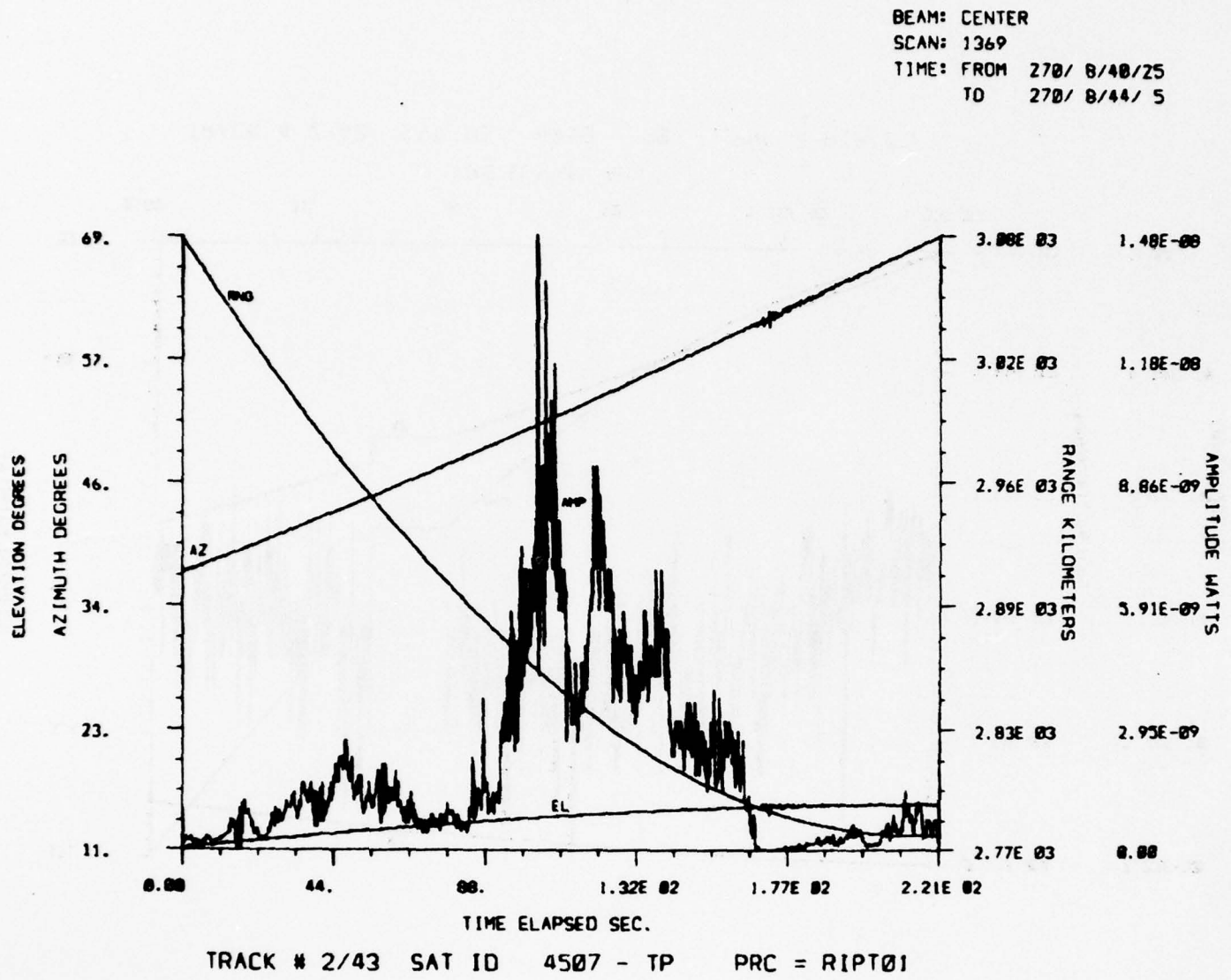
BEAM: CENTER
SCAN: 1369
TIME: FROM 270/ 0/40/25
TO 270/ 0/44/ 5
69.
57.
46.
34.
23.
11.
ELEVATION DEGREES
AZIMUTH DEGREES
RNG
AZ
AMP
EL
3.08E 03
3.02E 03
2.96E 03
2.89E 03
2.83E 03
2.77E 03
RANGE KILOMETERS
1.48E-08
1.18E-08
8.86E-09
5.91E-09
2.95E-09
0.00
AMPLITUDE WATTS
0.00
44.
88.
1.32E 02
1.77E 02
2.21E 02
TIME ELAPSED SEC.
TRACK # 2/43 SAT ID 4507 - TP PRC = RIPT01

Figure A-27

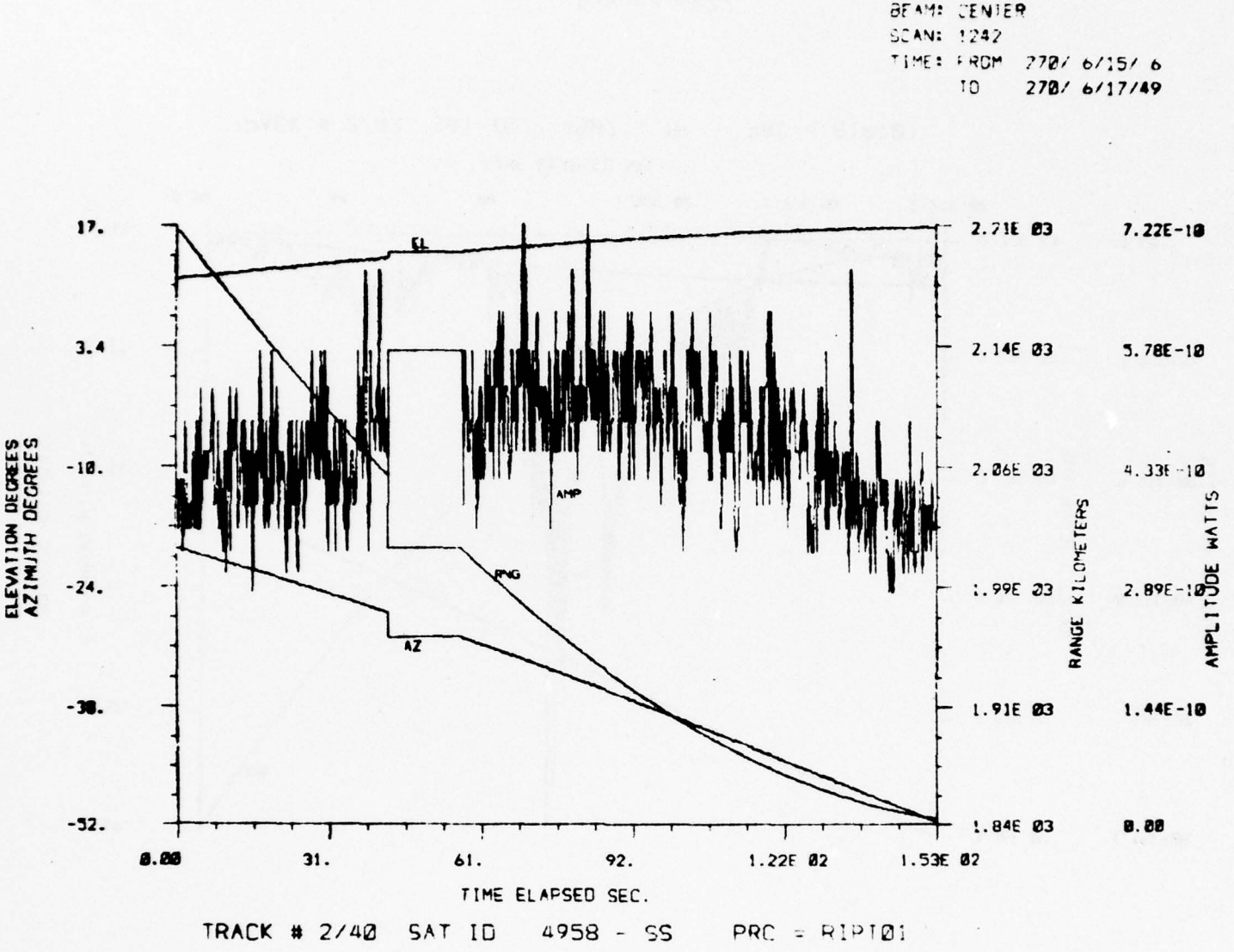
BEAM: CENTER
SCAN: 1242
TIME: FROM 270/ 6/15/ 6
TO 270/ 6/17/49
17.
3.4
-10.
-24.
-38.
-52.
EL
AMP
RNG
AZ
ELEVATION DEGREES
AZIMUTH DEGREES
2.21E 03
2.14E 03
2.06E 03
1.99E 03
1.91E 03
1.84E 03
RANGE KILOMETERS
7.22E-10
5.78E-10
4.33E-10
2.89E-10
1.44E-10
0.00
AMPLITUDE WATTS
0.00
31.
61.
92.
1.22E 02
1.53E 02
TIME ELAPSED SEC.
TRACK # 2/40 SAT ID 4958 - SS PRC = RIPI01

Figure A-26

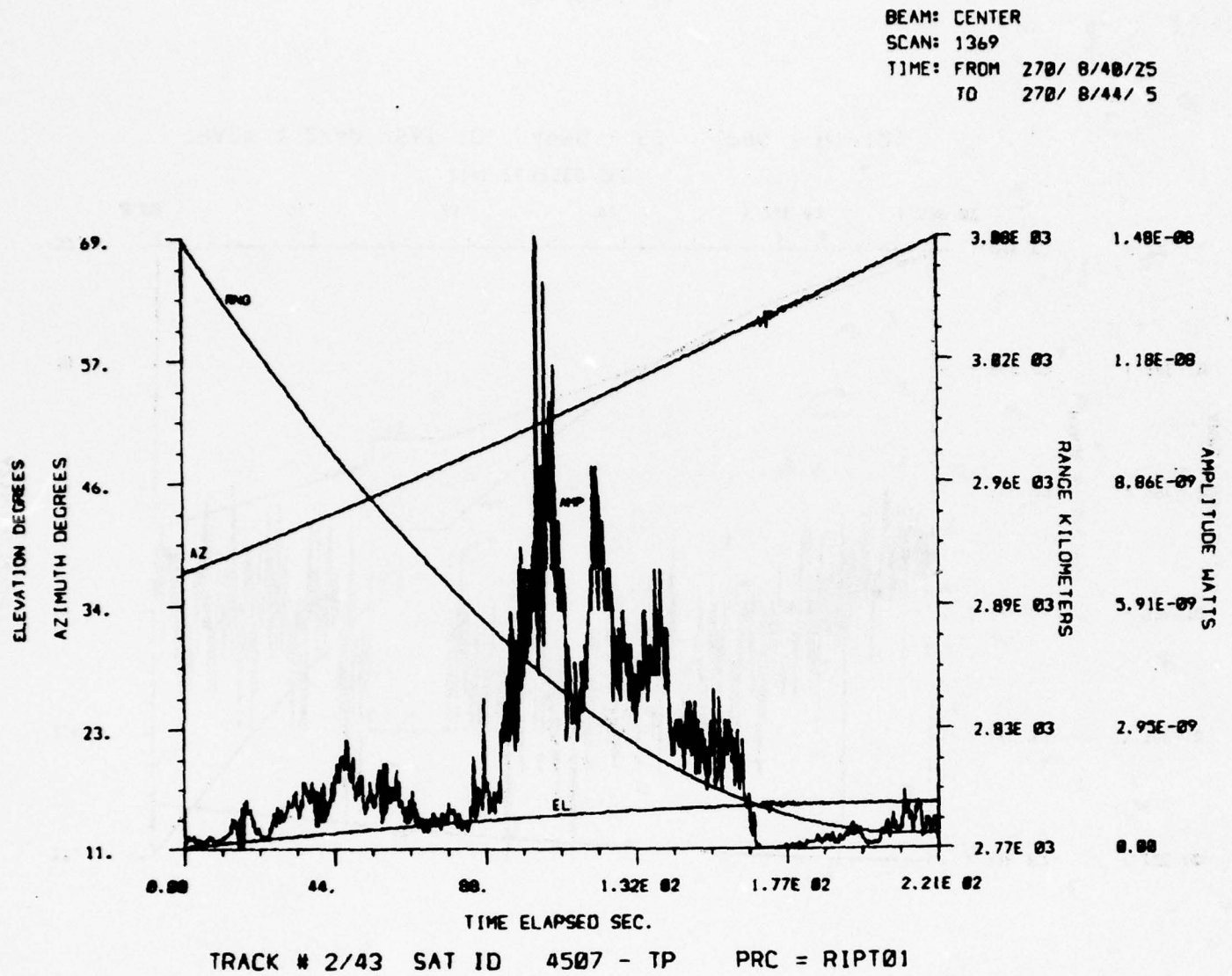
BEAM: CENTER
SCAN: 1369
TIME: FROM 270/ 8/40/25
TO 270/ 8/44/ 5
69.
57.
46.
34.
23.
11.
ELEVATION DEGREES
AZIMUTH DEGREES
RNG
AZ
AMP
EL
3.08E 03
3.02E 03
2.96E 03
2.89E 03
2.83E 03
2.77E 03
RANGE KILOMETERS
1.48E-08
1.18E-08
8.86E-09
5.91E-09
2.93E-09
0.00
AMPLITUDE WATTS
0.00
44.
88.
1.32E 02
1.77E 02
2.21E 02
TIME ELAPSED SEC.
TRACK # 2/43 SAT ID 4507 - TP PRC = RIPT01

Figure A-27

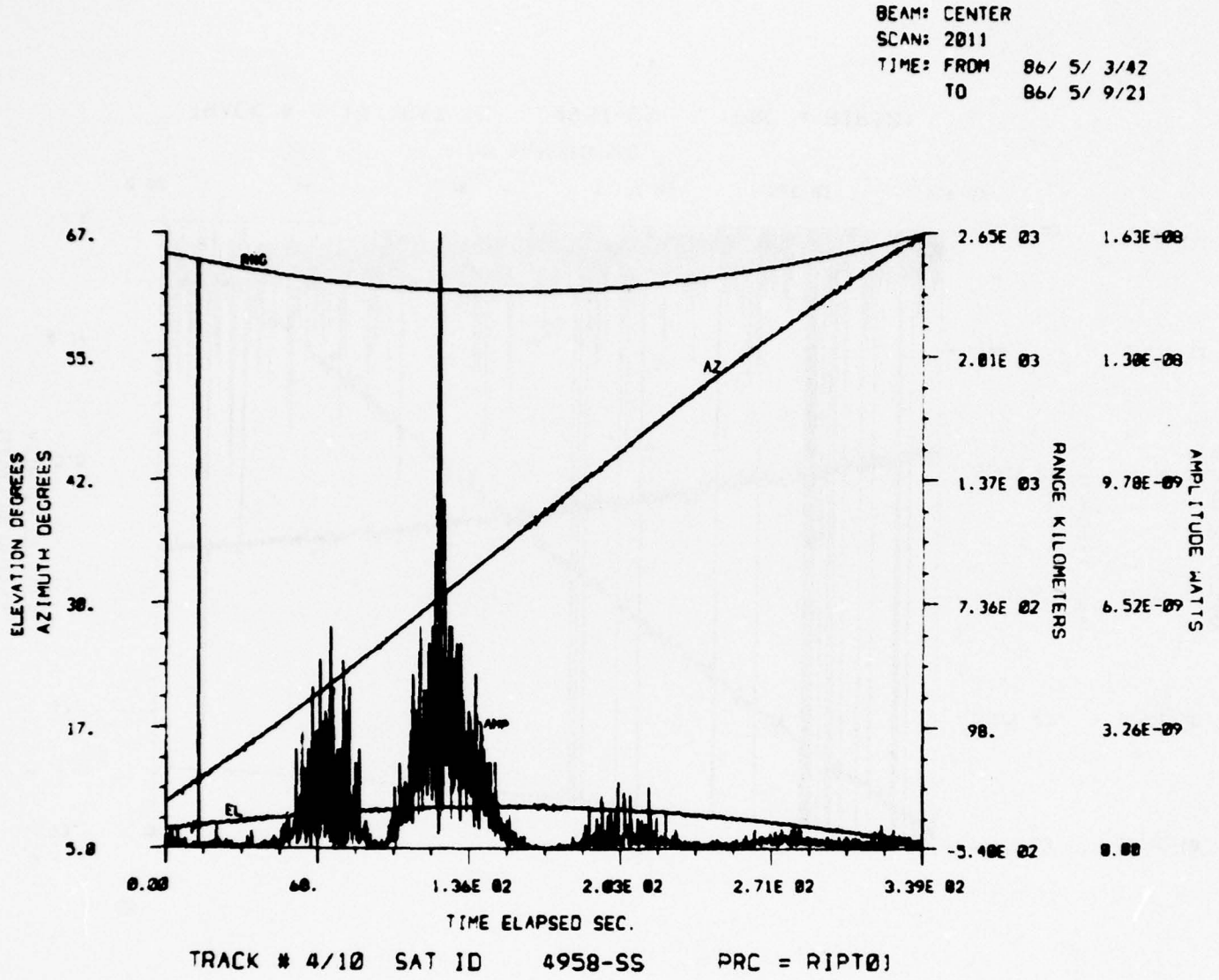
BEAM: CENTER
SCAN: 2011
TIME: FROM 86/ 5/ 3/42
TO 86/ 5/ 9/21
67.
55.
42.
30.
17.
5.0
ELEVATION DEGREES
AZIMUTH DEGREES
RNG
AZ
AMP
EL
2.65E 03
2.01E 03
1.37E 03
7.36E 02
98.
-5.40E 02
RANGE KILOMETERS
1.63E-08
1.30E-08
9.78E-09
6.52E-09
3.26E-09
0.00
AMPLITUDE WATTS
0.00
68.
1.36E 02
2.03E 02
2.71E 02
3.39E 02
TIME ELAPSED SEC.
TRACK # 4/10 SAT ID 4958-SS PRC = RIPT01

Figure A-28

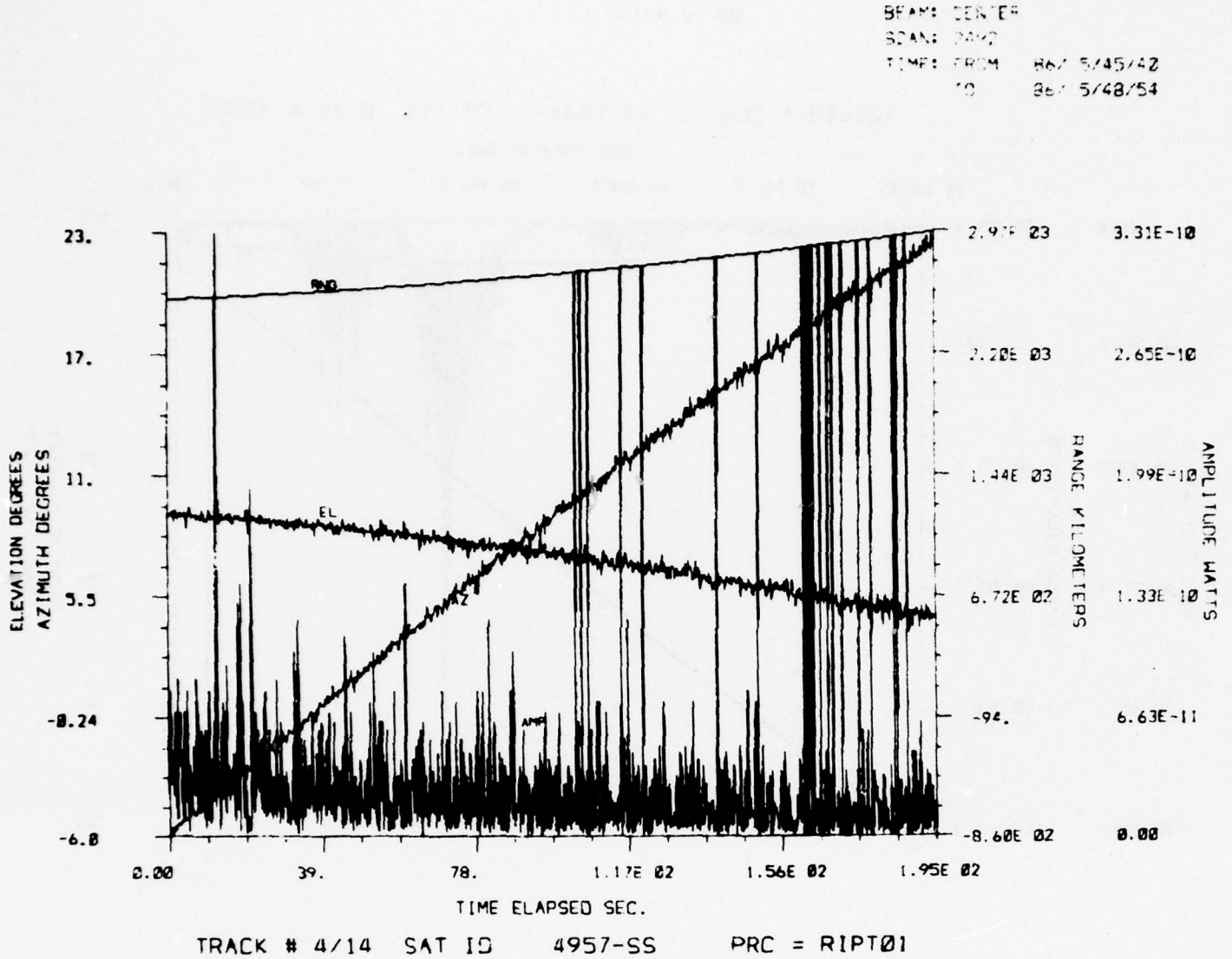
BEAM: CENTER
SCAN: ZONE
TIME: FROM 86/ 5/45/42
TO 86/ 5/48/54
23.
17.
11.
5.5
-8.24
-6.8
ELEVATION DEGREES
AZIMUTH DEGREES
RNG
EL
AZ
AMP
2.97E 03
2.20E 03
1.44E 03
6.72E 02
-94.
-8.60E 02
RANGE KILOMETERS
3.31E-10
2.65E-10
1.99E-10
1.33E-10
6.63E-11
0.00
AMPLITUDE WATTS
0.00
39.
78.
1.17E 02
1.56E 02
1.95E 02
TIME ELAPSED SEC.
TRACK # 4/14 SAT ID 4957-SS PRC = RIPT01

Figure A-29

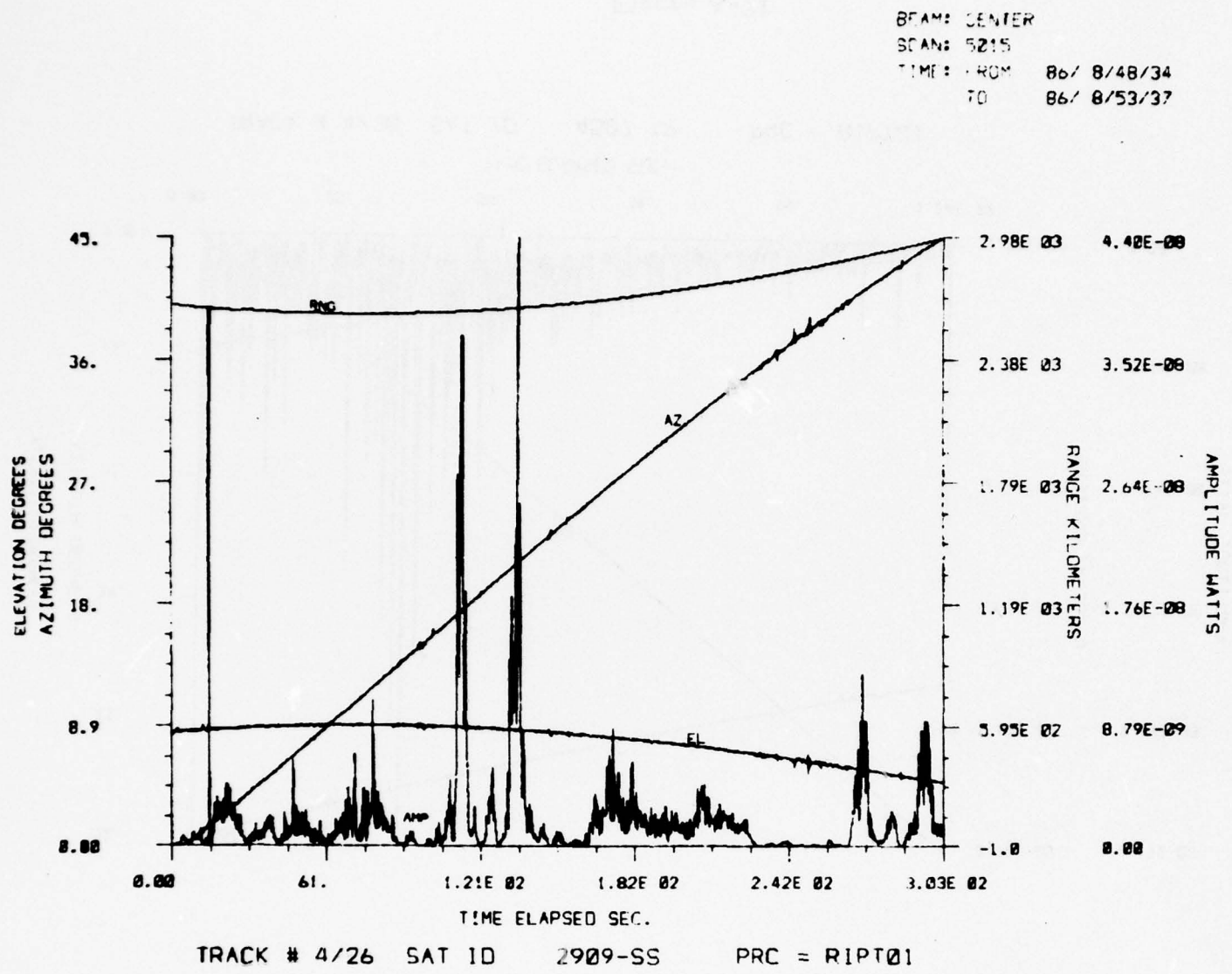
BEAM: CENTER
SCAN: 5215
TIME: FROM 86/ 8/48/34
TO 86/ 8/53/37
45.
36.
27.
18.
8.9
0.00
RNG
AZ
EL
AMP
2.98E 03
2.38E 03
1.79E 03
1.19E 03
5.95E 02
-1.0
4.40E-08
3.52E-08
2.64E-08
1.76E-08
8.79E-09
0.00
ELEVATION DEGREES
AZIMUTH DEGREES
RANGE KILOMETERS
AMPLITUDE WATTS
0.00
61.
1.21E 02
1.82E 02
2.42E 02
3.03E 02
TIME ELAPSED SEC.
TRACK # 4/26 SAT ID 2909-SS PRC = RIPT01

Figure A-30

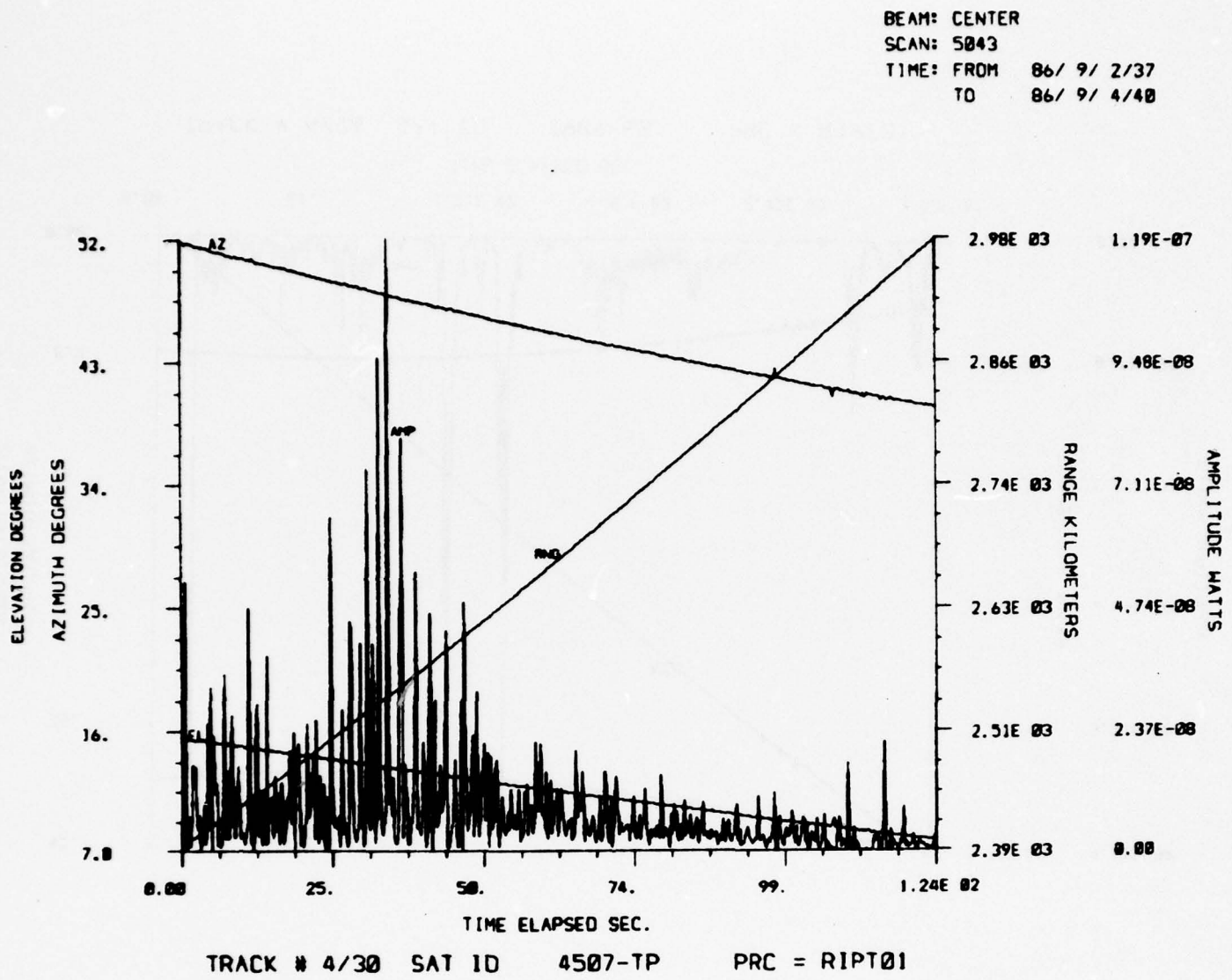
BEAM: CENTER
SCAN: 5043
TIME: FROM 86/ 9/ 2/37
TO 86/ 9/ 4/40
AZ
AMP
RNG
EL
52.
43.
34.
25.
16.
7.8
ELEVATION DEGREES
AZIMUTH DEGREES
2.98E 03
2.86E 03
2.74E 03
2.63E 03
2.51E 03
2.39E 03
RANGE KILOMETERS
1.19E-07
9.48E-08
7.11E-08
4.74E-08
2.37E-08
0.00
AMPLITUDE WATTS
0.00
25.
50.
74.
99.
1.24E 02
TIME ELAPSED SEC.
TRACK # 4/30 SAT ID 4507-TP PRC = RIPT01

Figure A-31

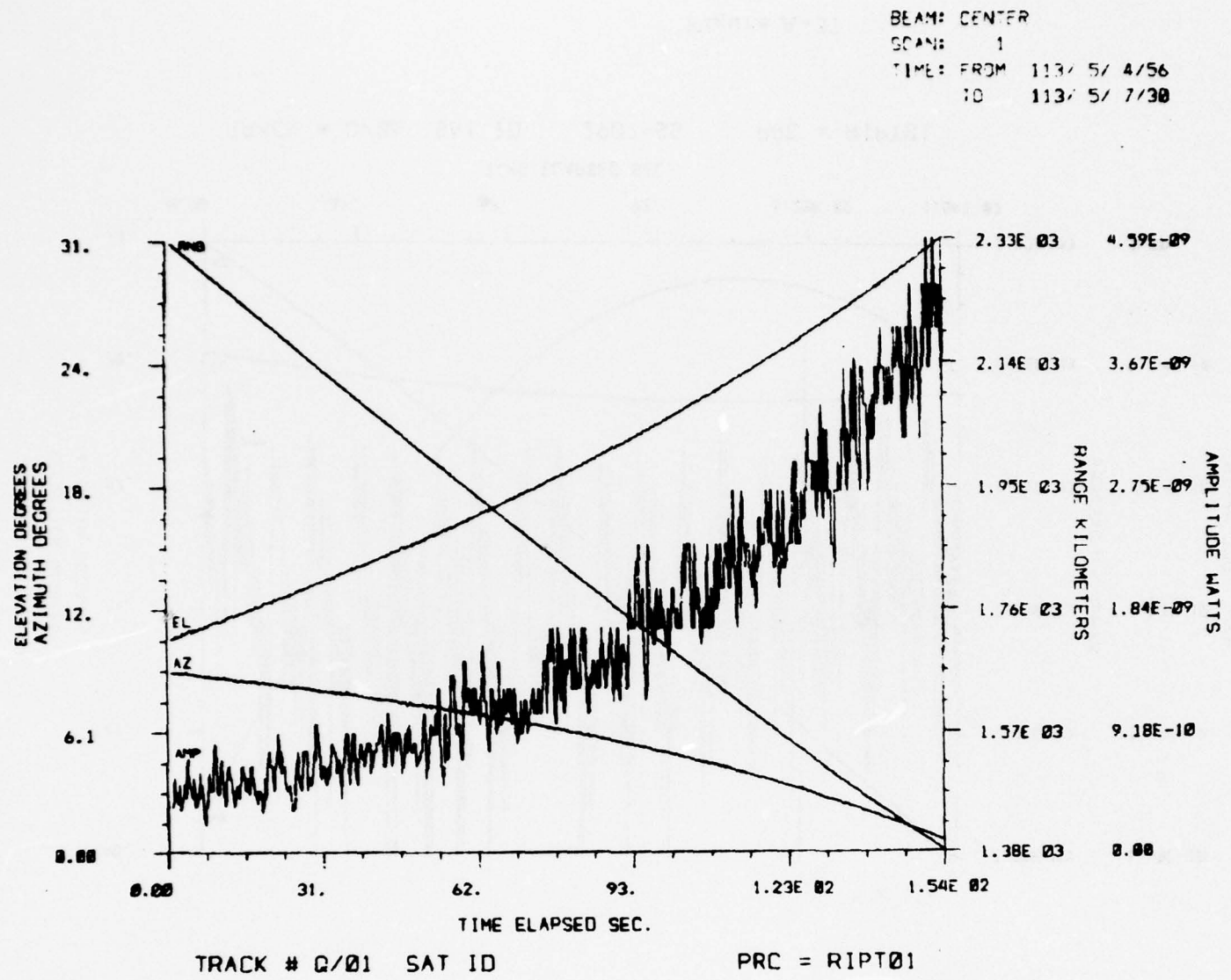
BEAM: CENTER
SCAN: 1
TIME: FROM 113/ 5/ 4/56
TO 113/ 5/ 7/30
31.
24.
18.
12.
6.1
0.00
ELEVATION DEGREES
AZIMUTH DEGREES
EL
AZ
AMP
0.00
31.
62.
93.
1.23E 02
1.54E 02
TIME ELAPSED SEC.
2.33E 03
2.14E 03
1.95E 03
1.76E 03
1.57E 03
1.38E 03
RANGE KILOMETERS
4.59E-09
3.67E-09
2.75E-09
1.84E-09
9.18E-10
0.00
AMPLITUDE WATTS
TRACK # Q/01 SAT ID
PRC = RIPT01

Figure A-32

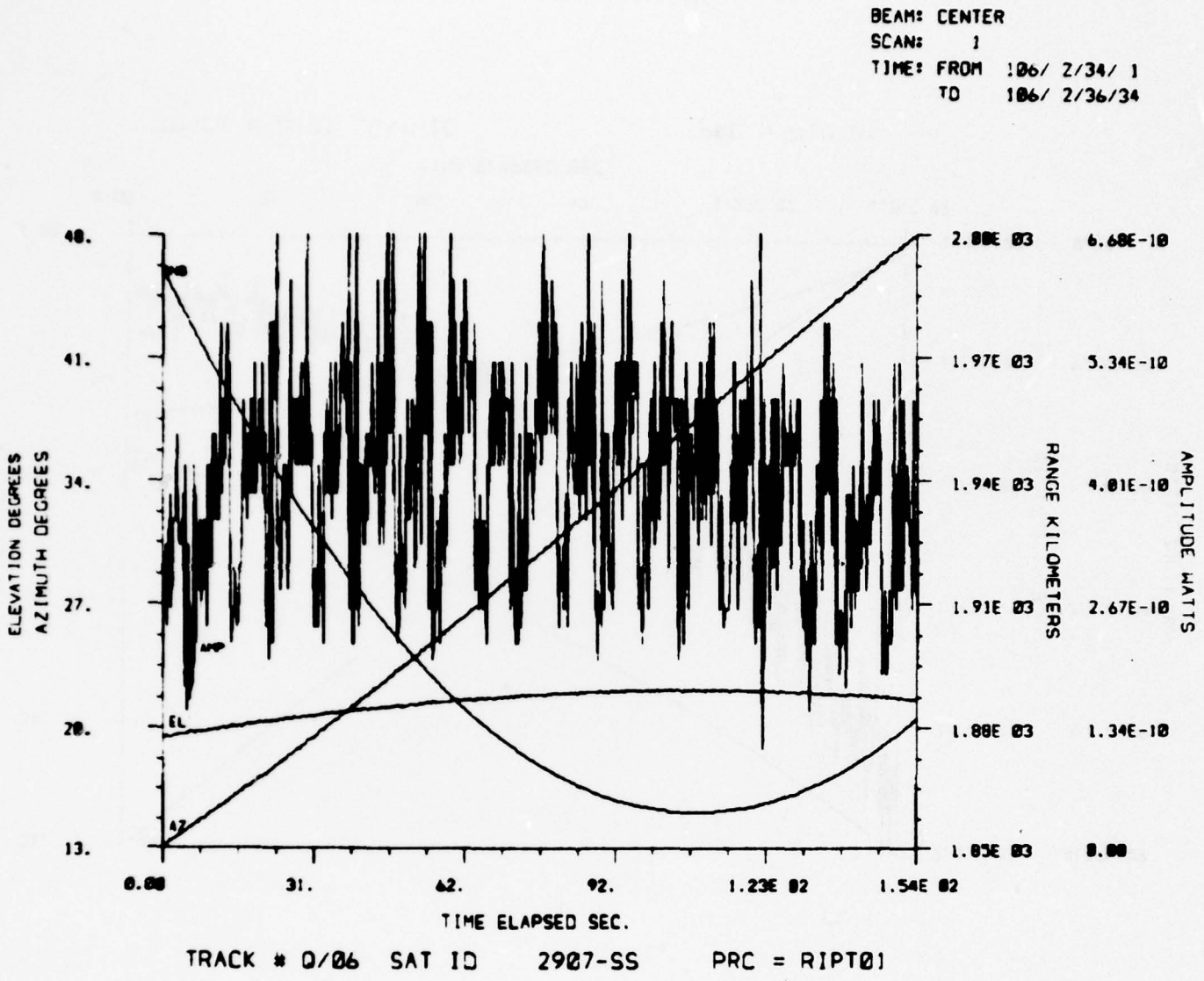
BEAM: CENTER
SCAN: 1
TIME: FROM 106/ 2/34/ 1
TO 106/ 2/36/34
48.
41.
34.
27.
20.
13.
EL
AZ
2.00E 03
1.97E 03
1.94E 03
1.91E 03
1.88E 03
1.85E 03
6.68E-10
5.34E-10
4.01E-10
2.67E-10
1.34E-10
0.00
0.00
31.
62.
92.
1.23E 02
1.54E 02
ELEVATION DEGREES
AZIMUTH DEGREES
RANGE KILOMETERS
AMPLITUDE WATTS
TIME ELAPSED SEC.
TRACK # 0/06 SAT ID 2907-SS PRC = RIPT01

Figure A-33

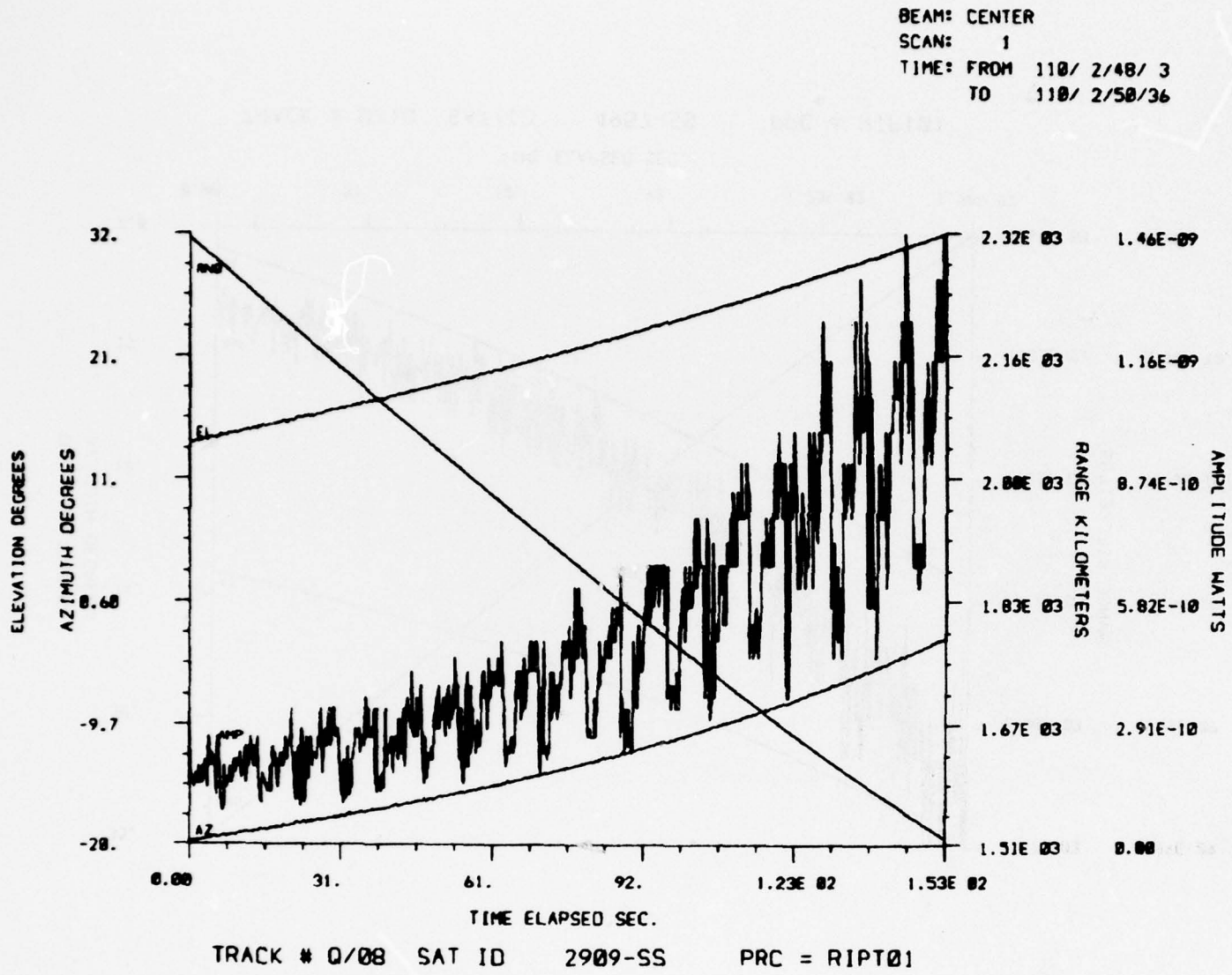
BEAM: CENTER
SCAN: 1
TIME: FROM 110/ 2/48/ 3
TO 110/ 2/50/36
32.
21.
11.
0.60
-9.7
-20.
ELEVATION DEGREES
AZIMUTH DEGREES
EL
AZ
2.32E 03
2.16E 03
2.00E 03
1.83E 03
1.67E 03
1.51E 03
RANGE KILOMETERS
1.46E-09
1.16E-09
8.74E-10
5.82E-10
2.91E-10
0.00
AMPLITUDE WATTS
0.00
31.
61.
92.
1.23E 02
1.53E 02
TIME ELAPSED SEC.
TRACK # 0/08 SAT ID 2909-SS PRC = RIPT01

Figure A-34

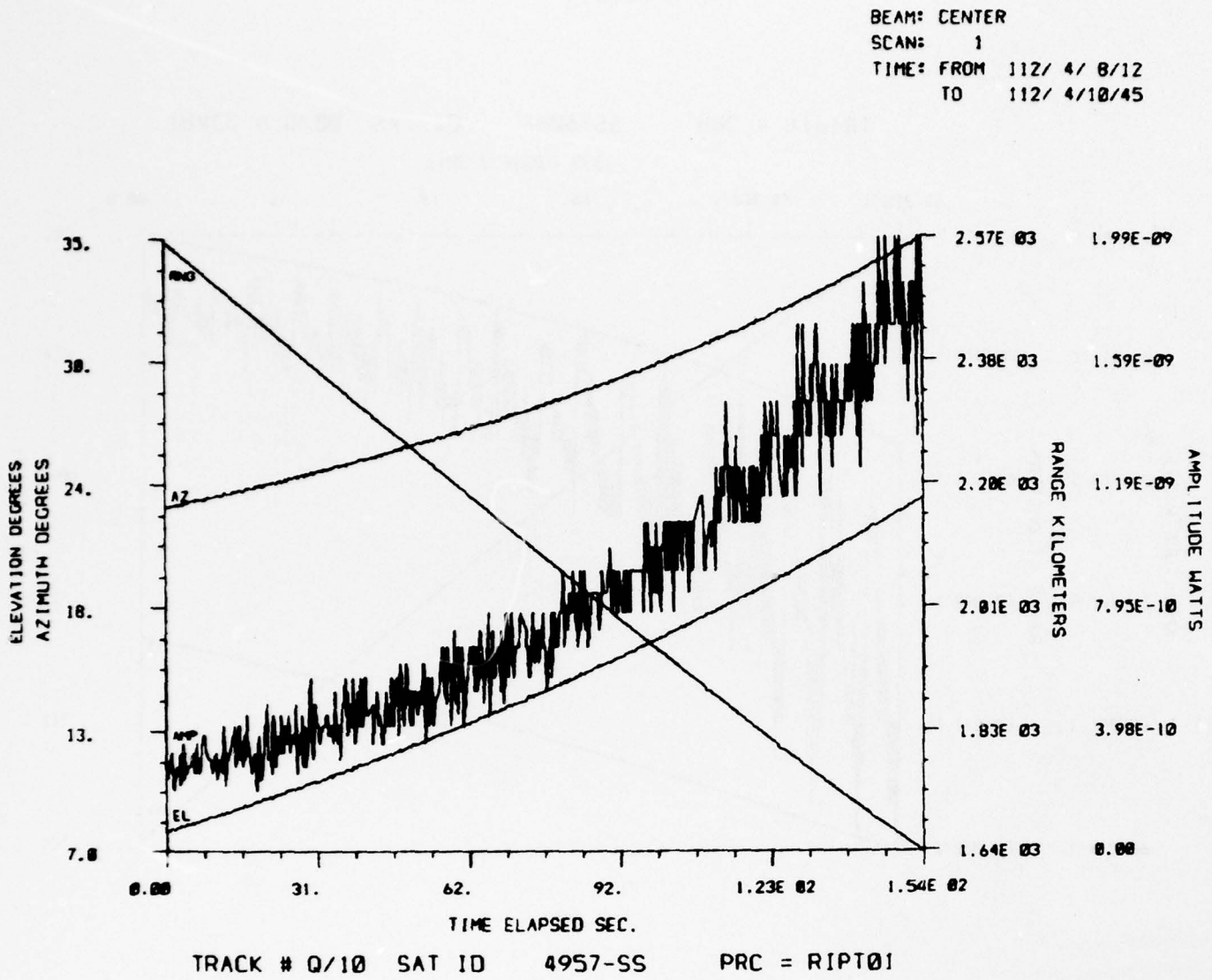
BEAM: CENTER
SCAN: 1
TIME: FROM 112/ 4/ 8/12
TO 112/ 4/10/45
35.
30.
24.
18.
13.
7.0
ELEVATION DEGREES
AZIMUTH DEGREES
AZ
EL
2.57E 03
2.38E 03
2.20E 03
2.01E 03
1.83E 03
1.64E 03
RANGE KILOMETERS
1.99E-09
1.59E-09
1.19E-09
7.95E-10
3.98E-10
0.00
AMPLITUDE WATTS
0.00
31.
62.
92.
1.23E 02
1.54E 02
TIME ELAPSED SEC.
TRACK # 0/10 SAT ID 4957-SS PRC = RIPT01

Figure A-35

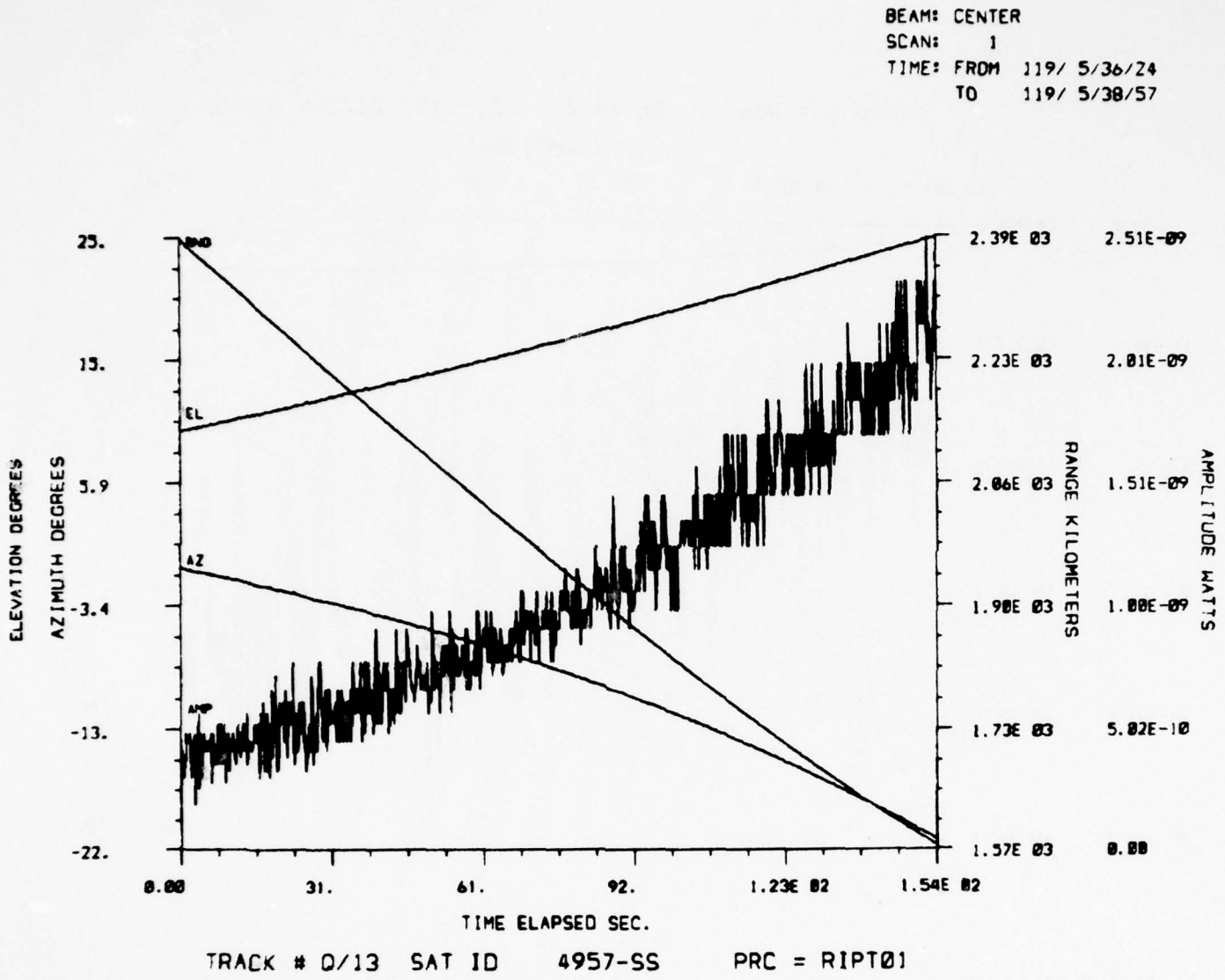
BEAM: CENTER
SCAN: 1
TIME: FROM 119/ 5/36/24
TO 119/ 5/38/57
25.
15.
5.9
-3.4
-13.
-22.
ELEVATION DEGREES
AZIMUTH DEGREES
EL
AZ
AMP
2.39E 03
2.23E 03
2.06E 03
1.90E 03
1.73E 03
1.57E 03
RANGE KILOMETERS
2.51E-09
2.01E-09
1.51E-09
1.00E-09
5.02E-10
0.00
AMPLITUDE WATTS
0.00
31.
61.
92.
1.23E 02
1.54E 02
TIME ELAPSED SEC.
TRACK # 0/13 SAT ID 4957-SS PRC = RIPT01

Figure A-36

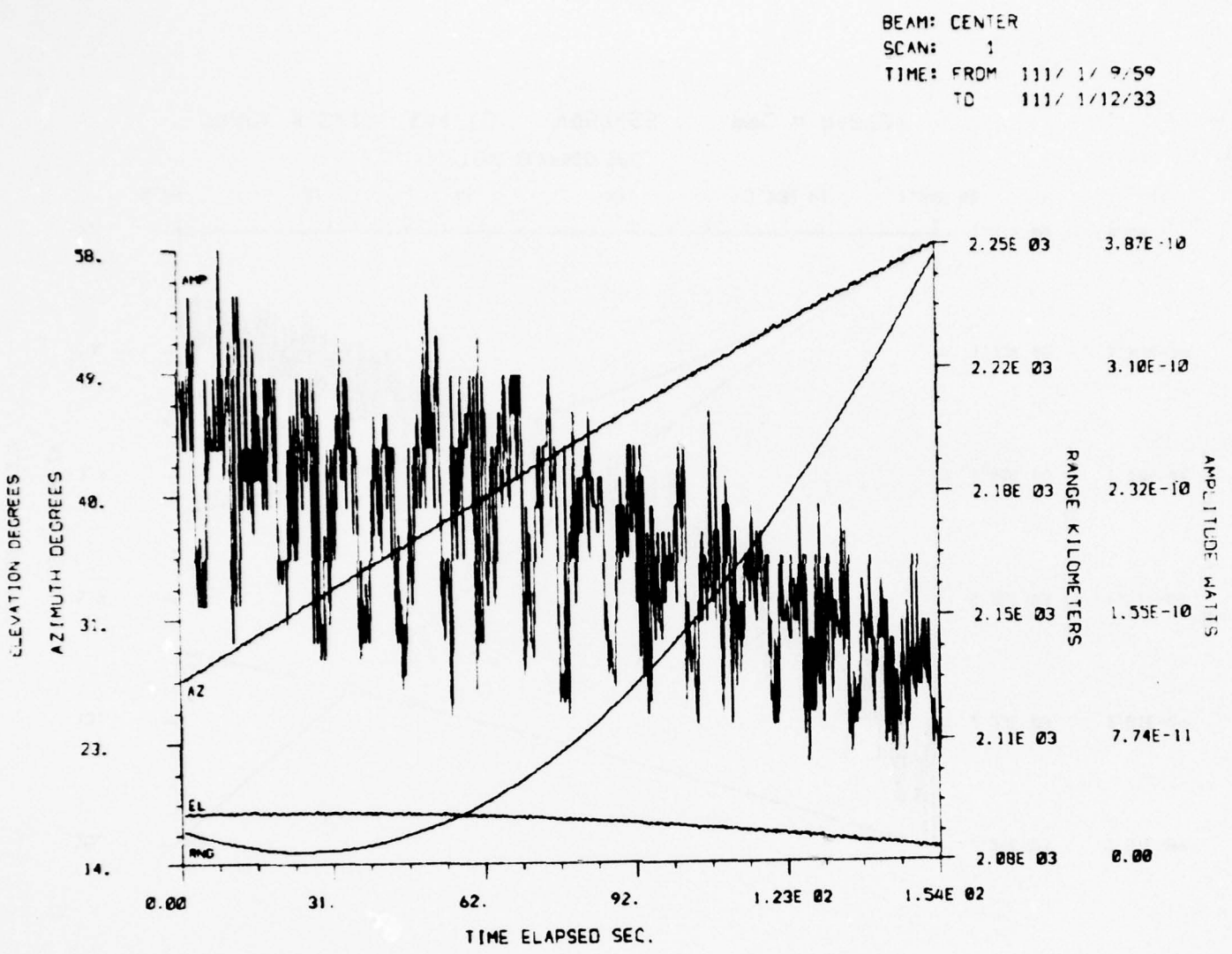

Figure A-37

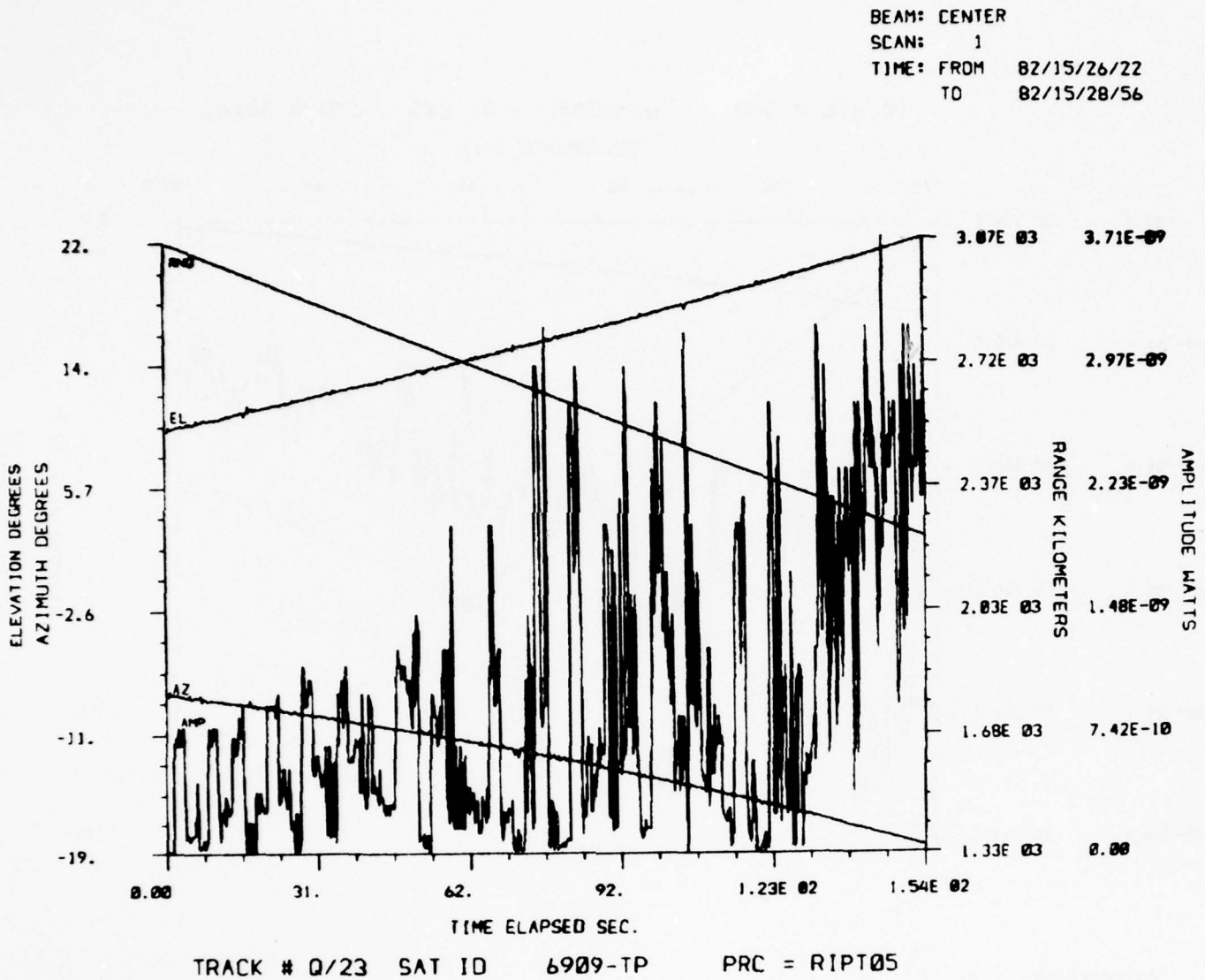
BEAM: CENTER
SCAN: 1
TIME: FROM 82/15/26/22
TO 82/15/28/56
22.
14.
5.7
-2.6
-11.
-19.
EL
AZ
AMP
ELEVATION DEGREES
AZIMUTH DEGREES
3.07E 03
2.72E 03
2.37E 03
2.03E 03
1.68E 03
1.33E 03
RANGE KILOMETERS
3.71E-09
2.97E-09
2.23E-09
1.48E-09
7.42E-10
0.00
AMPLITUDE WATTS
0.00
31.
62.
92.
1.23E 02
1.54E 02
TIME ELAPSED SEC.
TRACK # Q/23 SAT ID 6909-TP PRC = RIPT05

Figure A-38

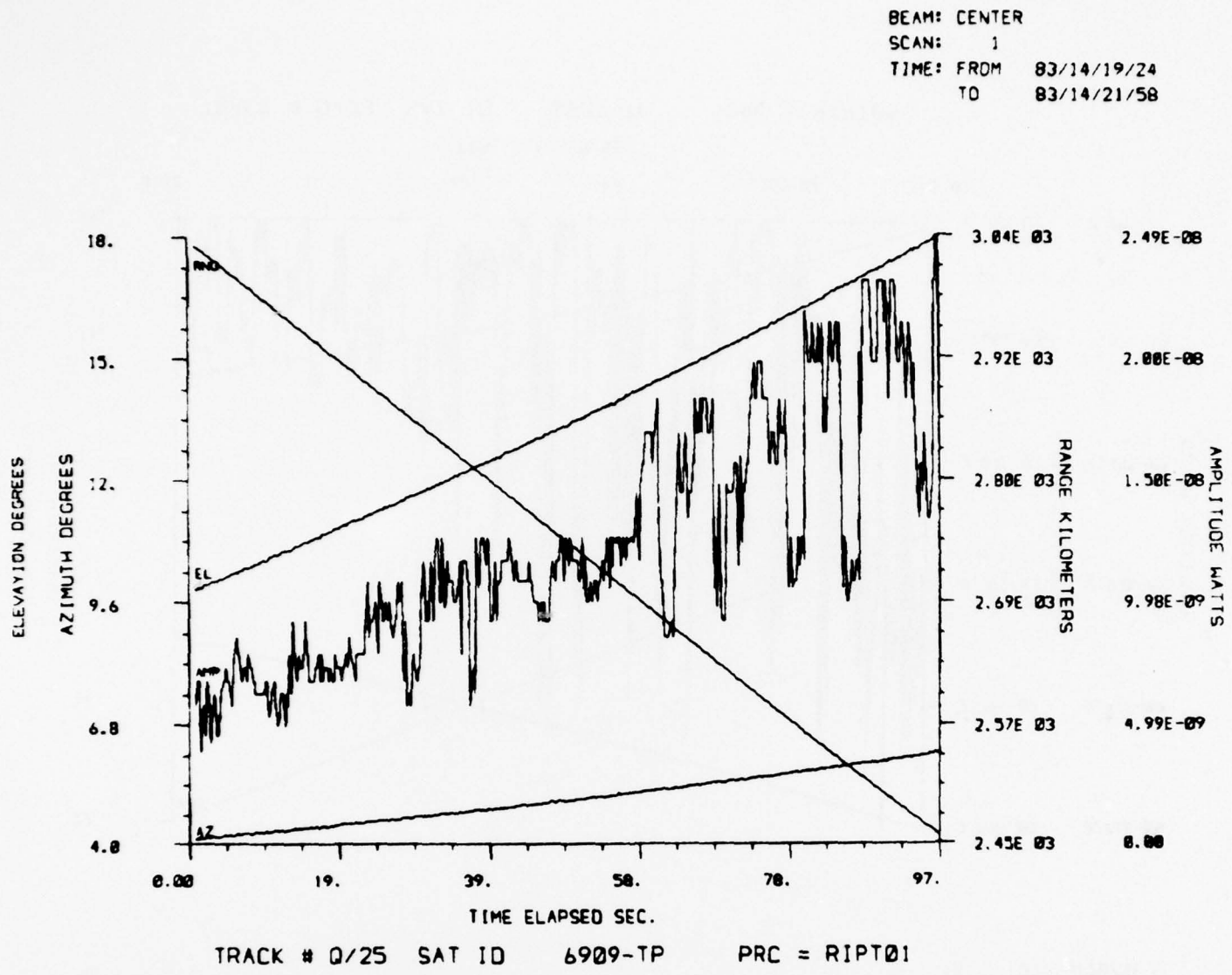
BEAM: CENTER
SCAN: 1
TIME: FROM 83/14/19/24
TO 83/14/21/58
ELEVATION DEGREES
AZIMUTH DEGREES
18.
15.
12.
9.6
6.8
4.0
RNG
EL
AMP
AZ
3.04E 03
2.92E 03
2.80E 03
2.69E 03
2.57E 03
2.45E 03
RANGE KILOMETERS
2.49E-08
2.00E-08
1.50E-08
9.98E-09
4.99E-09
0.00
AMPLITUDE WATTS
0.00
19.
39.
58.
78.
97.
TIME ELAPSED SEC.
TRACK # 0/25 SAT ID 6909-TP PRC = RIPT01

Figure A-39